

Recovery of gallium and indium from end-of-life LEDs by ionic liquid technology

Willem VEREYCKEN

Promotor: Prof. Koen Binnemans

Co-promotor: Dr. Tom Vander Hoogerstraete

Begeleider: Drs. Arne Van den Bossche

Proefschrift ingediend tot het
behalen van de graad van
Master of Science in Chemie

Academiejaar 2017-2018

© Copyright by KU Leuven

Without written permission of the promotors and the authors it is forbidden to reproduce or adapt in any form or by any means any part of this publication. Requests for obtaining the right to reproduce or utilize parts of this publication should be addressed to KU Leuven, Faculteit Wetenschappen, Geel Huis, Kasteelpark Arenberg 11 bus 2100, 3001 Leuven (Heverlee), Telephone +32 16 32 14 01.

A written permission of the promotor is also required to use the methods, products, schematics and programs described in this work for industrial or commercial use, and for submitting this publication in scientific contests.

Table of contents

Dankwoord	i
Abstract	ii
Samenvatting.....	iii
Summary	v
Thesis Outline	vii
List of Abbreviations	viii
1 Literature	1
1.1 Gallium and indium	1
1.2 Light-Emitting diodes	2
1.2.1 Working principle	3
1.2.2 Construction	5
1.2.3 Applications	6
1.2.4 Recycling	6
1.3 Ionic liquids	8
1.3.1 Brief history.....	8
1.3.2 Synthesis	10
1.3.3 Properties	13
1.3.4 Applications	15
1.3.5 Polyhalide ionic liquids	16
1.4 Extractive metallurgy	18
1.4.1 Solvent extraction.....	18
1.4.2 Gallium and indium solvent extraction	21
2 Techniques.....	23
2.1 Nuclear magnetic resonance spectroscopy	23
2.2 Karl Fischer titration.....	24
2.3 Raman spectroscopy	25
2.4 Rolling-ball viscometry.....	25
2.5 Total reflection X-ray fluorescence (TXRF).....	26

2.6	Inductively coupled plasma – optical emission spectrometer (ICP-OES)	27
2.7	Microwave digestion	29
3	Health, Safety and Environment	30
4	Materials and methods	31
4.1	Materials	31
4.2	Synthesis of ionic liquids	32
4.2.1	Tributyldecylphosphonium bromide [P ₄₄₄₁₀][Br]	32
4.2.2	Tribromide ionic liquids	32
4.3	Oxidative dissolution of semiconductor materials	33
4.4	Measuring metal concentrations	33
4.4.1	Total reflection X-ray fluorescence (TXRF)	33
4.4.2	Inductively coupled plasma – optical emission spectrometer (ICP-OES)	36
4.5	Extraction/stripping of metals from ionic liquids	38
5	Results and discussion	39
5.1	Solubility study	39
5.1.1	<i>N</i> -dodecane	39
5.1.2	Influence of extractant	40
5.1.3	Water	42
5.2	Synthesis of ionic liquids	42
5.3	Oxidative dissolution of semiconductor materials	44
5.3.1	Leaching kinetics	46
5.4	Choice of ionic liquid	47
5.5	Extraction/stripping of metals from ionic liquids	48
5.5.1	Initial experiments	48
5.5.2	Sulphate salts	49
5.5.3	MilliQ water	51
5.5.4	Multi-step strippings	51
5.5.5	Development of stripping procedure	55
5.5.6	Optimization of the NaBr – MilliQ procedure	59

5.5.7	Extraction/stripping of indium	60
5.5.8	Flowsheet for the selective stripping of arsenic, gallium and indium	62
5.6	Mechanistic study	63
5.7	Light emitting diodes.....	67
5.7.1	Grinding and milling.....	67
5.7.2	Thermal treatment.....	67
5.7.3	Fractionalisation of the powders	69
5.7.4	Analysis of the different fractions	70
5.7.5	Stripping of LED leachates.....	72
5.7.6	Conceptual flowsheet.....	73
6	Conclusion and outlook	75
7	Bibliography	77

Dankwoord

Vooreerst ben ik veel dank verschuldigd aan mijn promotor Prof. Koen Binnemans en copromotor Dr. Tom Vander Hoogerstraete voor het interessante en uitdagende projectvoorstel. Bedankt voor de goede begeleiding en al het advies die dit project tot een goed einde brachten.

Daarnaast wil ik iedereen van het LIC bedanken voor alle hulp, tips en de gezellige sfeer in de labo's en bureaus. In het bijzonder Martina voor de hulp met het ball millen, Recai voor het disc millen en de thermal treatment van de LEDs en Emir voor de hulp met de microwave digestions.

Graag zou ik ook mijn collega thesisstudenten willen bedanken voor het fijne jaar. In het bijzonder Brent, het was een genoegen om vijf jaar met jou op kot te zitten. Bedankt om het zo lang met mij uit te houden! En Rayco, merci voor al onze gezellige middagen.

Uiteraard wil ik ook mijn ouders bedanken. Vijf jaar studeren en op kot gaan is achteraf bekeken zeker geen evidentie. Bedankt voor al de kansen en vrijheid die jullie mij hebben gegeven!

Mijn vriendin, Charlien, die mij steeds wist op te fleuren en de stress als sneeuw voor de zon kon doen verdwijnen. Dikke merci voor al de leuke weekends en die talloze bezoeken aan Leuven!

En dan natuurlijk, last maar zeker niet least, Arne. Ik weet dat je de rol van begeleider vrij onverwachts hebt moeten opnemen. Bedankt voor je onvoorwaardelijke hulp en het beantwoorden van al mijn vragen. Zonder jou had deze thesis er ongetwijfeld helemaal anders uitgezien!

Merci iedereen!

Willem

Abstract

Starting in 2005, the light-emitting diode (LED) industry has experienced an enormous growth. It is expected that this trend will continue and that the global market will account for 54 billion USD by 2022. The growth is fuelled by the many advantages of LEDs over the conventional light sources. They are characterised by a low energy consumption, long lifespan, reduced dimensions and the absence of mercury. The first end-of-life LEDs are now leaving the market. However, there is currently a lack of specific recycling routes and many of the LED semiconductors contain gallium and/or indium. Both are considered as critical raw materials for the EU, implying a significant supply risk in the near future. In this project, tribromide ionic liquids (ILs) are proposed for the recovery of gallium and indium from end-of-life LEDs. ILs are solvents that consist entirely of ions and are characterised by negligible vapour pressures, which makes them ideal substitutes for many of the commonly used volatile organic solvents. The tribromide ILs are strongly oxidizing and capable to oxidatively dissolve an array of metals while being non-volatile at ambient temperatures.

A suitable IL was determined based on its mutual solubility with other solvents and its dissolution characteristics of common semiconductors. Both 1-ethyl-3-methylimidazolium bromide ([EMIM][Br]) and tributyldecylphosphonium bromide ([P₄₄₄₁₀][Br]) showed a sufficiently low miscibility with *n*-dodecane. [EMIM][Br] was however completely miscible with water whereas [P₄₄₄₁₀][Br] was not. In addition, [P₄₄₄₁₀][Br₃] showed superior dissolution characteristics of GaAs and InAs. [P₄₄₄₁₀][Br₃] was therefore used for the remainder of the project. An extraction/stripping procedure was developed and optimized for the selective stripping of gallium, arsenic and indium from the [P₄₄₄₁₀][Br₃] phase. Arsenic is stripped quantitatively using three stripping steps with 4 M NaBr and an O:A ratio of 2. Hereafter, gallium can be stripped with MilliQ water and an O:A ratio of 1. Indium can be precipitated using a dilute NaOH solution. Finally, the optimized stripping procedure was applied to a [P₄₄₄₁₀][Br₃] leachate of semiconductor material derived from real LEDs. Despite some contamination of other metals, the metal concentrations in the strip solutions indicated that the procedure worked as intended.

Samenvatting

Sinds 2005 kende de licht-emitterende diode (LED) industrie een enorme groei. In 2016 was de wereldmarkt goed voor 26 miljard USD. Er wordt verwacht dat deze groei zich zal voortzetten en dat de wereldmarkt 54 miljard USD waard zal zijn tegen 2022. De enorme groei werd gevoed door de vele voordelen die LEDs bieden ten opzichte van de meer conventionele lichtbronnen zoals de gloei- en fluorescentielampen. Hun grootste voordeel is de lage energieconsumptie, daarnaast hebben ze ook een lange levensduur, kleinere dimensies en bevatten ze geen kwik. Het eerste LED-afval is zich nu aan het opstapelen, maar er bestaan echter nog geen specifieke recyclage routes. Bovendien bevatten veel LEDs gallium en/of indium in hun halfgeleider. Beide elementen worden beschouwd als kritieke materialen voor de EU, wat voor de nabije toekomst een potentieel bevoorradingsrisico inhoudt. In deze masterproef worden tribromide ionische vloeistoffen (ILs) gebruikt voor de winning gallium en indium van LED-afval. ILs zijn solventen die enkel uit ionen bestaan en vloeibaar zijn onder 100 °C. Ze worden gekenmerkt door een verwaarloosbare dampspanning. Dit maakt hen de ideale substituten voor vluchtige organische solventen. Tribromide ILs kunnen eenvoudig gesynthetiseerd worden door toevoeging van moleculair broom aan een bromide IL. Deze tribromide ILs zijn sterk oxiderend en kunnen een hele reeks aan metalen oxidatief oplossen. Het doel van dit project is om het gallium en indium aanwezig in LED-afval op te lossen in een tribromide IL waarna de metalen gescheiden kunnen worden door middel van solventextractie.

Het eerste deel van dit project bestond uit het kiezen van een geschikte IL. De keuze was voornamelijk gebaseerd op de onderlinge mengbaarheid van de IL met andere solventen zoals *n*-dodecaan en water. Deze is bij voorkeur zo laag mogelijk om een adequate fasescheiding te verkrijgen tijdens de solventextracties. De mengbaarheid van tien ILs met *n*-dodecaan werd onderzocht. [EMIM][Br] en [P₄₄₄₁₀][Br] waren de beste kandidaten aangezien ze niet oplossen in de *n*-dodecaan fase en de oplosbaarheid van *n*-dodecaan in de IL ook voldoende laag bleef. De invloed van de drie extractanten PC-88a, D2EHPA en Cyanex 923 op de onderlinge mengbaarheid werd ook onderzocht. In het geval van [P₄₄₄₁₀][Br] verbleven de extractanten voornamelijk in de IL. Bovendien was de oplosbaarheid van *n*-dodecaan in de IL ook toegenomen. Bij [EMIM][Br] bleven de extractanten volledig in de *n*-dodecaan fase. [EMIM][Br], in tegenstelling tot [P₄₄₄₁₀][Br], was echter wel volledig mengbaar met water wat de mogelijkheid van extractie naar een waterige fase uitsluit voor de deze IL. Het oplossen van halfgeleidermaterialen werd ook overwogen bij de keuze van de geschikte IL. [P₄₄₄₁₀][Br₃] en [EMIM][Br₃] werden beiden gesynthetiseerd en gebruikt in een oplossingsexperiment met GaAs, InAs en GaN. GaN loste niet op in de tribromide ILs. GaAs en InAs losten op in beide

ILs maar het proces verliep trager in [EMIM][Br₃] en stagneerde na verloop van tijd. Daarnaast was [P₄₄₄₁₀][Br₃] vloeibaar bij kamertemperatuur en [EMIM][Br₃] vast. [P₄₄₄₁₀][Br₃] werd uiteindelijk gekozen als de IL voor het verdere verloop van dit project. De oplossingskinetiek van GaAs en InAs in [P₄₄₄₁₀][Br₃] werd ook onderzocht. InAs loste iets sneller op dan GaAs door de zwakkere bindingssterkte. Globaal gezien waren de oplossingsnelheden van beide halfgeleiders echter gelijkaardig.

Het tweede grote deel van dit project bestond uit de ontwikkeling van een extractieprocedure voor de selectieve verwijdering van gallium, arseen en indium van de [P₄₄₄₁₀][Br₃]-fase. Gallium en arseen konden beide gemakkelijk en kwantitatief geëxtraheerd worden naar een waterige fase. Door gebruik te maken van een hoge O:A ratio en NaBr concentratie kon de extractie van gallium nagenoeg volledig onderdrukt worden. Indium daarentegen vertoonde een hoge affiniteit voor de IL-fase en kon niet geëxtraheerd worden naar een waterige fase. Extractie naar een *n*-dodecaan fase met opgeloste extractanten toonde ook geen selectiviteit voor indium, bovendien bleef de extractie-efficiëntie laag (<30%). Gebruikmakende van 5 equivalenten NaOH kon indium uiteindelijk kwantitatief neergeslagen worden als hydroxide. In de geoptimaliseerde procedure wordt eerst arseen geëxtraheerd met behulp van 3 strippingsstappen met 4 M NaBr en een O:A verhouding van 2. Vervolgens kan gallium geëxtraheerd worden met MilliQ water en een O:A verhouding van 1. Als laatste wordt indium neergeslagen met een verdunde NaOH oplossing. Aan de hand van een mechanistische studie werden de extractieverschillen tussen gallium en arseen ook aangetoond.

In het laatste gedeelte van dit project werd de geoptimaliseerde extractieprocedure toegepast op een [P₄₄₄₁₀][Br₃] loging van halfgeleidermateriaal afkomstig van LEDs. Hiervoor werden LEDs met een GaAs halfgeleider aangekocht. Na het vermalen werden de bekomen poeders gescheiden door middel van verschillende mechanische en fysische technieken. Karakterisatie van de verschillende fracties leidde tot de conclusie dat de halfgeleider voornamelijk aanwezig was in de plasticfracties. Deze fracties werden geloofd met [P₄₄₄₁₀][Br₃] en de extractieprocedure werd hierop toegepast. Ondanks de aanwezigheid van enkele andere metalen, bewezen de metaalconcentraties dat de procedure naar behoren werkte. Tenslotte werd nog een conceptuele flowsheet voorgesteld voor de winning van gallium en indium uit LED-afval met behulp van tribromide IL.

Summary

Starting in 2005, the light-emitting diode (LED) industry has experienced an enormous growth and in 2016 the global LED-market accounted for 26 billion USD. It is expected that this trend is to continue and that the global market will reach 54 billion USD by 2022. The growth is fuelled by the many advantages LEDs possess over the conventional light sources such as the incandescent and fluorescent lamps. The biggest asset is their low energy consumption, in addition they are characterised by a long lifespan, reduced dimensions and the absence of mercury. The first end-of-life LEDs are now leaving the market. However, there is currently a lack of specific recycling routes. Additionally, many of the LED semiconductors contain gallium and/or indium which are both considered as critical raw materials for the EU, implying a significant supply risk in the near future. In this master thesis project tribromide ionic liquids (ILs) are applied for the recovery of gallium and indium from end-of-life LEDs. ILs are solvents that consist entirely of ions and are liquid below 100 °C. They are characterised by negligible vapour pressures, which makes them ideal substitutes for many of the commonly used volatile organic solvents. Tribromide ILs can easily be synthesised by the addition of molecular bromine to a bromide IL. The tribromide ILs are strongly oxidizing and capable to oxidatively dissolve an array of metals while being non-volatile at ambient temperatures. The aim of the project is to dissolve gallium and indium from end-of-life LEDs using a tribromide IL after which they are separated by means of a selective extraction and/or stripping from the IL phase.

The first part of this master thesis project consisted of the determination of a suitable IL. This choice was largely based on the mutual solubility of the IL with other solvents such as *n*-dodecane and water. This mutual solubility is preferably as low as possible to achieve an adequate phase separation during the solvent extraction and stripping steps. The miscibility of ten monobromide ILs with *n*-dodecane was investigated. [EMIM][Br] and [P₄₄₄₁₀][Br] were the best candidates as they showed no dissolution into the *n*-dodecane phase and the *n*-dodecane content of the IL phase remained minimal. The influence of the three extractants PC-88a, D2EHPA and Cyanex 923 on this mutual solubility was also investigated. In the case of [P₄₄₄₁₀][Br], the extractant resided almost entirely in the IL phase. In addition the *n*-dodecane content of IL phase increased. [EMIM][Br] showed no changes compared with pure *n*-dodecane as the extractant remained in the *n*-dodecane. [EMIM][Br], in contrast to [P₄₄₄₁₀][Br], was however completely miscible with water ruling out the possibility of stripping to an aqueous phase for this IL. The second property which was considered in the choice of IL was the dissolution of commonly used semiconductor materials. [P₄₄₄₁₀][Br₃] and [EMIM][Br₃] were prepared and used in dissolution experiments on GaAs, InAs and GaN.

GaN showed no dissolution in the ILs. GaAs and InAs dissolved into both ILs however the dissolution in [EMIM][Br₃] was slower and stagnated before completion. In addition, [P₄₄₄₁₀][Br₃] was a liquid at room temperature while [EMIM][Br₃] was not. [P₄₄₄₁₀][Br₃] was therefore the IL of choice for the remainder of the project. The dissolution kinetics of GaAs and InAs into [P₄₄₄₁₀][Br₃] were also compared. InAs showed a slightly faster dissolution because of its weaker bond strength. However, overall the dissolution rates were quite similar.

The second major part of the project was the development of an extraction/stripping procedure for the selective removal of gallium, arsenic and indium from the [P₄₄₄₁₀][Br₃]-phase. Gallium and arsenic could easily be stripped in quantitative amounts to an aqueous phase. Using an increased O:A ratio and NaBr concentration, the stripping of gallium could largely be suppressed. Indium showed a high affinity for the IL phase and was unable to be stripped to any aqueous phase. Extraction to an extractant containing *n*-dodecane phase showed no particular selectivity for indium and the extraction efficiencies remained low (<30%). Using 5 equivalents of NaOH indium could be precipitated quantitatively as an hydroxide. In the optimized procedure arsenic is stripped first using three stripping steps with 4 M NaBr and an O:A ratio of 2. Hereafter, gallium can be stripped with MilliQ water and an O:A ratio of 1. Lastly, indium can be precipitated using a dilute NaOH solution. Using a mechanistic study, the differences between the stripping of gallium and arsenic were clarified.

In the last section of this project, the optimized stripping procedure is applied to a [P₄₄₄₁₀][Br₃] leachate of semiconductor material derived from real LEDs. For this purpose LEDs with a GaAs semiconductor were bought. After milling or grinding, the resulting powders were fractionalised using different mechanical and physical techniques. Characterisation of the different fractions revealed that the majority of the semiconductor was present in the plastic fractions. These fractions were subsequently leached with [P₄₄₄₁₀][Br₃] and subjected to the stripping procedure. Despite some contamination of other metals, the metal concentrations in the strip solutions indicated that the procedure worked as intended. Lastly, a conceptual flow sheet for the recovery of gallium and indium from end-of-life LEDs using tribromide ILs was proposed.

Thesis Outline

The objective of this master thesis project is the application of tribromide ILs for the recovery of gallium and indium from end-life-life LEDs.

Chapter 1 contains a literature study to introduce firstly gallium and indium and their use in light emitting diodes (LEDs). The advantages, working principle, composition, applications and recent studies on the recycling of LEDs are also discussed. Secondly, ionic liquids (ILs) are introduced together with their synthesis, properties and applications after which polyhalide ILs are shortly discussed. Finally, the typical metallurgical flow sheet is mentioned with a focus on solvent extractions and the separation of gallium and indium.

In chapter 2, all used techniques are introduced. NMR, Karl fisher titration, Raman spectrometry, rolling-ball viscometry, TXRF, ICP-OES and microwave digestion are all shortly discussed.

Chapter 3 is the health, safety and environment (HSE) chapter.

Chapter 4 contains a list of the used materials and a detailed description of all synthetic routes, experimental and measuring procedures.

Chapter 5 deals with the results and their discussion. Firstly, the solubility study of ILs with *n*-dodecane and water is discussed. Hereafter, the synthesis of ILs and the dissolution of semiconductor materials in the tribromide ILs are treated. Next, the stripping and/or extraction of metals from the tribromide IL is discussed. Lastly, the composed stripping procedure is applied to LEDs.

Chapter 6 resumes the most important conclusions and achievements of this project. In addition, an outlook to future research is given.

List of Abbreviations

Symbol/abbreviation	Full description
%E	Percentage extraction or extraction efficiency
α	Separation factor
cP	Centipoise
<i>D</i>	Distribution ratio
D2EHPA	Di-(2-ethylhexyl)phosphoric acid
DIBK	Diisobutyl ketone
GaAs	Gallium arsenide
GaN	Gallium nitride
IC	Integrated circuit
ICP-OES	Inductively coupled plasma – optical emission spectrometer
IL	Ionic liquid
InAs	Indium arsenide
ITO	Indium tin oxide
LCD	Liquid crystal display
LED	Light emitting diode
LEP	Light emitting polymer
NMR	Nuclear magnetic resonance
O:A ratio	Organic to aqueous volume ratio
OLED	Organic light emitting diode
rpm	Revolutions per minute
RT	Room temperature
RTIL	Room temperature ionic liquid
SSL	Solid-state lighting
TBP	Tributyl phosphate
TOPO	Trioctylphosphine oxide
TXRF	Total reflection X-ray fluorescence
VOC	Volatile organic compound
XRF	X-ray fluorescence

1 Literature

1.1 Gallium and indium

Gallium (atomic number 31) is a soft, silvery-white metal. It is a good conductor of both electricity and heat. Gallium does not occur in its elemental form in nature and mostly substitutes other elements in minerals. It is rarely found in sufficient quantities by itself to enable economic extraction and is currently almost exclusively extracted as a by-product of aluminium production.¹ To a lesser degree, gallium is also obtained as a by-product of zinc production.² In 2016, the worldwide low-grade primary gallium production was estimated to be 375 tons, refined high-purity gallium production was estimated to be about 180 tons.³ Gallium has been on the list of critical raw materials for the EU since it was first published in 2011.¹

Currently, the largest consumption of gallium is its use in semiconductors, the most popular being gallium arsenide (GaAs), followed by gallium nitride (GaN) with respective shares of 92% and 8%.¹ Both compounds display exceptional semiconductor properties with an electron mobility six times higher than silicon. GaN is produced in reduced quantities compared to GaAs because of a more difficult and costly production process. Both semiconductors are incorporated in integrated circuits (ICs), light emitting diodes (LEDs) and solar cells (copper-indium-gallium-selenide, CIGS). These applications require gallium of at least 99.9999% (6N) purity. Both vacuum refining and zone refining are used for the purification of gallium.⁴

Today, pre-consumer recycling (from industrial scrap generated during production) is common and a consequent secondary supply for gallium. Even though semiconductor devices represent the highest volumes of gallium consumption, the gallium content per device is extremely low. The thickness of the semiconductor layer in a LED is approximately 4 μm . The recovery of gallium from end-of-life products is therefore nearly non-existent.^{1,5} Current recycling processes of electronic equipment favour the recovery of precious metals or copper, while gallium ends up as an impurity in the recycled metals or in waste slags. The absence of primary gallium ores and the steady increase in gallium use necessitate the development of new recycling routes for end-of-life products or urban mining.^{2,5}

Indium (atomic number 49) is a soft, silvery metal with a high thermal conductivity. Like gallium, indium is not concentrated enough to be a major commodity in deposits.¹ Indium is associated with different sulphide based minerals such as sphalerite ((Zn,Fe)S), galena (PbS) and chalcopyrite (CuFeS₂) but it is mainly recovered as a by-product during zinc ore

processing.⁶ The total worldwide production of primary indium was estimated to be 655 tons in 2016.⁷ Just as gallium, indium has been on the list of critical raw materials for the EU since 2011.¹

Indium is predominantly used in the form of indium tin oxide (ITO) as a transparent conductive oxide material which bonds strongly to glass.⁸ ITO thin-film coatings are primarily used for electrical conductive purposes in flat-panel displays such as liquid crystal displays (LCDs) and organic light emitting diode (OLED) displays. ITO thin films are also applied to car and aircraft windshields for defogging and de-icing. Indium is also used in the CIGS solar cells. Other indium end-uses include alloys and lead-free solders, electrical components (e.g. InP, InN and InSb in transistors and microchips) and semiconductors (e.g. InGaN in LEDs).

Just as for gallium, recovery of indium from manufacturing waste (pre-consumer recycling) is common but recovery from end-of-life products is practically non-existent.^{1,5} The same reason as for gallium applies, the indium content per device is considered to be too low. Also here, urban mining and the development of new recycling routes can play an essential role in ensuring the future supply of indium.⁸

1.2 Light-Emitting diodes

Light-emitting diodes (LEDs) together with organic light-emitting diodes (OLEDs) or light-emitting polymers (LEPs) are referred to as solid-state lighting (SSL).⁹ These devices create visible light by means of electroluminescence. They have the potential to greatly exceed the energy efficiencies of incandescent and fluorescent lighting.

Electroluminescence was first observed by H. J. Round in 1907, who also invented the first light-emitting diode (LED).⁹ But it was only in the 1960s that the first LEDs were commercialized. Among the first applications were indicator lights on circuit boards, calculators and wristwatches. It was not until 2005 that a large number of firms began to enter the LED-industry and since 2010 the industry has experienced an enormous growth.¹⁰ The industry is expected to grow even further, completely replacing the conventional lighting industry.¹¹ The total global LED-market accounted for 26.09 billion USD in 2016 and is expected to reach 54.28 billion USD by 2022.¹²

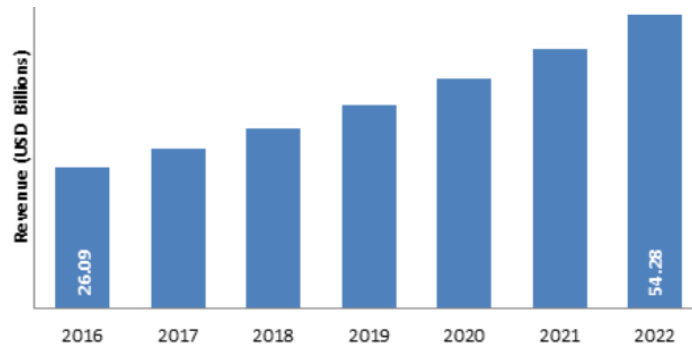


Figure 1: Expected market growth of the global LED industry.¹²

Lighting accounts for 19% of the world's electricity consumption.¹¹ Since the most commonly used lighting source is still the incandescent bulb, the energy savings potential of lighting is very high.¹³ The incandescent bulb has a low luminous efficiency and a short lifespan, creating a major environmental impact. Fluorescent lamps are a step in the right direction as they are more energy efficient and have a longer lifespan. However, they suffer from a high lumen depreciation and they contain mercury. LEDs on the other hand have the potential for electricity conversion of nearly 100%. Other advantages of LEDs include: long lifespan (over 50 000 h), high-speed response time (micro-second level on-off switching), reduced dimensions, flexibility in design, they are unaffected by vibrations, better thermal management than conventional lighting sources, absence of mercury and they are dimmable without loss of efficiency.^{9,11,13}

Although LEDs offer many advantages over the conventional light sources, they also possess some downsides. Waste LEDs have more potential to impact human health and the ecosystem than incandescent bulbs because they require more metal-containing components in order to function.¹⁴

1.2.1 Working principle

To clarify the working principle of a LED, the electronic structure of semiconductors has to be treated first. The electronic structure of solids can be represented using bands resulting from the overlap of an infinite amount of molecular orbitals. The valence band and conduction band are the most important when discussing conductivity.¹⁵ Just as insulators, semiconductors possess a completely filled valence band and an empty conduction band which are separated by a band gap with energy E_g . At 0 K semiconductors act as insulators since movement of electrons is impossible in the completely filled valence band. At higher temperatures thermal excitation results in the occupation of the lower energy levels of the conduction band. This makes the material conducting since the movement of electrons is now possible, left side Figure 2. The difference between insulators and semiconductors is the width of the band gap, it is much bigger for insulators. The result is that at room temperature

conduction is still limited in insulators while it is not in semiconductors. Doping, or the controlled introduction of impurities, of semiconductors with elements with fewer or more electrons allows to significantly alter the conductive properties. As such, a *p*-type semiconductor contains an excess of holes in the valence band and an *n*-type semiconductor has an excess of electrons in the conduction band (right side Figure 2).

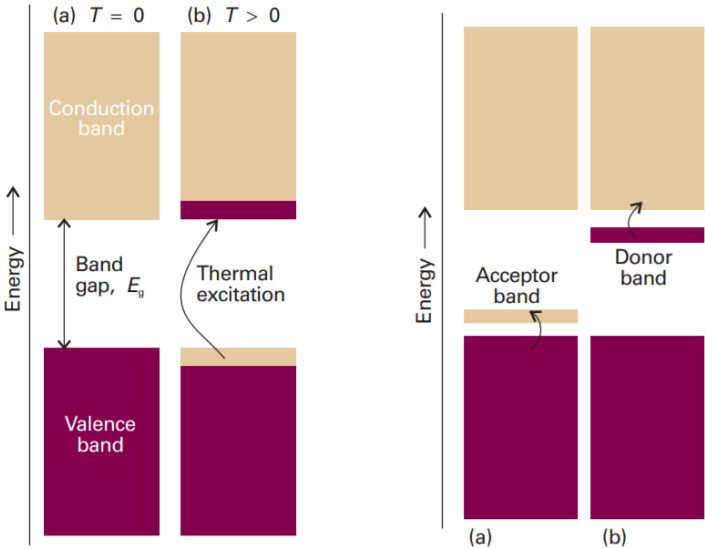


Figure 2: Left: Electronic band structure of a semiconductor. Right: Electronic band structure of a *p*-type (a) and *n*-type (b) semiconductor.¹⁵

The working principle of a LED is based on a forward biased *p-n* junction. *P-n* junctions consist of the interface between a *p*-type and an *n*-type semiconductor.¹⁰ The term forward biased indicates that the *p*-type semiconductor is connected to the positive side of the energy source and the *n*-type semiconductor is connected to the negative side. The charge carriers are therefore pushed towards the interface and the electrons of the *n*-side are able to recombine with the holes of the *p*-side.¹⁶

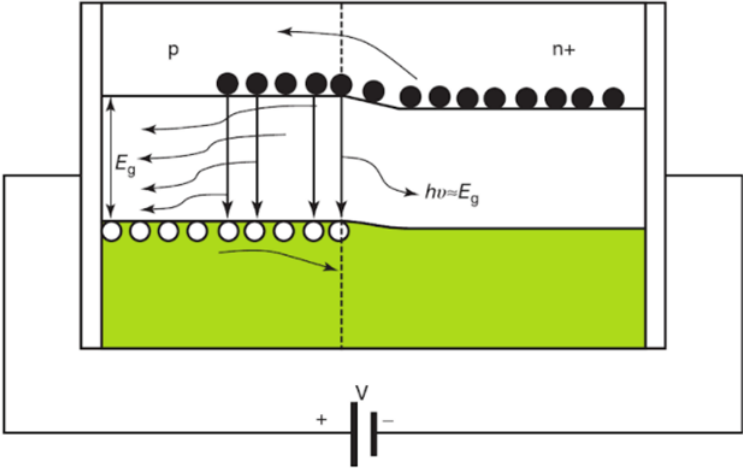


Figure 3: Working principle LED.¹⁷

The electrons must lose some of their energy in order to recombine with the holes because of the energy difference (E_g , or band gap) between the valence band of the p -type semiconductor and the conduction band of the n -type semiconductor. This is depicted in Figure 3. There are two types of recombination: radiative and non-radiative recombination.¹⁷ Radiative recombination allows LEDs to emit photons while non-radiative recombination results in the production of heat. In most semiconductor materials the excess energy is dissipated as heat. But in some semiconductors such as e.g. gallium arsenide phosphide (GaAsP) the electrons dissipate energy as photons. Different semiconductors, with different band gaps, are available for different colours as illustrated in Table 1. Slight changes in the composition of the semiconductor will also influence the band gap and the emitted colour.¹⁶

Table 1: Different semiconductor materials used for different colours.¹⁶

Semiconductor	LED emission colours
AlGaAs	Red and infrared
AlGaInP	Bright orange red, orange, yellow
AlGaIn	Near to far ultraviolet
AlGaP	Green
AlN	Near to far ultraviolet
GaAs	Infrared
GaAsP	Red, orange and red, orange, yellow
GaN	Green
GaP	Red, yellow, green
InAs	Infrared
InGaIn	Bluish green, blue, near ultraviolet
SiC	Blue
ZnSe	Blue

Other colours can also be achieved by coating the LED with phosphors. The phosphor absorbs the emitted light and reemits it as a new colour through fluorescence.^{9,17} Examples of the use of these phosphors can be found in the production of white LEDs. The most commonly used method for the production of white LEDs is the combination of a blue LED chip, such as InGaIn, with the yellow phosphor Ce³⁺-doped yttrium aluminium garnet (YAG/Ce). Another possibility is combining a UV-LED with a mixture of red, green and blue phosphors.¹⁸

1.2.2 Construction

A basic LED is composed of a p - n junction (which can be coated with a phosphor), two electrical contacts from which the electric current that is applied flows through the chip, a heat sink slug usually made of aluminium or copper and a plastic case which serves as protection and a lens to direct the beam of light.¹³ This is visualised in Figure 4.

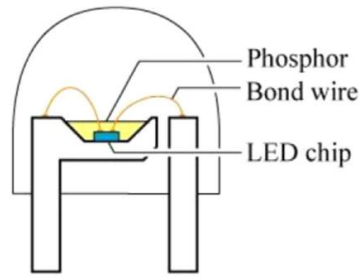


Figure 4: Basic LED construction.⁹

Two basic configurations are possible based on the direction of light emitted. The surface emitting LED emits light perpendicular to the plane of the $p-n$ junction. And the edge emitting LED which emits light in a plane parallel to the junction. In the latter configuration the light can be confined to a narrow angle. The $p-n$ junctions are normally grown by liquid phase or vapour phase epitaxy.⁵ The substrates are chosen to have a close lattice match to the semiconductors used.⁹ Poor alignment could cause strain and defects in the semiconductor's crystal structure and inhibit the desired electronic and optical properties.¹⁰

1.2.3 Applications

In 2016 residential applications dominated the market as they accounted for more than 40% of the LED market share.¹² Visible LEDs have found applications in displays, indicators, optical switches, visual signals, aviation lighting, automotive lighting, advertising, general lighting and traffic signals. Infrared LEDs can be used as a source in optical fibre communications, in the remote control units of many commercial products including televisions, DVD players, and other domestic appliances.⁹

1.2.4 Recycling

Observing the different semiconductors in use in Table 1 the conclusion can be made that end-of-life LEDs could serve as a potential source for both gallium and indium. However, the number of studies on the recovery of gallium and indium from end-of-life LEDs is rather limited.¹⁹ One reason is that very little end-of-life LEDs have entered the waste streams because of their relatively long life-time. Another reason is that the LED-module not only consist of the semiconductor but also of plastic, different resins and metallic electrodes, as can be seen in Figure 4. These other components lower the concentration of the elements of interest in the material. Also the contacting surface during leaching and the diffusion rate are dramatically reduced by these exogenic components.²⁰ An efficient recycling route for LEDs must thus be a combination of mechanical and chemical methods. This paragraph is aimed at presenting a brief overview of the available literature.

Zhan *et al.* reported pyrolysis of the organic compounds of InGaN and GaN LEDs, followed by crushing and sieving.²¹ The residue was then introduced into a vacuum furnace at 1100 °C with a pressure of 0.01-0.1 Pa. Gallium and indium were recovered after sublimation and condensation with efficiencies of 93.48% and 95.67% respectively. Zahn *et al.* also reported the use of sulfurization and evaporation for the recycling of arsenic from GaAs scraps.²² GaAs was contacted with solid sulphur for 40 min at 180 °C forming As_2S_3 , As_4S_4 , GaS and Ga_2S_3 . Further heating at 800 °C allowed for the evaporative separation of gallium and arsenic with an 88.2% recovery for arsenic. Chen *et al.* leached GaAs semiconductors with a 4 M nitric acid solution followed by a coagulation and annealing step.²³ Vacuum separation and sublimation by heating to 1000 °C resulted in As_2O_3 of 99.2% purity and Ga_2O_3 of 99.9% purity. The aforementioned methods all require a very high energy input and cannot be considered as environmentally friendly recycling routes. On top of that, high temperatures are usually accompanied by high operating costs and strict safety regulations. Hu *et al.* reported a more environmentally friendly recycling route of GaAs scrap from LED waste.²⁴ The GaAs was dissolved in 1.5 M HNO_3 and selective precipitation of arsenic was performed with Na_2S .

Nagy *et al.* on the other hand have developed a mechanical and chemical approach to the recycling of gallium from GaN LEDs.²⁰ The first step consisted of cutting and milling the LEDs and sieving to the 106-1000 μm fraction. This was followed by an electrostatic separation step. The non-conducting fraction consisted of the LED chips and the conductive fraction consists of metallic parts such as copper wiring. The non-conducting material was then mechano-chemically activated by roasting and mixing in the presence of Na_2CO_3 . The produced $NaGaO_2$ was then dissolved in 4 M HCl with recoveries up to 99%. Swain *et al.* developed a similar procedure for the recovery of gallium from MOCVD (metalorganic chemical vapour deposition) dust, a by-product from the LED-industry. In a first research they reported leaching 64.62% of the gallium and 99.99% of the indium present in the material using a 4 M HCl solution.²⁵ However, they were only able to leach the $Ga_{0.97}N_{0.9}O_{0.09}$ phase, the GaN phase remained in the residue. GaN needs some form of pre-treatment before leaching. In a following research they reported ball milling the waste dust with Na_2CO_3 with a subsequent annealing step at 1100 °C to form $NaGaO_2$.²⁶ This material was then leaching using a 4 M HCl solution.

1.3 Ionic liquids

Because of their large scale use and volatile nature, organic solvents have a high environmental impact. These volatile organic compounds (VOCs) cause safety concerns and concerns on increasing air pollution. In the context of climate change, the development of more efficient and environmentally friendly processes is necessary. Ionic liquids have been proposed as environmentally friendly or 'green' solvents, since they are inflammable and have a negligible vapour pressure at room temperature.^{27,28}

Ionic liquids (ILs) are liquids which only consist of ions. Typical ionic liquids are organic salts with a melting point below 100 °C, although this threshold is arbitrary. In reality, most ionic liquids reported in the literature that meet our present definition are also liquid at room temperature, therefore called room temperature ILs (RTILs).^{29,30} Some remarkable physical properties make them interesting solvents compared to organic solvents. They have a negligible volatility, are non-flammable, conducting, have a very wide liquidus range and are good solvents for a range of organic and inorganic compounds.²⁸ Their most prominent downsides are their high viscosity (which lowers the rate of mass transfer and increases stress on equipment such as pumps)³¹ and high price, which are serious drawbacks for their large-scale application.^{32,33} On average, ILs cost 20 times more than common solvents. This implies that, to develop an economically viable process, ILs should be recycled at least 20 times.

Due to the high variety in the choice for cation and anion, it is estimated that there are 10^{18} possible combinations for ILs. ILs are sometimes called 'designer solvent' because this vast number allows for tailoring the IL properties for each specific application. Such compounds are referred to as task-specific ionic liquids since they are especially designed and suited for a specific purpose or application.^{30,34}

1.3.1 Brief history

The first report of a room temperature molten salts dates back to 1914 with Walden reporting that ethylammonium nitrate had a melting point of 12 °C. However, this discovery attracted only limited attention in scientific circles.^{30,34} The progress in IL studies was particularly impacted by a series of studies conducted in the 1960s and 70s at the U.S. Air Force Academy.³⁴ These studies were aimed at finding an electrolyte for the thermal battery. A cell was developed containing an ionic liquid as electrolyte produced by the reaction of aluminium chloride with 1-ethylpyridinium halides. Later on dialkylimidazolium chloroaluminate ILs were also synthesised because of their higher stability towards reduction.³⁰ The ILs based on aluminium chloride can be considered as the first generation of

ILs, but their use was restricted due to their hygroscopic nature. These chloroaluminates were even sensitive to atmospheric moisture, producing gaseous hydrogen chloride.^{27,28}

Replacing the chloroaluminate anion with other more hydrolytically stable anions such as BF_4^- , PF_6^- , NO_3^- , SO_4^{2-} and CH_3COO^- resulted in ILs that were more water and air stable. Initially it was however not fully realized that BF_4^- and PF_6^- do hydrolyse when in contact with water forming HF.³⁵ ILs based on these two anions should still be handled under an inert atmosphere. Also anions such as trifluoromethanesulfonate (CF_3SO_3^-) and bis(trifluoromethylsulfonyl)imide ($\text{N}(\text{SO}_2\text{CF}_3)_2^-$) were used.³⁰ This resulted in the formation of relatively inert and water-immiscible ionic liquids with low viscosities. New cations based on phosphonium, ammonium and pyrrolidinium ions were also introduced. These ILs can be considered as the second generation and were developed in the 1990s.^{27-29,34} The main disadvantages of these second generation ionic liquids are their high cost and toxicity.³⁶

The third generation of ionic liquids, which was introduced around 2010, tries to solve the problem of high cost and toxicity by using readily available and biodegradable cations and anions.^{27,36} For example, the cation can be choline and the anions may be sugars, sugar analogues, amino acids, organic acids, alkylsulfates or alkylphosphates. These ionic liquids often display some form of biological activity, such as bactericidal or fungicidal activity.³⁴

The structures of the cations and anions of the three generations of ILs are given in Figure 5.

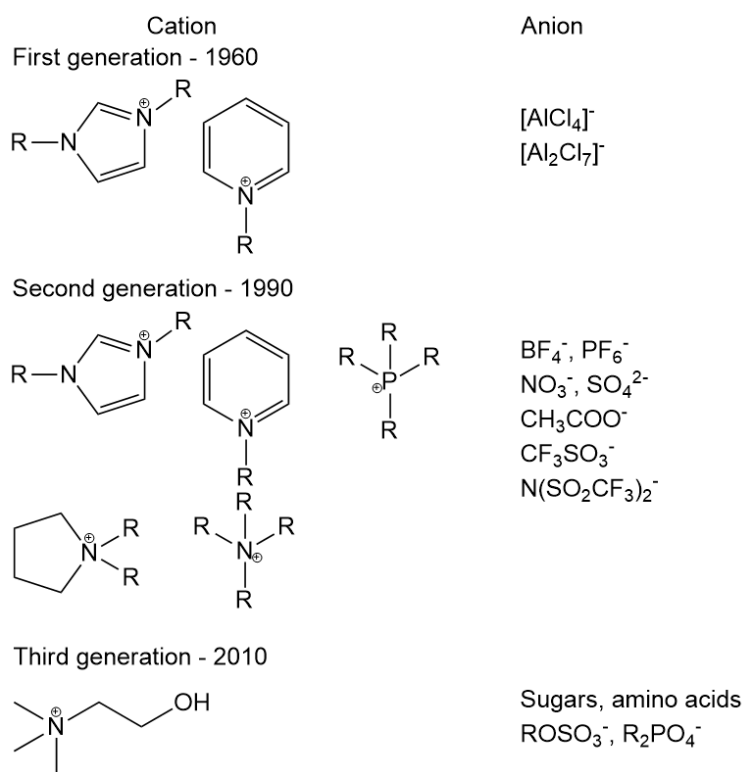


Figure 5: Structures of the cations and anions of the three generations of ILs.

1.3.2 Synthesis

The synthesis of ionic liquids can generally be split into two steps: the formation of the cation and anion exchange.^{27,29,37} In some cases only the first step is required. Examples of this include the synthesis of the aforementioned ethylammonium nitrate through the reaction of ethylamine with nitric acid and the production of halide ILs through the quaternization of phosphines, amines, ... with haloalkanes.

Formation of the cation

The formation of the cation can be performed in one of two ways. The first option is a protonation reaction with a Brønsted acid, as in the example of ethylammonium nitrate. ILs produced with a protonation reaction are called 'protic ILs'. The second option is the quaternization of an amine, phosphine, imidazole, pyridine, pyrrolidine,... with a haloalkane (or any alkyl compound with a sufficiently good leaving group). The protonation of suitable starting materials is the easiest method for the synthesis of ILs, but it can only be used for a small range of salts. An additional downside is the possible decomposition of the IL through deprotonation. Synthesis of the cation through a quaternization reaction using haloalkanes is therefore preferred.^{27,29} Furthermore, the formed halide salts can easily be converted into salts with other anions as is explained hereafter.

Quaternization reactions can be performed easily in the lab, the starting product (amine, phosphine, imidazole,...) is simply mixed with the desired haloalkane. The mixture is then stirred and heated. Often the reaction is carried out in a round-bottom flask with a reflux condenser.²⁹ Depending on the starting product, the reaction is carried out under an inert atmosphere. This is necessary to exclude water and/or oxygen which might react with the starting product lowering the total yield. Phosphines, for example, require the use of an inert atmosphere to prevent the formation of phosphine oxides. The quaternization reaction can be carried out with chloro-, bromo- and iodoalkanes with the reaction conditions required becoming more gentle in the order $\text{Cl} \rightarrow \text{Br} \rightarrow \text{I}$.^{27,29} This is in accordance with the increasing leaving group properties of the halides. Fluoride salts cannot be formed in this manner because of the strong carbon-fluorine bond.²⁷ The reaction can be performed without a solvent as often both reagents are liquid and miscible. However, the reaction is usually performed in a solvent to lower the viscosity of the system and improve the reaction kinetics. Subsequent removal of this solvent can easily be done using a rotary evaporator.

As stated earlier, not only halide salts can be synthesised using a quaternization reaction but any alkyl compound with a sufficiently good leaving group can be used. As such, triflates and

tosylates which display excellent leaving group characteristics can be used in quaternization reactions at room temperature.²⁹

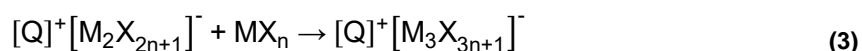
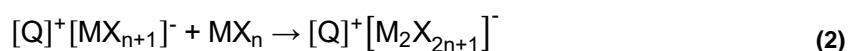
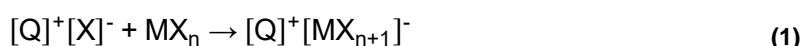
Protonation and quaternization are the two most important mechanisms for cation formation. There exist however some other possibilities like the Debus-Radziszewski synthesis of imidazolium salts.³⁸

Anion exchange

There are several possibilities to alter the anion of ILs. The first option is the treatment of the halide IL with a Lewis acid. Secondly, the anion can be changed by anion metathesis.^{27,29} A third possibility makes use of anion exchange resins. Finally, the anion does not always have to be exchanged, it can also be modified.

- Lewis acid treatment

Treatment of quaternary halide salts, $[Q]^+[X]^-$, with Lewis acids of the form MX_n results in the formation of new anionic species depending on the relative proportions of both compounds as is illustrated in Equations (1), (2) and (3).^{28,29} It is possible to tune the acidity of the IL depending on the molar ratio of MX_n added. With molar ratios smaller than 0.5 the IL is said to be basic. A neutral IL is obtained with a molar ratio of 0.5, here only the $[MX_{n+1}]^-$ anion is present. When the molar ratio is larger than 0.5 the IL is acidic with the $[M_2X_{2n+1}]^-$ and $[M_3X_{3n+1}]^-$ anions acting as strong Lewis acids.³⁷



In fact, this is the method that was used to synthesise the chloroaluminate ILs which were discussed earlier. This method is not limited to the chloroaluminates, other Lewis acids such as $AlEtCl_2$, BCl_3 , $CuCl$, $SnCl_2$ and $FeCl_3$ can be used as well.^{28,37} The reaction can be carried out by contacting the two compounds, but the reaction is often quite exothermic. It is therefore advised to use some form of cooling or to perform the reaction in a dry solvent which helps dissipate the heat. It should be noted again that this kind of ILs are not stable in the presence of water.²⁹

- Anion metathesis

The occurrence of anion exchange can be predicted based on the Hofmeister series, Figure 6. Anions with a low charge density (Tf_2N^- , SCN^- , ClO_4^- and I^-) prefer to be in the less polar IL phase, while more hydrophilic anions (Cl^- and SO_4^{2-}) prefer to be in the water phase where they are better solvated.³⁹ The anion exchange reaction depends on the position of both anions in the Hofmeister series. The methatesis reaction will only be complete when the desired anion is placed higher in the series than the current anion.

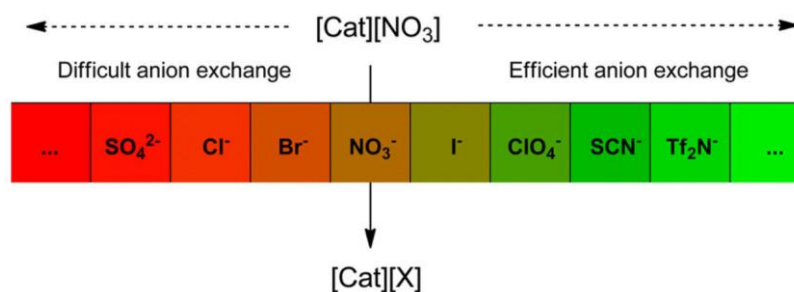


Figure 6: Prediction tool for the occurrence of anion exchange based on the Hofmeister series.³⁹

Anion metathesis can be carried out by contacting the halide salt of the cation with an aqueous solution of the desired anion. Where available use of the free acid of the anion is favoured as this leaves only HCl, HBr, or HI as the by-product. Metal or ammonium salts of the anion can also be used if the free acid is not available. The synthesis of water-immiscible ILs is considerably more straightforward than the preparation of their water-soluble analogues since in the latter case it is not possible to remove the by-products by washing with water. A possible solution is the use of silver salts to perform the metathesis reaction, as the silver halides precipitate from the solution. Other possibilities include the use of other solvents, such as dichloromethane, to purify the IL with the use of solvent extraction.^{27,29}

- Anion exchange resins

Anion exchange resins have also been used to alter the anion of ionic liquids.²⁹ Ion exchange resins are usually made out of functionalized, crosslinked, polystyrene-derived resins.³² These resins are charged with a specific anion after which the IL can be poured through.

- Anion modification

An example of anion modification is the formation of polyhalide anions which will be discussed in paragraph 1.3.5. Since X_2 molecules are in fact Lewis acids, the formation of polyhalide ILs can also be classified as a Lewis acid treatment.

1.3.3 Properties

Liquidus range and melting point

The liquidus range is the temperature range in which a compound is in the liquid state. ILs exhibit liquidus ranges much wider than those found in common solvents. The upper limit, which is the boiling point for common solvents, is for ILs usually characterised by thermal decomposition. This thermal decomposition or pyrolysis is accompanied by mass loss and volatilization of some components. Pyrolysis of the organic cation generally occurs between 350 and 450 °C.²⁹ The lower temperature limit is characterised by solidification, this can either be crystallization or vitrification. The charge, size and charge distribution of both the cation and anion influence the melting point of salts. The dominant force in salts, and also in ILs, is the Coulombic attraction between ions which can be represented by Equation (4).^{29,31}

$$F = k \frac{Q_1 Q_2}{r^2} \quad (4)$$

With F the Coulombic force, k Coulomb's constant, Q_1 the charge of the cation, Q_2 the charge of the anion and r the distance between the charges. This formula shows that low ionic charges (+1 and -1) and large ion sizes will reduce the attractive force between the ions and as such lower the melting point.²⁹ However not only the Coulombic attraction should be taken into account. Additional attractive interactions, such as hydrogen bonding or aromatic π - π stacking, can also increase the melting temperature.³⁰

Also the symmetry of the ions has an influence on the melting point.^{29,30} Increasing symmetry in the ions increases the melting point by allowing a more efficient ion packing in the crystal lattice. Manipulation of alkyl chain length can thus produce major changes in the melting point. For example, an increase in the substituent length initially reduces the melting point of the ionic liquid because of reduced symmetry and less efficient packing in the crystal cell. The melting points of the salts start to increase again with increasing chain length, as van der Waals interactions between the long alkyl chains contribute to local structure. This initial decrease and subsequent increase in melting point as a function of chain length is displayed in Figure 7.

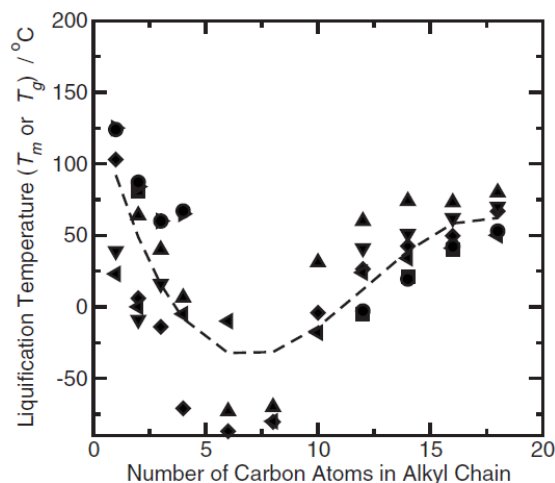


Figure 7: Variation of melting point as a function of alkyl chain length for 1-alkyl-3-methylimidazolium chloride (●), bromide (■), tetrafluoroborate (◆), hexafluorophosphate (▲), bis(triflyl)imide (◄), triflate (▼), and tetrachloroaluminate (►).²⁹

Viscosity

The viscosity describes the internal resistance of a fluid to shear stress. The viscosity of ILs can range from about 10 to 5000 cP. Comparing this with the viscosity of water which is only 0.89 cP, it is obvious that ILs are considerably more viscous than most common solvents.^{29,40}

Roughly the same trends apply to the viscosity as those which were found for the melting point of ILs. Longer alkyl chains will increase the viscosity (because of the increased van der Waals interactions) while asymmetric substitution of the cation leads to lower viscosities.²⁷ The presence of other intermolecular interactions such as hydrogen bonding and π - π stacking can strongly influence the viscosity.^{37,40} Also the molar mass of the ions affects the viscosity.³¹ A higher molar mass results in a slower diffusion of the ions and thus a higher viscosity. Additionally, the viscosity of ionic liquids is strongly influenced by temperature and purity. Higher temperatures and the addition of solvents can drastically lower the viscosity.^{29,31,33}

Density

In general, the density of ILs ranges between 0.8 and 1.6 g/mL. The density of the IL decreases with an increasing cation size or with an increase in alkyl chain length on the cation.^{37,40} The anion also greatly influences the density. Small and heavy anions result in higher densities.²⁷

Vapour pressure

ILs are characterised by negligible vapour pressures at ambient conditions. However, that does not mean that their vapour pressure is non-existent. Under the appropriate conditions of

high temperature (200-300 °C) and low pressure (0.1 mbar) some ionic liquids can be distilled and separated. The volatility decreases as the substituent chain-length increases.⁴¹ The nature of the gas-phase species has been identified as tightly bound, discrete ion-pairs.³⁰ The distillation rates are very low (0.01 g/h) and for all practical purposes, ILs may be considered as non-volatile.^{27,42}

Conductivity and electrochemical window

Based on the fact that ILs consist only of ions, it would be expected that they have high conductivities. However, the conductivity is not only dependent on the amount of charge carriers present but also on the viscosity, ion size, ion mobility and aggregate formation. The cations of ILs are usually quite large which results in a low ion mobility and a reduced conductivity. Strong ion-pair formation also reduces the ion mobility. Furthermore, the high viscosity of ILs also negatively influences their conductivity.²⁷

The electrochemical window is by definition the electrochemical potential range over which the electrolyte is neither reduced nor oxidized. ILs have electrochemical windows in the range of 5-6 V, which is significantly larger than the 1.23 V window of water.^{30,34} ILs have been proposed as new systems for the electrodeposition of metals such as Al, Mg, Si, Ge and some rare earths which were formerly only deposited from high temperature molten salts.²⁸

1.3.4 Applications

ILs have been used in a wide variety of applications. The most obvious and maybe the most important is their use as alternative solvents. ILs can easily replace common solvents which are used in large quantities in the chemical processing industries. Because of their negligible vapour pressure they are often characterized as 'green' solvents.³⁰ Additionally, this gives the opportunity to use them in high vacuum systems.²⁷ As was already mentioned, it is possible to tune the properties of ILs by changing the nature of the ions. It is therefore possible to tune the miscibility with water or other solvents or to tune the solubility of reagents and products.³⁷ This gives rise to the possibility of designing a multiphase reaction procedure. ILs have been used as solvents for many organic and inorganic compounds, ranging from metal salts to polymers and cellulose.^{34,43} ILs have even been used as solvents for some gasses, especially CO₂ and oxygen.³⁰

ILs have also been used as solvents for synthetic and catalytic applications. For example, ILs have been used to tune the *endo/exo* selectivity of Diels-Alder cycloadditions. An example of the catalytic application of ILs is the use of imidazolium chloroaluminates for Friedel-Crafts

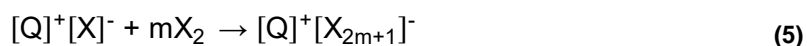
alkylations and acylations.^{28,37} ILs have even been used as solvents for enzyme catalysed reactions.³⁶

Some ILs have already been implemented in industrial processes.³⁰ The most known example is the BASIL process at BASF where 1-methylimidazole is used to scavenge the acid that is released during the alkoxyphenylphosphines synthesis forming 1-methylimidazolium chloride. This is an IL that forms a separate phase and can easily be separated from the reaction mixture. Recovery of the 1-methylimidazole is done via base decomposition of the IL. Another well-known example is that of the Dimersol process at IFP. Dimerization of alkenes is performed in a biphasic system where the nickel catalyst is dissolved in a chloroaluminate IL.³⁷ Because the reaction products form a second layer, separation of catalyst and reaction products is straightforward.

1.3.5 Polyhalide ionic liquids

The tendency of halide ions to complex elemental halogens forming polyhalide complexes has been known since 1819.⁴⁴ But it was only in the last 20 years that many new interesting polyhalides were explored. Many mono-, di-, tri- and tetra-anions of polyiodides are known varying between I_3^- and I_{26}^{4-} , yet the chemistry of the lighter halogens is much less explored.⁴⁵ Tri- and tetra-anions are unknown for fluorine, chlorine, and bromine. This is mainly due to their higher volatility compared with iodine, which results in a higher tendency towards loss of halogen. The known polyhalides of bromine vary between Br_3^- and Br_{20}^{2-} . For chlorine, Cl_3^- is currently the only known polyhalide. However it has been shown that Cl_5^- should be able to exist as well.⁴⁶ Under cryogenic conditions the existence of F_3^- was also confirmed.⁴⁴ Also mixed trihalide anions such as ICl_2^- and IBr_2^- are known. Here the X-Y-X⁻ anions, with Y the heavier halogen, are more stable than Y-X-X⁻. The reason is that in the former configuration there is more room for the 5 electron pairs on the central atom. The Y-X-X⁻ anions therefore easily isomerize to the more stable X-Y-X⁻ anion.⁴⁷

Polyhalide salts, and subsequently also ILs, can be synthesized by the reaction of elemental halogens with the halide salt. These polyhalides can be described as donor-acceptor complexes between the Lewis base X⁻ (X_3^- , X_5^- , ...) and the Lewis acid X_2 .^{44,48} The reaction can be carried out without solvent even when the ionic liquid is a solid.⁴⁹ For mono-anionic species, the reaction is described in Equation (5). Trihalide ILs are relatively stable and can be stored for several months. Storage has to occur in the dark to avoid radical dissociation of the anion, which might subsequently damage the cation.⁴⁷

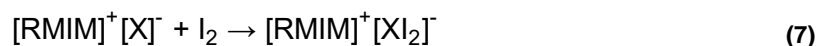


The cation also influences the formation of these polyhalide anions. ILs such as tetraalkylammonium or phosphonium halides more easily produce higher order polyhalides than for example imidazolium ILs. This is a result of the more sterically hindered cations in the former. The shielding of the cation lessens the electronic influence of the cation over the halide ion allowing it to more readily participate in halogen bonding.⁴⁸

These polyhalide ILs have mostly been used in organic chemistry as halogenating agents. They are preferred over classical halogenating methods because they are easier to handle as the molecular halogens.^{47,49} Other advantages include high yields, the ability to tune the selectivity and reactivity and the easy separation of the ILs from the reaction products. Phosphonium ILs are preferred over ammonium or imidazolium ILs because of the larger size, greater polarizability and lower binding energy to the anions.⁴⁹ Polyhalide anions also have interesting electrochemical properties because the total negative charge is smaller than the number of atoms, resulting in a charge deficit. The tribromide ion, for example, reduces according to Equation (6) and can act as an oxidant.⁴⁴



These oxidative properties can be used for the oxidative dissolution of metals. An example where this has been applied is the absorption of elemental mercury from flue gas of coal fired power plants.⁵⁰ 1-Alkyl-3-methyl imidazolium halides were transformed into polyhalide ILs by the addition of iodine. The mercury containing gas was then passed through the IL. This resulted in the oxidation of the mercury forming mercury iodide which is bound to the IL. Exposure to a sodium formate solution results in the precipitation of elemental mercury and the ability to recycle the IL. The reactions that are involved are summarized in Equations (7), (8) and (9).



Comparing the standard reduction potential of the tribromide ion in Equation (6) with those of gallium and indium in Equations (10) and (11) respectively, it is clear that the tribromide ion should be able to oxidize both elements.



The use of tribromide ILs is therefore proposed for the leaching of metals from semiconductors or scrap LEDs. This approach can be considered as more environmentally friendly than the previously mentioned methods in paragraph 1.2.4. The main advantages of this approach include the use of low-volatile ILs and the fact that it works at ambient temperatures. Additionally it avoids the use of acids which can, in the case of arsenide semiconductors, lead to the formation of the highly toxic arsine gas.³²

1.4 Extractive metallurgy

A typical flow sheet of an extractive metallurgical process is comprised of three steps as shown in Figure 8.⁵¹ The first step is the dissolution or leaching of the solid material. In this master thesis project the leaching will be performed using the aforementioned tribromide ILs. In the next step, the leached metals are to be separated and concentrated using solvent extraction techniques. Lastly, the metal can be regenerated by reduction.

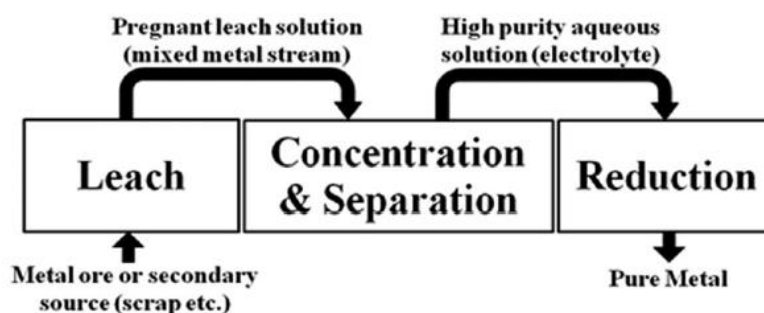


Figure 8: Typical flow sheet of an extractive metallurgical process.⁵¹

1.4.1 Solvent extraction

Solvent extraction is an important technique used for the separation and purification of metals. The technique is fairly straightforward as all that is required are two immiscible liquid phases. Metal ions are distributed over the two mutually immiscible phases. Various metal ions distribute differently over both phases and a separation can be achieved. An important remark is that the mutual solubility of two liquid phases is dependent on both temperature and the concentration of dissolved salts or extractants.³²

A distinction can be made between solvometallurgy and hydrometallurgy based on the choice of the two immiscible phases. In solvometallurgy no discrete water phase is present. When ionic liquids are used in solvometallurgical processes sometimes the term ionometallurgy is preferred.³² The fact that only very little water is present in solvometallurgy offers many advantages. One of the more important advantages is the fact that water sensitive products can be separated. Additionally the consumption of water is very limited, and thus the production of waste water is also minimal. Often the leaching and extraction

steps can be combined into a single step. Solvent leaching is usually also more selective than leaching with acidic aqueous solutions.³²

In conventional (hydrometallurgical) solvent extractions, the metal ions are distributed between an aqueous phase and a water-immiscible organic phase. The distribution ratio D of a certain metal ion M is defined by Equation (12). An important remark here is that the concentrations in Equation (12) are total concentrations at equilibrium, they are the sum over all the species containing M .⁵² In the case of solvometallurgy the same definition cannot be used as no water phase is present. It is then better to use the terms more-polar and less-polar phase.³²

$$D = \frac{C_{M,org}}{C_{M,aq}} \quad (12)$$

Other important quantities used in the description of solvent extractions are the percentage extraction ($\%E$) and the separation factor between two elements (α). The percentage extraction reflects the amount of the element of interest that has been transferred to the less polar phase and can be calculated using Equation (13) with D the distribution ratio for the particular element. Separation factors quantify the separation between two elements. The separation factor between elements A and B is calculated according to Equation (14).⁵²⁻⁵⁴

$$\%E = 100 \frac{DV_{aq}}{DV_{org} + V_{aq}} \quad (13)$$

$$\alpha_{A/B} = \frac{D_A}{D_B} \quad (14)$$

Single stage solvent extractions often result in insufficient separation, purity or recovery of the metals of interest. Therefore, industrial solvent extraction processes generally make use of multi stage flow sheets.⁵²

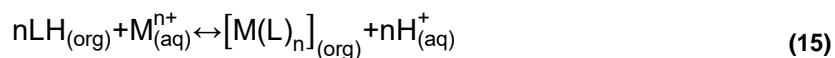
Extractants

The distribution of metal ions over both phases is often aided by extractants.³² Based on the extraction mechanism, extractants are divided into 3 classes.^{51,53} For simplicity, the three classes are explained for hydrometallurgical solvent extractions.

- Cation exchangers

These extractants extract metal cations, M^{n+} , from the aqueous phase to the organic phase by exchanging the metal ion for another cation, usually an ionisable proton of the extractant

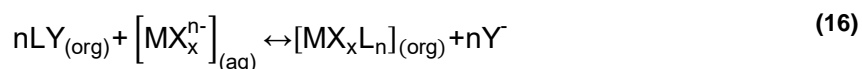
molecule. This is displayed in Equation (15).⁵¹ When the extractant is not acidic enough and as a result the metal loading is too low, the extractant may be converted to the alkali salt first. The cation exchange is then facilitated because of the higher hydration energy of the alkali cation compared with the M^{n+} cation, favouring its transfer to the aqueous phase.



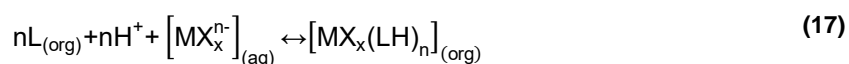
Because of the pH dependence of the equilibrium in Equation (15), subsequent stripping of the organic phase is possible by using an acidic aqueous solution. Typical examples of these cation exchangers include the commercially available phosphinic and phosphonic acid derivatives such as D2EHPA, PC-88a and Cyanex 272. Other examples include carboxylic acids such as Versatic acid 10 and 8-hydroxyquinoline derivatives such as Kelex-100.

- Anion exchangers

This type of extractants extract metal ions as anionic complexes, MX_x^{n-} . Hence, they are only effective in the presence of strong anionic ligands.⁵³ Extractants that carry a permanent positive charge can be employed as anion exchangers according to Equation (16).⁵¹ Loading and stripping the organic phase can be controlled through variation of the Y^- concentration. An example of this type of extractant is Aliquat 336.

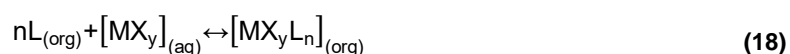


Alternatively, protonation of neutral extractant molecules can also form anion exchangers. Loading and stripping are now pH dependent, Equation (17).⁵¹ Several amines, ketones and phosphine oxides such as Alamine 336, DIBK and TOPO have been used for this.



- Solvating extractants

This category of extractants transports the metal cation from the aqueous phase to the organic phase as a neutral species, MX_y . The extraction mechanism can be written as Equation (18).⁵¹ Examples of commonly used extractants of this type are TBP and Cyanex 923. Attention needs to be made to the conditions under which this type of extractants is used. When contacted with highly acidic solutions the oxygen atom of e.g. TBP can be protonated transforming it into an anion exchanger.



1.4.2 Gallium and indium solvent extraction

Solvent extraction is an ideal tool for the extraction and separation of gallium and indium after leaching both elements from end-of-life LEDs. In this section some examples are given of the literature describing gallium and indium solvent extraction and separation.

Both Ga^{3+} and In^{3+} display a strong affinity for oxygen and/or nitrogen donors.⁵⁵ Extractants with these donor atoms are therefore often used for the extraction and separation of these elements. Popular extractants include D2EHPA, Cyanex 272 and Kelex-100.

Gallium extraction

Gupta *et al.* used a 0.50 M Cyanex 923 solution in toluene to extract Ga^{3+} from acidic media.⁵⁶ Extraction efficiency increased with increasing chloride concentration because of the increased chance of the formation of the GaCl_3 species, reaching a maximum at 3.0 M HCl. Extraction from nitrate and sulphate solutions was poor across the entire concentration range.

In another study Gupta *et al.* recovered gallium from Bayer's liquor.⁵⁷ Carbon dioxide was first bubbled through the solution to precipitate the bulk of the aluminium. Next, the pH was adjusted to 1 and the solution was extracted with 0.50 M of Cyanex 301 (the sulphur analogue of Cyanex 272) in toluene. Subsequent stripping of the organic layer was performed with 0.50 M of HCl.

Solvent extraction of gallium from highly alkaline Bayer's liquor can also be performed with Kelex-100 in *n*-dodecane. Deprotonation of the alcohol function in the alkaline conditions is an essential part of the extraction mechanism.^{58,59}

Indium extraction

Gupta *et al.* also studied the extraction of In^{3+} from acidic media to a 0.20 M Cyanex 923 solution in toluene.⁶⁰ The extraction is quantitative at 0.001 M $\text{H}_2\text{SO}_4/\text{HNO}_3/\text{HCl}$. A decrease in extraction efficiency was observed with increasing acid concentration for H_2SO_4 and HNO_3 . This was attributed to the decreasing possibility to form hydroxide complexes. The extraction from HCl media was rather unaffected by the acid concentration because of the formation of the extractable InCl_3 at higher acid concentrations.

Kang *et al.* efficiently extracted In^{3+} from HCl media with acid concentrations varying between 0.1 and 0.5 M using a 1 M solution of PC-88a in kerosene.⁶¹ The In^{3+} was selectively stripped, and thus separated from the co-extracted impurities, from the organic layer using a 2.0 M acid solution.

Gallium/indium separation

0.50 M of Cyanex 301 or Cyanex 923 in kerosene was used by Gupta *et al.* to selectively extract indium from a 0.50 M HCl solution containing both gallium and indium. Gallium remained completely in the aqueous phase at this chloride concentration.^{56,57} Another possible separation process presented by Gupta *et al.* also makes use of Cyanex 923.⁶⁰ This time both gallium and indium are transferred from the 0.01 M HCl/H₂SO₄/HNO₃ aqueous phase to the organic phase using 0.20 M Cyanex 923. Ga³⁺ is then stripped using a 1.0 M HCl solution followed by In³⁺ stripping using a 1.0 M H₂SO₄ solution.

Lee *et al.* reported the use D2EHPA for the selective extraction of indium from mixed gallium and indium sulphate solutions.⁵⁴ They found that D2EHPA had a selectivity for indium over gallium. The separation factor between indium and gallium decreased with increasing pH. A maximum value of the separation factor was obtained for extractions with a stoichiometric amount of D2EHPA for indium extraction. Complete separation of gallium and indium was accomplished by a two-stage extraction process.

Sec-octylphenoxy acetic acid in kerosene was used by Zhang e.a. for the selective extraction of gallium and indium from chloride solutions.⁶² Ga³⁺ was quantitatively extracted from a solution at pH 4.2 using an extractant concentration of 0.0046 M. Approximately 10% of In³⁺ was co-extracted but Ga³⁺ was selectively stripped with a 3.0 M HCl solution.

2 Techniques

2.1 Nuclear magnetic resonance spectroscopy

^1H and ^{31}P NMR were used to determine the structure and purity of synthesized products. In addition it was also used to determine the mutual solubility of ionic liquids and *n*-dodecane, both in the absence and presence of extractants. The ^1H measurements were performed on a Bruker Avance 300 or 400 spectrometer, which operated at respectively 300 and 400 MHz with tetramethylsilane (TMS) as the reference material. The ^{31}P measurements were all performed on the Bruker Avance 400 spectrometer operating at 162 MHz. For the ^{31}P measurements the delay time (d1) was adjusted to 5 s and 128 scans were recorded, the reference was a solution of 25 wt% H_3PO_4 in water. All samples were dissolved in deuterated chloroform (CDCl_3). Analysis of the spectra was done using the Bruker Topspin software.

NMR is a powerful, non-destructive technique capable of structural and conformational analysis of molecules and quantitative analysis of complex mixtures.⁶³ Nuclei possessing a spin angular momentum I have an associated dipole moment μ . The spin angular momentum is quantized and can only take $(2I + 1)$ discrete values. The isotopes of interest for chemists (^1H , ^{13}C , ^{15}N , ^{19}F and ^{31}P) possess a spin angular momentum equal to $\frac{1}{2}$, this makes the analysis of the spectra straightforward as there are only two possible spin states.⁶⁴ The energy levels are degenerate in the absence of an external magnetic field B_0 . When a magnetic field is present the magnetic moments of these nuclei will orient parallel or anti-parallel with B_0 resulting in an energy difference between the levels, Figure 9. In addition, the interaction causes a precession of the magnetic moments around the B_0 axis. The angular frequency of this precession depends on the strength of the local magnetic field. This in turn depends on the electrons which surround a particular nucleus.⁶⁴ Different chemical environments will thus result in a different local magnetic field and a different precession frequency.

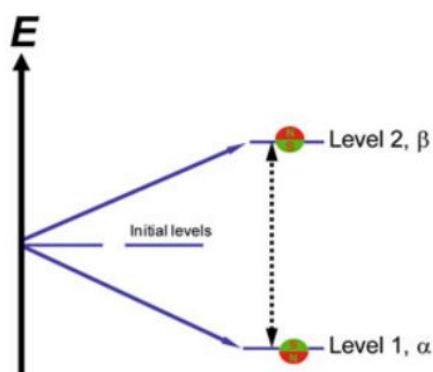


Figure 9: Splitting of the nuclear spin states in the presence of a magnetic field.⁶⁴

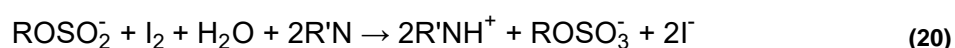
The most stable and lowest energy state in a system will be the most populated at equilibrium as dictated by the Boltzmann distribution. In this case, the nuclear magnetic moments oriented parallel with B_0 have the lowest energy. Electromagnetic radiation with a frequency equal to the precession frequency can be used to pump the nuclei in the lowest energy state (α -state) to the upper state (β -state). Relaxation from the β -state to the α -state will result in fluctuations of the magnetic field which can be converted to the signals in the NMR spectrum. Nuclei with different chemical environments will cause different signals in the spectrum. The strength of these signals is proportional to the amount of nuclei undergoing the transition. The NMR spectrum can thus be used to determine the relative abundances of these nuclei. The resonance frequencies are usually converted to a number called the 'chemical shift'. This value is independent of the used equipment as it describes the resonance frequency relative to a reference point. Tetramethylsilane (TMS) is most frequently used as the reference material in ^1H and ^{13}C NMR. For ^{31}P measurements a reference solution of 25 wt% H_3PO_4 in water is often used.

In practice, the continuous wave technique (CW-NMR) in which the entire range of electromagnetic frequencies is scanned is too time consuming. Therefore another technique is used called Fourier Transform NMR (FT-NMR).⁶⁴ Here, the entire range of frequencies is pulsed at once and all nuclei are excited at the same time. The nuclei start relaxation at the same time, but the relaxation times are different because of the different chemical environments. The spectrum is recorded as a function of time and the overlapping relaxation signals are subjected to a Fourier transformation. This transforms the signal-time spectrum to the usual signal-frequency spectrum.

2.2 Karl Fischer titration

Karl Fischer titration was used to determine the water content of ionic liquid samples. The measurements were performed on a Mettler Toledo V30S Volumetric Titrator.

Karl Fischer titration is the preferred technique for moisture content determination because of its ease and speed.⁶⁵ The technique is based on the reaction of sample water, an alcohol, a base, sulphur dioxide and iodine according to Equations (19) and (20).^{65,66} One mole of I_2 is consumed for each mole of sample water.



Two set-ups are possible: coulometric and volumetric titration.⁶⁷ In the coulometric Karl Fischer titration I_2 is constantly regenerated at an electrode. As long as water is present, the solution contains little I_2 , but at the equivalence point excess I_2 appears. This excess I_2 is accompanied by a voltage drop at a detector electrode. This marks the end point of the titration and the amount of charge used to generate I_2 can be recalculated to the amount of water. The coulometric titration is preferred when the water content is relatively low. The volumetric Karl Fischer titration is based on the volume of a standard solution with a known I_2 concentration that must be added to react with the sample water. This configuration is preferred for samples where water is present as a major component.

2.3 Raman spectroscopy

Raman spectroscopy was used to verify the synthesis of the tribromide ion and to determine its stability in the presence of water. All spectra were measured on a Bruker Vertex 70 spectrometer coupled to a RAM II FT-Raman module with a Nd:YAG laser of wavelength 1064 nm. Analysis of the spectra was performed using the OPUS software.

Raman spectroscopy is a technique which is based on the inelastic scattering of incident radiation with vibrating molecules.⁶⁸ A change in the polarizability of the molecule during the molecular vibration is an essential requirement to obtain a Raman spectrum. Raman spectroscopy can thus be used to analyse homonuclear molecules in contrast to IR analysis which requires the presence of a dipole moment. To record the Raman spectrum the sample is illuminated with a monochromatic laser which interacts with the molecular vibrations. A large portion of the scattered light will have the same frequency as the incident radiation. This is called elastic scattering or Rayleigh scattering. Only a small fraction of the scattered radiation has a frequency different from the frequency of the incident radiation. When the scattered photon possesses less energy than the incident photon, this is called a Stokes shifted Raman band. When it possesses more energy it is called an anti-Stokes shifted Raman band. The scattered radiation is usually measured perpendicular to the incident radiation. The intensity of the Raman scattered radiation is given as a function of its energy difference from the incident radiation in cm^{-1} . This results in a spectrum which is independent from the instrumental properties.

2.4 Rolling-ball viscometry

Rolling-ball viscometry was used to determine the viscosity of the $[P_{44410}][Br]$ and $[P_{44410}][Br_3]$ ionic liquids. Both measurements were performed on an Anton-Paar Lovis 2000 ME viscometer.

A rolling-ball viscometer determines the viscosity of a liquid by measuring the time it takes a gold coated steel ball to roll through a tilted capillary filled with sample fluid. Varying the inclination angle allows for adjusting the driving force. When high viscosities are expected, relatively large inclination angles (e.g. 70°) are used to limit the length of the measurement. However, the inclination angle cannot be too large as this would result in a turbulent flow regime and an inaccurate measurement. Additionally, the diameter of the capillary is usually increased to e.g. 2.5 mm when measuring viscous liquids. The dynamic viscosity, expressed in cP, can be calculated according to Equation (21).⁶⁹

$$\eta = K(\rho_0 - \rho_s)t \quad (21)$$

With η the dynamic viscosity, K a calibration constant which is specific for each capillary, ρ_0 and ρ_s the densities of the ball and sample fluid respectively and t the rolling time.

2.5 Total reflection X-ray fluorescence (TXRF)

TXRF was used to determine the metal content of ionic liquid and aqueous phases. The measurements were performed on a Bruker S2 Picofox TXRF, operating with a molybdenum X-ray source at 50 kV.

X-ray fluorescence (XRF) is based on the effect that when a sample is irradiated with primary X-rays of sufficient energy, inner electrons of atoms can be ejected.⁷⁰ The atom with the vacancy is in an instable state and will try to regain its stable ground state. A possibility is that an outer electron fills this vacancy. On doing so, the electron must lose some of its energy which is emitted in the form of a secondary X-ray photon. Since the energy states of atomic electrons are quantized, the X-ray photons emitted have energies which are equal for all atoms of the same element. Consequently, these photons cause discrete sharp line in the spectrum which can be used to identify elements in the sample. A differentiation is made between K, L and M lines in the spectrum depending on whether a vacancy is filled in the K, L or M shell. The signals are then further classified on the basis of intensity. The most intense peak is denoted with α , the next less intense peaks are called β , γ , η and ι . The intensity of the characteristic radiation is related to the amount of the element present. Because the signal depends heavily on matrix, the addition of an internal standard is needed for a quantitative analysis.

In contrast to XRF, where the primary beam strikes the samples at an angle of about 40°, TXRF uses a glancing angle of less than 0.1°. Figure 10 compares the instrumental arrangement of conventional XRF (a) with that of TXRF (b). It is the high reflectivity of the

sample support at these small angles that eliminates nearly all the spectral background off the support. This makes that TXRF can be used for micro- and trace analysis.

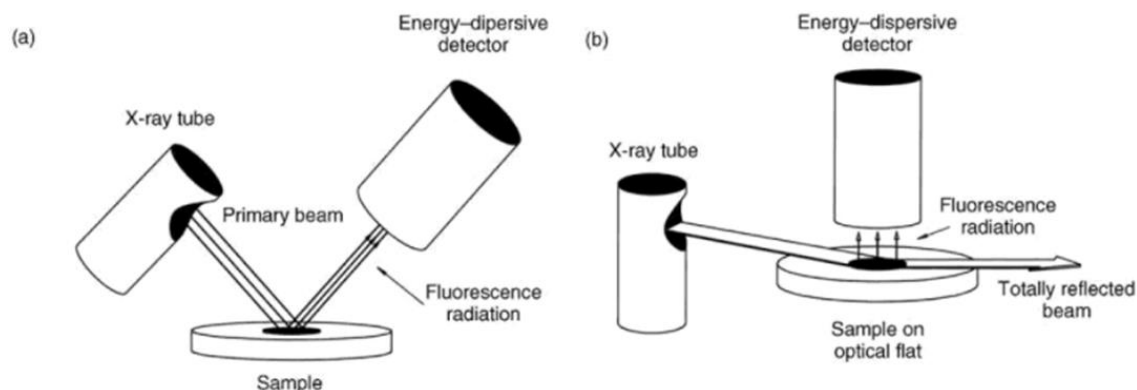


Figure 10: Instrumental arrangement conventional XRF (a) and TXRF (b).⁷⁰

The Bruker S2 Picofox TXRF produces the primary X-ray beam using an X-ray tube.⁷¹ Here, electrons are generated by a heated tungsten cathode and accelerated by a voltage difference between 20 and 60 kV towards a metal (Rh, Mo or Cr) anode. This results in the production of a continuous X-ray spectrum and a characteristic spectrum dependent on the anode material. In total, less than 1% of the supplied energy is transformed into X-rays, the rest produces heat. Using a monochromator, most of the continuum is filtered and the sample is irradiated with only the characteristic spectrum of the anode. The secondary X-rays are detected using a silicon-drift detector. When an X-ray hits the detector it is transferred into a certain charge, which is conducted to the electrode by means of an electric field and causes a charge burst. This charge burst is amplified and converted in a voltage pulse whose intensity is proportional to the energy of the X-ray. The voltage pulses are digitalized and saved through a multi-channel analyser. The spectrum can then be produced by showing the number of detected X-rays per energy interval or channel.

2.6 Inductively coupled plasma – optical emission spectrometer (ICP-OES)

ICP-OES analysis was used to determine the metal content of ionic liquid and aqueous phases. All measurements were performed on a Perkin Elmer Optima 8300 instrument.

The ICP-OES technique can be used for the determination of a large number of elements with detection limits in the ppb range.⁷² A major advantage of this technique is that many elements can be determined in the same analytical run. This arises from the fact that all emission signals are emitted from the plasma simultaneously.

An ICP-torch is constructed out of three concentric tubes of quartz and a copper coil, which is connected to a radio frequency (RF) generator, surrounds the top end of the torch. With an alternating current moving through the coil, an intense electromagnetic field is created at the top of the torch. With argon gas being swirled through the outer tube of the torch, a spark is applied to the gas causing some electrons to be stripped from their argon atoms. These electrons are then accelerated by the electromagnetic field. These high-energy electrons in turn collide with other argon atoms, stripping them of their electrons. A chain reaction is set off which forms what is known as an inductively coupled plasma (ICP). The gas temperature in the centre is about 6800 K. This high temperature improves the excitation and ionization efficiencies and reduces many of the chemical interferences found in flames or furnaces.

A peristaltic pump delivers the sample solution to the nebulizer where it is changed into an aerosol. The samples are then introduced into the plasma through the inner quartz tube. The plasma first removes the solvent (desolvation), leaving the sample as microscopic salt particles. These salt particles are then decomposed into individual molecules (vaporization) and atoms (atomization). The plasma is then able to excite and/or ionize the atoms. This whole process is depicted in Figure 11.

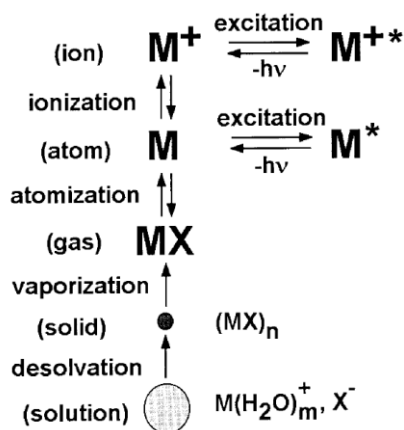


Figure 11: Visualisation of process that takes place when a sample droplet is introduced into the plasma.⁷²

Every element has its own characteristic set of energy levels and its own unique set of emission wavelengths. The light emitted by the excited atoms and ions in the plasma can be used to obtain information about the elements present in the sample. Detection of the emission light can be either axially or radially with respect to the plasma. The axial view results in a longer path length which improves sensitivity. Along with this enhancement, there are also increased spectral interferences and matrix effects. For the detection of the emitted light, the Perkin Elmer Optima 8300 instrument combines an echelle polychromator with a two-dimensional CCD array solid-state detector.⁷³

ICP-OES analysis can be used to extract both qualitative and quantitative information about the elements present in the sample. Qualitative analysis is fairly straightforward, it involves identifying the presence of emission at wavelengths characteristic of the elements of interest. Quantitative information can be extracted using calibration plots which are constructed using solutions with a known concentration of the element of interest.

2.7 Microwave digestion

Microwave digestion was used to solubilize the ionic liquid phases prior to elemental analysis with ICP-OES. All digestions were performed in a Berghof Speedwave Xpert.

Microwave digestion is performed by exposing a sample to a strong acid in a closed vessel and raising the pressure and temperature through microwave irradiation. The main advantage of heating the sample through microwave irradiation over other heating techniques is that the energy is directly delivered to the sample, this avoids the lag time of heating the container. The advantage of using a closed vessel in comparison with open digestions lies in the significantly higher working temperatures which can be achieved. This in turn has a drastic effect on the reaction kinetics, shortening the digestion time. Other advantages of the closed system include reduced acid consumption and no loss of volatile elements.⁷⁴

Naturally, the selection of the specific reagents depends on the sample to be digested. Organic samples are generally decomposed to carbon dioxide with the aid of oxidizing acids (mostly HNO₃). For inorganic samples the employed range of reagents or reagent mixtures is much broader. Here, acid mixtures of hydrochloric and/or hydrofluoric acid are often used. The solubility of the resulting salts must also be considered so that the solutions remain stable for a sufficiently long period.

The employed vessels must be transparent for microwaves and resistant to high temperature and the used reagents. Teflon and quartz are mainly used.⁷⁴ In the Berghof Speedwave Xpert, the temperature and pressure of the sample within the vessels can be monitored directly and without delay throughout the digestion.⁷⁵ The temperature measurement is based on the detection of the temperature dependent infrared (IR) radiation emission of the sample. To improve the accuracy, the radiation must be measured in a frequency range where the vessel material is transparent and the radiation emitted by the vessel itself must be filtered out. As a safety feature, the surface temperature of the vessels is also measured using a second IR sensor. The pressure measurement is performed by monitoring the colour change of polarized light send through a glass ring integrated in the vessel lid. The internal pressure is transferred to this glass ring and causes a change in the photo elastic behaviour.

3 Health, Safety and Environment

Prior to any activity in the lab, the hazards of the used products and the potential risks associated with the performed reactions were evaluated. All risk assessments are collected on the KU Leuven groupware platform. In the case of a new experiment, new risk assessments were added to the platform. Overnight experiments required the registration of an additional document which contains all information about experiment termination and safety. These documents are displayed at the entrance of the lab and at the fume hood.

All experimental procedures were performed according to the *Code of Good Practice for safety in the lab*.⁷⁶ The standard personal protection equipment such as gloves, safety goggles and a lab coat were worn at all times during the experiments. All experimental details and observations were recorded in the lab notebook. Depending on the reagents used additional precautions were taken such as working in the fume hood or wearing face protection. For example, the synthesis of the $[P_{44410}][Br]$ ionic liquid required the use of tributylphosphine. This product is classified as E4+ and is flammable when in contact with oxygen and water. The reaction was therefore carried out in an inert atmosphere. In addition, the conversion of this ionic liquid to its tribromide equivalent $[P_{44410}][Br_3]$ required the use of molecular bromine, another E4+ reagent. This is a volatile liquid that gives off suffocating fumes and is corrosive to the skin. Before use, the bromine was cooled using dry ice to reduce its vapour pressure. Next, the bromine was handled with gloves in the fume hood. In case of a spillage, a saturated $NaHSO_3$ solution was present to allow for immediate neutralisation.

The measurement of metal concentrations using TXRF holds a potential risk because of ionizing radiation which may cause DNA damage and cancer. A certificate of the training '*Radiation Protection for open and sealed sources*' was acquired prior to working with this device. The microwave digestion of samples also holds a certain risk due to the use of concentrated acids at elevated temperatures and pressures. The digestion vessels were thus left to cool down for a sufficiently long period before opening.

All chemical wastes were collected in the appropriate waste containers. For example, digested ionic liquids were disposed of in the container for oxidants because of the nitric acid content.

4 Materials and methods

4.1 Materials

Tetrabutylphosphonium bromide (> 95%), tetraoctylphosphonium bromide (> 95%), 1-butyl-3-methylimidazolium bromide (99%), 1-ethyl-3-methylimidazolium bromide (99%) and 1-ethyl-2,3-dimethylimidazolium bromide (99%) were purchased from Iolitec (Heilbron, Germany). Methyltriphenylphosphonium bromide (98%), hexadecyltrimethylammonium bromide (> 99%) and di-(2-ethylhexyl)phosphoric acid (D2EHPA, 95%) were purchased from Acros Organics (Geel, Belgium). Cyphos[®] IL 101 (triethyl(tetradecyl)phosphonium chloride, 97%), Cyphos[®] IL 102 (triethyl(tetradecyl)phosphonium bromide, 97%) and Cyanex 923 were purchased from Cytec Industries (Niagara Falls, Canada). 2-Ethylhexylphosphoric acid mono-2-ethylhexyl ester (PC-88a, > 95%) was purchased from Carbosynth (Compton, UK). Dodecane (> 99%) and deuterated chloroform (99.8 atom% D) which was used for the preparation of all NMR samples was purchased from Sigma Aldrich (Diegem, Belgium). Tri-*n*-butylphosphine (95% with Acroseal[®]), 1-bromodecane (98%), dry acetonitrile (99.9% with Acroseal[®]) and bromine (99.6%) were purchased from Acros Organics (Geel, Belgium). *N*-heptane (> 99%) was purchased from Chem-Lab nv (Zedelgem, Belgium). The semiconductor materials gallium nitride (99.99%), gallium arsenide (99.999%) and indium arsenide (99%) were all purchased from Alfa Aesar (Haverhill, US). Hydrogen bromide (48%) and sodium sulphite (> 98%) were purchased from Sigma Aldrich (Diegem, Belgium). Trisodium citrate (99.5%), sodium chloride (99.53%), sodium hydroxide (99.25%) and toluene (> 99.5%) were purchased from Fisher Scientific (Geel, Belgium). Sodium sulphate (> 99%) and calcium chloride (> 99.5%) were purchased from Chem-Lab nv (Zedelgem, Belgium). Ammonium sulphate (99.8%) was bought from VWR Chemicals (Oud-Heverlee, Belgium). 1-Butyl-3-methylimidazolium hydrogensulphate (99%) was purchased from Iolitec (Heilbron, Germany). Sodium hydrogensulphate (95%) and potassium hydrogensulphate (> 98%) were acquired from Honeywell (Diegem, Belgium). Sodium bromide (> 99%) was purchased from Acros Organics (Geel, Belgium). Ethanol (> 99.5%) was purchased from Fisher Scientific (Geel, Belgium). Triton X-100 was purchased from Merck (Overijse, Belgium). Nitric acid (65%) as well as the 1000 ppm standard solutions of arsenic, gallium, indium, scandium and copper with 2-5% HNO₃ matrix were purchased from Chem-Lab nv (Zedelgem, Belgium). The 1000 ppm standard solution of platina with 2-5% HNO₃ matrix was bought from Sigma Aldrich (Diegem, Belgium). The silicone solution in isopropanol was acquired from SERVA Electrophoresis GmbH (Heidelberg, Germany). All MilliQ water was obtained through a Merck Millipore system (Overijse, Belgium). All chemicals were used as received without any further purification.

4.2 Synthesis of ionic liquids

4.2.1 Tributyldecylphosphonium bromide [P₄₄₄₁₀][Br]

[P₄₄₄₁₀][Br] was synthesized by the quaternization of tri-*n*-butylphosphine (250 mmol, 61.68 mL) with 1-bromodecane (1.1 eq., 275 mmol, 57.09 mL) as presented in Figure 12. The reaction is an S_N2-type nucleophilic addition of tri-*n*-butylphosphine to 1-bromodecane.⁷⁷

The reaction was performed in a three-way flask with a cap, septum and a reflux condenser. The glassware was dried in an oven at 110 °C. The system was subsequently purged with N₂ for 2 minutes and a N₂-atmosphere was ensured with a N₂-balloon. The reaction was performed under inert atmosphere to prevent the formation of a phosphine oxide and consequently a reduced yield. First dry acetonitrile and 1-bromodecane were added through the septum. The tri-*n*-butylphosphine was then added dropwise. This way the reaction of tri-*n*-butylphosphine with remaining traces of water and oxygen was minimized as it could immediately react with an excess of 1-bromodecane in dry acetonitrile.

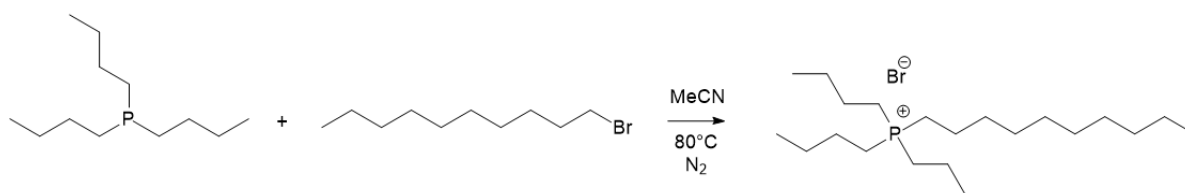


Figure 12: Quaternization of tri-*n*-butylphosphine with 1-bromodecane.

The mixture was stirred for 24 h at 80 °C and allowed to cool to RT. It was washed at least 4 times with *n*-heptane to remove the excess 1-bromodecane and the tri-*n*-butylphosphine oxide impurities. This was checked via ¹H and ³¹P NMR analysis. The acetonitrile was removed using a rotary evaporator and the remaining traces of water or acetonitrile were removed on a Schlenk line.

4.2.2 Tribromide ionic liquids

[P₄₄₄₁₀][Br₃] and [EMIM][Br₃] were prepared from their monobromide precursors by the addition of molecular bromine according to the reaction presented in Equation (22). The reagents were added together in a 1:1 molar ratio.



The dried monobromide ionic liquid was added to a roundbottom flask and Br₂ was added secondly. The advantage of adding the IL first is that the bromine is heavier and sinks to the bottom of the flask and no vapour is able to escape, allowing for a more precise addition of

bromine. The bromine was cooled beforehand using dry ice in order to reduce the vapour pressure. The addition of bromine was performed in a fume hood because of its volatile and corrosive nature. The roundbottom flask was covered with aluminium foil to prevent the homolytic cleaving of the bromine bond under the influence of light, the mixture was stirred for approximately 2 h at 200 rpm.

4.3 Oxidative dissolution of semiconductor materials

All oxidative dissolution experiments were performed in 20 mL glass vials. The semiconductor materials (GaN, GaAs and InAs) were mixed with the tribromide IL in a 1:10 molar ratio. The vials were fitted in an aluminium block to allow for efficient heating and an homogeneous temperature profile. Aluminium foil was then used to cover the vials and prevent homolytic cleaving of the bromine bond. The mixtures were heated to 60 °C and magnetically stirred at 200 rpm until the metals were completely dissolved.

4.4 Measuring metal concentrations

4.4.1 Total reflection X-ray fluorescence (TXRF)

Measuring IL phases

A certain amount of the $[P_{44410}][Br_3]$:metal mixture was weighed and diluted with ethanol to a concentration of 1.25 mg/mL.

A 100 μ L sample of a 1000 ppm solution of the standard element was brought in a 1.5 mL Eppendorf tube. Scandium was selected as the internal standard for the measurement of indium. Copper was chosen for measuring gallium and arsenic. These internal standards were used for all TXRF measurements. The internal standards were chosen based on their X-ray fluorescence energy, which is preferable as close as possible to the energy of the element of interest.⁷⁸ Next 800 μ L of the $[P_{44410}][Br_3]$:metal solution in ethanol was added. Finally, 100 μ L of MilliQ water was added. The solutions had a final IL concentration of 1 mg/mL and a 2:8 volume ratio of water:ethanol.

A 30 μ L sample of SERVA silicone solution in isopropanol was disposed on a quartz sample carrier. The carrier was then dried for 30 min at 60 °C. Next 1 μ L of the solution was disposed on the carrier. This was then dried again at 60 °C for 30 min. All samples were then measured for 300 s on the TXRF instrument. Of each solution two carriers were prepared.

The construction of calibration curves gives the opportunity to address the matrix effects caused by the high bromide concentration of the tribromide ionic liquid. These matrix effects can be quite significantly alter the measured metal concentrations. A plot of the average

measured concentration versus the actual concentrations allows for a recalculation of any results.

All calibration solutions for the TXRF instruments were prepared using the following method. 25 mg of $[P_{44410}][Br_3]$ was dissolved in 20 mL of ethanol. A 800 μ L sample of this solution was brought in a 1.5 mL Eppendorf tube. A 100 μ L sample of a 1000 ppm internal standard solution was added. Lastly 5, 20 or 100 μ L of a 1000 ppm solution of In, Ga or As was added. MilliQ water was added to obtain a total volume of 1 mL. All calibration solutions had an IL concentration of 1 mg/mL and a 2:8 volume ratio of water:ethanol.

A 30 μ L sample of SERVA silicone solution in isopropanol was disposed on a quartz sample carrier. The carrier was then dried for 30 min at 60 °C. Next 1 μ L of a calibration solution was disposed on the carrier. This was then dried again at 60 °C for 30 min. All samples were then measured for 300 s on the TXRF instrument. Of each solution three carriers were prepared, except for the 100 ppm solutions of which four carriers were prepared.

The calibration curves for Ga, As and In are presented in Figure 13, Figure 14 and Figure 15 respectively. Linear regression with a fixed intercept at zero was used to fit the results for all three elements. The adjusted R^2 values are > 0.99, indicating a good fitting of the obtained results.

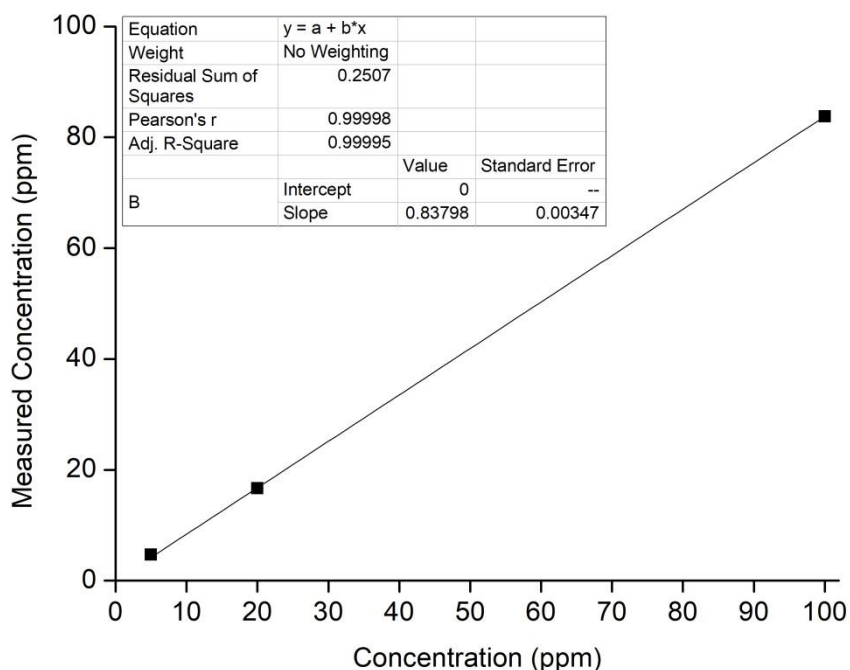


Figure 13: Calibration curve for Ga.

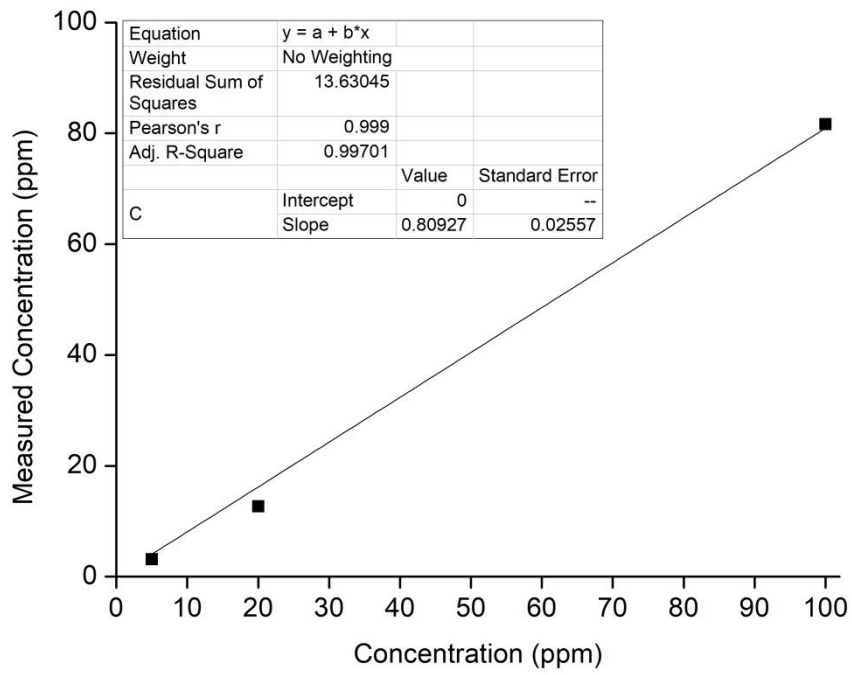


Figure 14: Calibration curve for As.

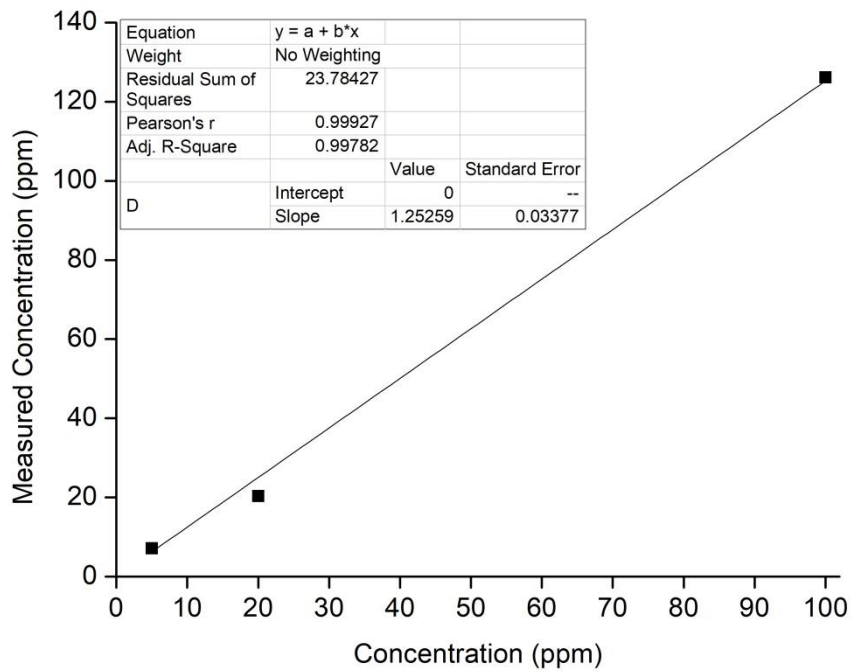


Figure 15: Calibration curve for In.

Measuring aqueous phases

A certain amount of the aqueous phase - varying between 20 and 100 μL depending on the salt concentration - was brought in a 1.5 mL vessel. For high salt concentrations only 20 μL of sample was used in order to prevent the formation of crystals on the sample carrier after drying. A 50 μL sample of a 1000 ppm solution of the standard element was then added. Next, 800 μL of a 5 vol% solution of Triton X-100 in water was added. Triton X-100 is a non-ionic surfactant which aids in the homogeneous drying of the sample droplet. Finally, MilliQ water was added to obtain a total volume of 1 mL.

A 30 μL sample of SERVA silicone solution in isopropanol was disposed on a quartz sample carrier. The carrier was then dried for 30 min at 60 $^{\circ}\text{C}$. Next 3 μL of the solution was disposed on the carrier. This was then dried again at 60 $^{\circ}\text{C}$ for 30 min. All samples were then measured for 300 s on the TXRF instrument. Of each solution two carriers were prepared.

4.4.2 Inductively coupled plasma – optical emission spectrometer (ICP-OES)

During the first part of this master thesis project, all metal concentrations were determined using TXRF measurements. It was however noticed that the measurements were not always accurate, reliable nor reproducible. It was suspected that the high bromide content of the IL was the issue for this inconsistency. ICP-OES analysis was therefore proposed as an alternative technique. Since most tribromide ILs are not soluble in water and direct measurement of the ionic liquid phase using ICP-OES is not possible, microwave digestion of the IL samples prior to ICP-OES analysis is necessary.

Method validation

To find out whether ICP-OES measurement after microwave digestion is an accurate and reliable method to determine metal concentrations, samples with a known metal content were digested and measured. Two leachates were chosen of which the first leachate had a lower metal loading than the second leachate. Of each leachate, two samples were digested. As a first trial 50 mg (ca. 40 μL) of the ionic liquid was digested in 7 mL of 65% HNO_3 using a digestion method which had proved to be ideal for ILs within the research group. The details of this digestion method are displayed in Table 2.

Table 2: Details of the digestion method for ILs.

Temperature ($^{\circ}\text{C}$)	Ramp (min)	Hold (min)
145	10	10
170	5	10
200	5	10
50	5	20

For each element (As, Ga and In) two wavelengths were analysed. Platinum was chosen as an internal standard for gallium and arsenic, scandium was the internal standard for indium. These internal standards for Ga, As and In were used for all ICP-OES measurements to determine the Ga, As and In concentration. Table 3 compares the results of these first tests to the actual metal concentrations.

Table 3: ICP-OES analysis after microwave digestion of two leachates with a known metal concentration. Measured metal concentration and deviation from actual concentration in % (small value).

Sample	As				Ga				In			
	188.979 nm		193.696 nm		417.206 nm		294.364 nm		230.60 nm		325.609 nm	
1	2758	1.8	867	-68	1296	5.8	1184	-3.4	2341	9.7	2214	3.7
1	2823	4.2	2305	-14.9	1350	10.2	1248	1.9	2256	5.7	2154	0.9
2	14737	-8.4	14922	-7.3	7797	4.1	7498	0.1	12435	0.8	12302	-0.3
2	16450	2.2	16569	2.9	8546	14.1	8222	9.8	13018	5.5	13575	10.1

These results show that ICP-OES analysis after microwave digestion is able to produce results which are both accurate and reproducible. For the measurement of arsenic 188.979 nm seemed to be the best line, gallium is best measured at 297.364 nm. For indium both lines seem to be equally good, yet 230.606 nm will be used for any further calculations.

Two additional digestions were performed, the first on pure $[P_{44410}][Br_3]$ and the second on pure $[P_{44410}][Br]$. These digestions were performed to determine the influence of the bromide content on the ICP-OES measurements, as this was suspected to be the issue with the inconsistent TXRF measurements. After digestion 5 ppm of arsenic, gallium and indium were added to the samples. Based on results in Table 4 the conclusion can be made that the additional bromine of the $[P_{44410}][Br_3]$ sample did not affect the measurements in any significant way when comparing its results with those of the $[P_{44410}][Br]$ sample.

Table 4: ICP-OES results of $[P_{44410}][Br_3]$ and $[P_{44410}][Br]$ after microwave digestion and addition of 5 ppm Ga, As and In.

Sample	As		Ga		In	
	188.979 nm	193.696 nm	417.206 nm	294.364 nm	230.606 nm	325.609 nm
$[P_{44410}][Br_3]$	5.285	5.296	5.417	5.116	5.328	5.364
$[P_{44410}][Br]$	5.431	5.001	5.35	4.878	5.452	5.107

A remark needs to be made on these first microwave digestions. In some digested samples a small droplet of ionic liquid was still present. Yet from the results in Table 3 it is clear that during the digestion all metals were stripped from the ionic liquid. However, to exclude any

future mistakes due to this incomplete digestion, new digestions will be performed with 10 mL of 65% HNO₃ and the method displayed in Table 5. This adjusted digestion method resulted in consequent and complete digestions.

Table 5: Details of adjusted digestion method.

Temperature (°C)	Ramp (min)	Hold (min)
150	10	10
180	5	10
230	5	10
50	5	20

Measuring samples

- IL phases

A 40 µL sample of IL:metal mixture was digested in 10 mL HNO₃ 65% using a Berghof Speedwave Xpert microwave digester. The digested sample was then diluted to 50 mL with a 2% HNO₃ solution. 5 mL of this solution was added to a 15 mL centrifuge tube and further diluted to 10 mL with 2% HNO₃ leading to a total dilution factor of 2500. A 50 µL sample of a 1000 ppm Pt and a 1000 ppm Sc solution were added as internal standards.

A blank and three calibration solutions were prepared according to the same procedure using a metal-free IL. The calibration solutions contained 1, 5 and 10 ppm of Ga, As and In.

- Aqueous phases

When aqueous phases are measured, microwave digestion is not necessary. A 100 µL sample of the metal containing aqueous phase was first diluted to a volume of 2 mL using a 2% HNO₃ solution. Next, 80 µL of this solution was added to a 15 mL centrifuge tube and further diluted to 10 mL with 2% HNO₃ leading to a total dilution factor of 2500. A 50 µL sample of a 1000 ppm Pt and a 1000 ppm Sc solution were added as internal standards.

A blank and three calibration solutions were prepared according to the same procedure. The calibration solutions contained 1, 5 and 10 ppm of Ga, As and In.

4.5 Extraction/stripping of metals from ionic liquids

All extraction/stripping experiments were performed in 4 mL glass vials. The volume ratio of extraction/stripping solution to ionic liquid was set at 1 unless otherwise indicated. The samples were then shaken at 2000 rpm for 1 h at 60 °C. Afterwards the samples were centrifuged for 3 min at 4500 rpm to accelerate phase separation.

5 Results and discussion

The first part of this research project is aimed at determining a suitable ionic liquid that will be used for all subsequent leaching, solvent extraction and stripping experiments. This choice will mainly be based on the mutual solubility of the ionic liquid with other solvents. The mutual solubility with the solvent used in solvent extractions should be as low as possible in order to have an efficient recovery and separation of metals and to minimize the loss of ionic liquid to the second phase. Additionally, the oxidative dissolution of semiconductors will also be considered in this choice.

5.1 Solubility study

5.1.1 *N*-dodecane

N-dodecane was chosen as the diluent for all solvent extractions performed in this master thesis project. This choice was based on its resemblance to kerosene, a commonly used solvent in industrial solvent extraction processes. The following ten ionic liquids were readily available in the lab and were selected to test their mutual solubility with *n*-dodecane.

1. Trihexyl(tetradecyl)phosphonium chloride (Cyphos IL 101) ([P₆₆₆₁₄][Cl])
2. Trihexyl(tetradecyl)phosphonium bromide (Cyphos IL 102) ([P₆₆₆₁₄][Br])
3. Methyltriphenylphosphonium bromide ([PMePh₃][Br])
4. Tetrabutylphosphonium bromide ([P₄₄₄₄][Br])
5. Tetraoctylphosphonium bromide ([P₈₈₈₈][Br])
6. Tributyldecylphosphonium bromide ([P₄₄₄₁₀][Br])
7. Hexadecyltrimethylammonium bromide ([N₁₁₁₁₆][Br])
8. 1-butyl-3-methylimidazolium bromide ([BMIM][Br])
9. 1-ethyl-3-methylimidazolium bromide ([EMIM][Br])
10. 1-ethyl-2,3-dimethylimidazolium bromide ([EMMIM][Br])

Each ionic liquid (1.5 g) was mixed with *n*-dodecane (1.5 g, 2 mL) and shaken at 2000 rpm for 1 h at 60 °C. The elevated temperature was chosen to lower the viscosity of the system and allow for an efficient mixing of the phases. After shaking the mixtures were allowed to cool down to room temperature and were centrifuged at 5000 rpm for 3 minutes to accelerate the phase separation.

The mutual solubility was tested for monobromide (and one monochloride) ILs and not for the tribromide ILs which would be used during the oxidative dissolution. It is expected that the observed trend in mutual solubility with *n*-dodecane is the same for both mono- and

tribromides. The absolute values however will be different as the tribromide IL displays a lower polarity compared to the monobromide due to the lower charge density of the tribromide anion.

The weight percentages of the ionic liquids and *n*-dodecane in both phases were calculated using ¹H NMR analysis and are presented in Table 6. The dissolution of the tested ionic liquids in the *n*-dodecane phase is overall low. The solubilities of *n*-dodecane in the ionic liquid phases are considerably higher. The solubility of *n*-dodecane in Cyphos IL 101 is higher than in Cyphos IL 102. Based on the lower charge density of the bromide anion this would be suspected to be reserved. Both ILs are commercially available and contain a significant amount of impurities, what could have caused this observation. Additionally, the solubility of *n*-dodecane in Cyphos IL 101 and Cyphos IL 102 is relatively high compared with the other ILs. Both ILs will therefore not be used in further experiments. [P₄₄₄₁₀][Br] did not dissolve into the *n*-dodecane but the IL took up 5.7 wt% of *n*-dodecane. [EMIM][Br] contains 0.1 wt% of *n*-dodecane, it seems that this small amount of *n*-dodecane has made it a liquid at room temperature. No other initially solid IL became liquid because of a dissolution of *n*-dodecane.

Table 6: Distribution of ILs and *n*-dodecane over both phases.

Ionic Liquid	<i>n</i> -dodecane phase		IL phase	
	IL (wt%)	<i>n</i> -dodecane (wt%)	<i>n</i> -dodecane (wt%)	IL (wt%)
Cyphos IL 101	1.9	98.1	51.1	48.9
Cyphos IL 102	0.5	99.5	36.1	63.9
[PMePh ₃][Br]	< 0.1 ¹	> 99.9 ¹	n.a. ¹	n.a.
[P ₄₄₄₄][Br]	< 0.1	> 99.9	n.a.	n.a.
[P ₈₈₈₈][Br]	0.4	99.6	n.a.	n.a.
[P ₄₄₄₁₀][Br]	< 0.1	> 99.9	5.7	94.3
[N ₁₁₁₁₆][Br]	< 0.1	> 99.9	n.a.	n.a.
[BMIM][Br]	< 0.1	> 99.9	n.a.	n.a.
[EMIM][Br]	< 0.1	> 99.9	0.1	99.9
[EMMIM][Br]	< 0.1	> 99.9	n.a.	n.a.

¹ n.a. indicates that the IL was solid and that no ¹H NMR analysis was performed. < 0.1 and > 99.9 are indicated when no IL was observed in the ¹H NMR spectrum of the *n*-dodecane phase.

5.1.2 Influence of extractant

In most solvent extraction applications the distribution of metal ions over both phases is aided by extractants. The addition of extractants can however significantly influence the mutual solubility of ILs and *n*-dodecane. Because [P₄₄₄₁₀][Br] and [EMIM][Br] were both liquid when in contact with *n*-dodecane and showed low mutual solubilities with the latter, only these ILs were investigated further. The commonly used extractants PC-88a, D2EHPA and Cyanex 923 were all tested. Their structures are shown in Figure 16. These three extractants

have been used in the extraction and separation of indium from other elements.^{54,60,61} PC-88a and D2EHPA are cation exchangers while Cyanex 923 is a solvating extractant. A concentration of 9 wt% extractant in *n*-dodecane was used. The same mixing procedure as before was used.

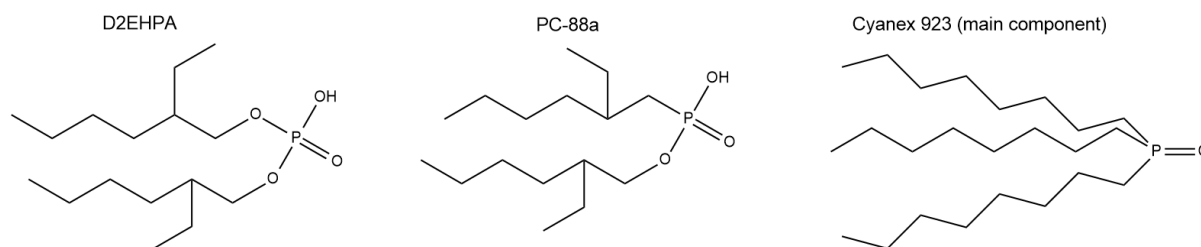


Figure 16: Structures of D2EHPA, PC-88a and Cyanex 923 (main component).

¹H NMR analysis proved insufficient to completely characterise both phases because of the overlapping signals of *n*-dodecane and the extractants. Additionally, ³¹P NMR analysis was used to determine the mutual solubilities. [PMePh₃][Br] was chosen as an internal standard. The distribution of *n*-dodecane, ionic liquid and extractant over both phases is displayed in Table 7. When comparing Table 6 with Table 7 it is clear that the addition of an extractant does not influence the solubility of the IL in the *n*-dodecane phase, it remains < 0.1 wt%. The addition of an extractant does however influence the solubility of *n*-dodecane in [P₄₄₄₁₀][Br]. The *n*-dodecane content rises from 5.7 wt% without extractant to > 10 wt% with extractant. In the case of [P₄₄₄₁₀][Br] the extractants are distributed over both phases with a preference for the IL phase. For [EMIM][Br] no significant changes are observed compared with Table 6.

Table 7: Distribution of *n*-dodecane, extractants and ionic liquids over both phases.

Ionic liquid	<i>n</i> -dodecane phase			IL phase		
	IL (wt%)	Extractant (wt%)	<i>n</i> -dodecane (wt%)	IL (wt%)	Extractant (wt%)	<i>n</i> -dodecane (wt%)
PC-88a						
[P ₄₄₄₁₀][Br]	< 0.1	2.5	97.5	83.6	5.5	10.9
[EMIM][Br]	< 0.1	9	91	> 99.8	< 0.1	< 0.1
D2EHPA						
[P ₄₄₄₁₀][Br]	< 0.1	0.6	99.4	80.1	7.8	12.1
[EMIM][Br]	< 0.1	10.6	89.4	> 99.8	< 0.1	< 0.1
Cyanex 923						
[P ₄₄₄₁₀][Br]	< 0.1	2	98	84.2	2.9	12.9
[EMIM][Br]	< 0.1	10.2	89.8	> 99.8	< 0.1	< 0.1

5.1.3 Water

Apart from extractions to an organic phase, the selective stripping of metals to an aqueous phase after oxidative dissolution of the solid material is also a possibility. The mutual solubility of [P₄₄₄₁₀][Br] and [EMIM][Br] with water was therefore investigated using a volumetric Karl Fischer titration device. Each ionic liquid (2 g) was mixed with 2 mL of demineralized water and shaken at 2000 rpm for 1 h at 60 °C. After shaking the mixtures were allowed to cool down to room temperature and were centrifuged at 5000 rpm for 3 minutes to accelerate the phase separation.

Only [P₄₄₄₁₀][Br] formed a phase separation with water. [EMIM][Br] inherently has a higher polarity compared to [P₄₄₄₁₀][Br] due to its shorter alkyl chains. The fact that only a single phase is formed means that this ionic liquid is not suitable to be used in a stripping step. Karl Fischer titration analysis determined that the saturation water content of the [P₄₄₄₁₀][Br] phase was 16.69 wt%. It is expected that its tribromide analogue will display a lower saturation water content because of the lower charge density of the anion. However, this cannot be confirmed as the tribromide ion interferes with the chemistry of the Karl Fischer device.

5.2 Synthesis of ionic liquids

The [P₄₄₄₁₀][Br] IL was synthesised in quantitative (> 99%) yield. The ¹H NMR spectrum of the synthesised IL is provided in Figure 17. It is a transparent, colourless and viscous liquid, left side Figure 18. The tribromide ILs [P₄₄₄₁₀][Br₃] and [EMIM][Br₃] are also shown in Figure 18. They have a dark yellow/brown colour compared to the colourless monobromide.

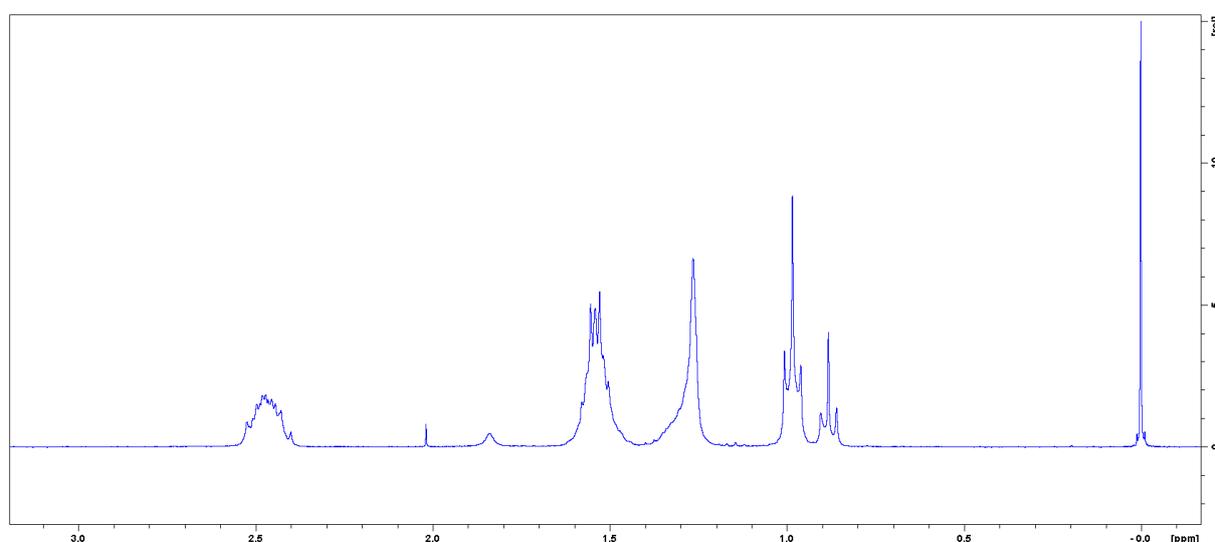


Figure 17: ¹H NMR of [P₄₄₄₁₀][Br] with small acetone (2.02) and water (1.83) impurity.

¹H NMR, 300 MHz, CDCl₃: 2.47 (m, 8H, CH₂-P), 1.54 (m, 16H, CH₂), 1.26 (m, 12H, CH₂), 0.98 (t, 9H, CH₃ (butyl)), 0.88 (t, 3H, CH₃ (decyl)).



Figure 18: Picture of synthesised $[P_{44410}][Br]$ (left), $[P_{44410}][Br_3]$ (middle) and $[EMIM][Br_3]$ (right).

The viscosity of the $[P_{44410}][Br_3]$ IL is remarkably lower than that of its bromide analogue which was confirmed experimentally. The dynamic viscosity of the monobromide is 2751.0 cP while that of the tribromide is 251.3 cP. This factor 10 difference finds its origin in the larger tribromide anion and the lower charge density of this anion, resulting in a smaller interaction with the $[P_{44410}]^+$ cation.⁷⁹ This decreased viscosity is an asset for the large scale application of tribromide ILs since high viscosities result in a slow mass transfer, slow reaction rates and stress on equipment. $[EMIM][Br_3]$ was found to be a solid with a melting point of about 49 °C.⁸⁰

In Figure 19 the Raman spectrum of $[P_{44410}][Br_3]$ is compared to that of $[P_{44410}][Br]$. The tribromide IL has two additional peaks compared to its bromide analogue. The first peak is situated around 160 cm^{-1} and arises from the symmetrical stretching vibration of the tribromide ion. The second peak, around 190 cm^{-1} , originates from the asymmetrical stretching vibration.⁸¹

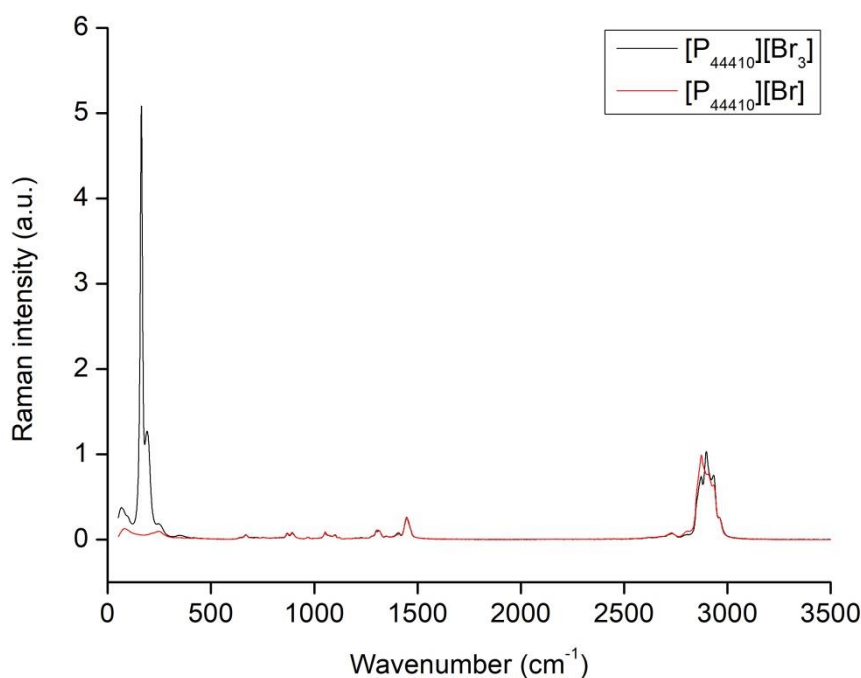


Figure 19: Raman spectra of $[P_{44410}][Br_3]$ and $[P_{44410}][Br]$.

5.3 Oxidative dissolution of semiconductor materials

GaAs, InAs and GaN, three commonly used semiconductor materials, were used in oxidative dissolution experiments with the tribromide ionic liquids $[P_{44410}][Br_3]$ and $[EMIM][Br_3]$.

In a first experiment, relatively large grains (\varnothing 2 mm) of GaAs and InAs were added to both tribromide ILs. It was visually confirmed that both materials were completely dissolved in $[P_{44410}][Br_3]$ after stirring for over 48 h at 60 °C. GaAs and InAs also dissolved slowly into $[EMIM][Br_3]$. Yet, after 48 h of stirring no complete dissolution was observed and the dissolution seemed to have stagnated. GaN did not seem to dissolve into the tribromide ILs. This observation can be explained by the fact that GaAs and InAs both are alloys while GaN identifies more as a salt. Thus, gallium is already in its oxidized state, making oxidative dissolution impossible. Additionally, the GaN crystal has a high bond energy ruling out dissolution by dissociation of the salt.⁵ Only molten KOH or NaOH at temperatures above 250 °C have been found to dissolve GaN at practical rates.⁸² In a second leaching experiment GaAs and InAs were grinded to a fine powder with a pestle and mortar prior to leaching. This grinding had a significant influence on the leaching time. Both GaAs and InAs were completely dissolved in $[P_{44410}][Br_3]$ after stirring for 24 h at 60 °C.

The fact that InAs and GaAs showed a slower and incomplete dissolution in $[EMIM][Br_3]$ compared to $[P_{44410}][Br_3]$ might be explained by the higher water content of $[EMIM][Br_3]$.

When preparing [EMIM][Br₃], the [EMIM][Br] was not completely solid (as it should with a melting point > 70 °C). [EMIM][Br] had most likely taken up water from the atmosphere. This water might have reacted with the tribromide ion and reduced the oxidative properties of the ionic liquid. The influence of water on the Br₃⁻ concentration was checked with Raman spectroscopy. 2 g of [P₄₄₄₁₀][Br₃] was mixed with an equal amount of demineralized water. The mixture was then shaken continuously for 72 h at 60 °C and 2000 rpm. Raman analysis was performed at different time intervals. The ratio of the intensity of the Br₃⁻ signal to the intensity of the P₄₄₄₁₀⁺ signal was plotted in function of time in Figure 20. Over a period of 72 h no decrease in Br₃⁻ was observed. Br₃⁻ does not react with water in a significant rate to explain the reduced oxidative dissolution in [EMIM][Br₃].

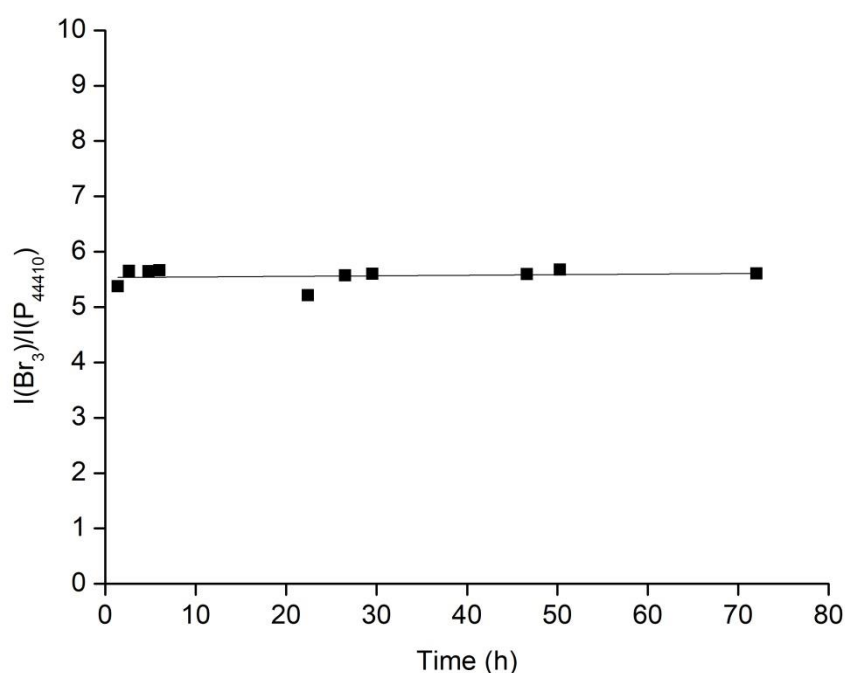


Figure 20: Ratio of the intensity of the Br₃⁻ signal to the intensity of the P₄₄₄₁₀⁺ signal plotted as a function of time.

Another possible explanation for the observation is the increased interaction between anion and cation for [EMIM][Br₃] compared to [P₄₄₄₁₀][Br₃]. Because of the fixed ring structure and relatively short alkyl chain lengths the [EMIM]⁺ cation is shielded less from the tribromide anion than the [P₄₄₄₁₀]⁺ with its longer and free alkyl chains. This increased interaction between both ions will result in a lower reactivity towards oxidative dissolution of the semiconductor materials.

5.3.1 Leaching kinetics

The kinetics of the oxidative dissolution of GaAs and InAs were investigated by performing dissolution experiments on both semiconductors. To be able to compare both experiments it is necessary that equal grain sizes are used. If not, the difference in surface area would dominate the results and no comparison can be made. To this extend both materials were grinded using a pestle and mortar and manually sieved using sieves of different pore sizes. The fraction between 63 and 125 μm was used for the dissolution experiments. The experiment was started at room temperature, however after 145 min it was decided to continue the experiment at 60 $^{\circ}\text{C}$. This decision was made after the observation that the dissolution was quite slow at room temperature. Both experiments were stirred at 300 rpm. Samples were taken regularly from the IL and these were analysed using ICP-OES after microwave digestion. The resulting plots are shown in Figure 21.

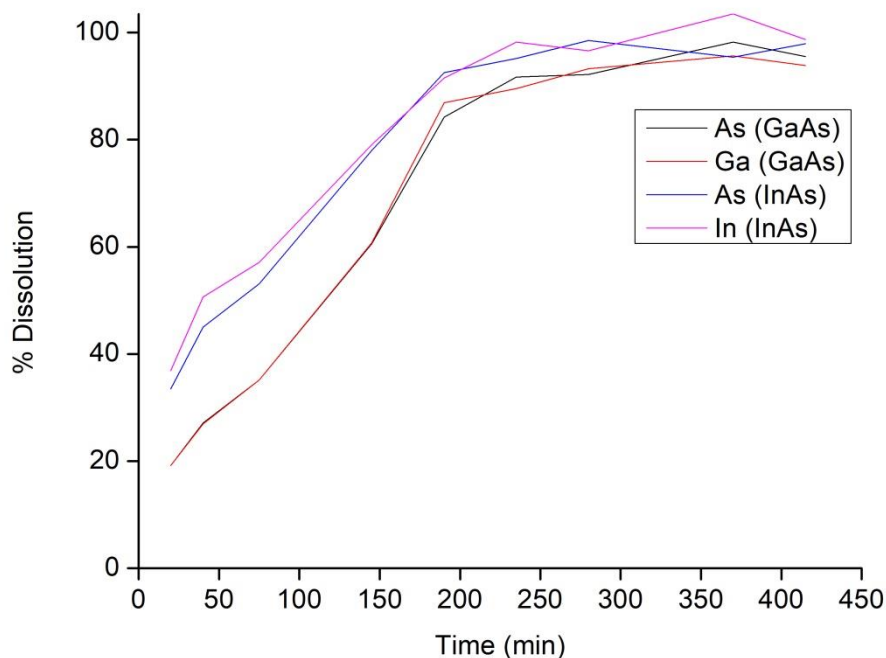


Figure 21: Dissolution of GaAs and InAs in function of time.

It seems that both semiconductor materials started dissolving quite quickly as after 20 min ca. 20% of GaAs and 35% of InAs has dissolved. However the data points of the first hour should not be taken too much into consideration because of the presence of small metallic particles in the samples which were taken, a problem that did not exist in the later samples. Nevertheless, during these first stages of the dissolution it is clear that InAs dissolves slightly faster than GaAs. This can be attributed to the decreased bond strength of InAs compared

with GaAs. The cohesive energy, a measure for the energy required to separate a solid into isolated atoms, of GaAs is 1.63 eV per bond while the value for InAs is 1.55 eV per bond.⁸³

After ca. 4 h both materials were dissolved for more than 90%. The final 10% of dissolution occurred a little slower because of the formation of aggregates which were stuck in the corner of the glass vials and limited the mixing. Overall it can be stated that the dissolution rates of GaAs and InAs are quite similar. This similarity can be related to a similar driving force behind the dissolution. The driving force behind a chemical reaction is usually expressed as the change in Gibbs free energy ΔG which can be related to the difference in standard reduction potential ΔE via Equation (24) with n the number of transferred electrons and F the Faraday constant.

$$\Delta G = -nF\Delta E \quad (23)$$

For gallium $\Delta E = 1.066 - (-0.53 \text{ V}) = 1.596 \text{ V}$ and for indium $\Delta E = 1.066 - (-0.34 \text{ V}) = 1.406 \text{ V}$. Based on the fact that ΔE is similar the overall dissolution rate can be expected to be similar as well. This reasoning is however entirely thermodynamic, kinetic effects are not taken into consideration.

Lastly, purely based on the standard reduction potentials of the metals (Ga (-0.53 V), In (-0.34 V) and As (+0.24 V)) one would expect that gallium and indium dissolve more quickly than arsenic because of a larger driving force for dissolution. From the graph can however be concluded that arsenic dissolves simultaneously with gallium and indium indicating that the metals are mixed on an atomic level.

5.4 Choice of ionic liquid

Several observations were taken into account when deciding which ionic liquid would be used in the following stages of this master thesis project.

The first element is the mutual solubility of the ionic liquid with other solvents. Based on the results presented in Table 7 one would prefer the use of [EMIM][Br] over [P₄₄₄₁₀][Br] because the former does not dissolve into *n*-dodecane (or vice versa) and the extractant remains entirely in the *n*-dodecane phase. However, later on it was noticed that [EMIM][Br] was not liquid at RT because of a limited dissolution of *n*-dodecane into the IL but because it was in an undercooled state. This undercooled state makes it unusable in an industrial setting because of the risk of solidification. In addition, [EMIM][Br] does not display any phase separation with water whereas [P₄₄₄₁₀][Br] does.

The second consideration is the oxidative dissolution of semiconductor materials such as GaAs, InAs and GaN. Both [EMIM][Br₃] and [P₄₄₄₁₀][Br₃] were unable to dissolve GaN. GaAs and InAs on the other hand dissolved in both ILs but the dissolution into [EMIM][Br₃] seemed to be slower and remained incomplete.

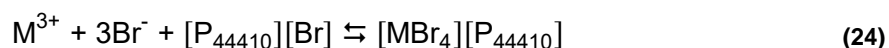
Finally, the melting temperature of the IL should preferably be below room temperature. This makes laboratory work easier as it avoids the need of constant heating when handling the IL. In addition, not needing to heat the IL throughout the leaching and solvent extraction process results in a lower energy input and a more environmentally friendly process overall. Based on the previously discussed arguments it was decided to only continue with [P₄₄₄₁₀][Br₃].

5.5 Extraction/stripping of metals from ionic liquids

After oxidative dissolution of semiconductor materials, different metals are present in the [P₄₄₄₁₀][Br₃] phase. The next step is the selective recovery of these metals from the ionic liquid so that this phase may be reused.

5.5.1 Initial experiments

There are two possibilities: stripping to an aqueous phase or extraction to an organic phase. Equation (24) presents the general equilibrium that is present when stripping/extracting trivalent metal ions from the [P₄₄₄₁₀][Br₃] phase. Initially the metal is present in the form on the right side of the equation. To strip/extract metals the equilibrium must be manipulated and shifted to the left.



There are several possibilities for stripping to an aqueous phase. A first possibility consist of stripping with an aqueous phase with very low Br⁻ concentration. Stripping with pure water might suffice since the reaction of water with Br₃⁻ is slow enough as previously proven. A second possibility is using a competitive reaction in the aqueous phase. The use of a highly concentrated HBr solution, might promote the formation of e.g. GaBr₄⁻, a strongly hydrated anion in the aqueous phase. Also the use of polydentate ligands (e.g. citrate ion) or strongly coordination anions (e.g. SO₄²⁻) can shift the equilibrium through the formation of a complex with the metal ion, lowering the free metal concentration.

When extracting to an organic phase using an extractant, one important thing needs be kept in mind. If there are any unsaturated c-c bonds present, a neutralization of Br₃⁻ needs to happen prior to the extraction to prevent a possible bromination of the double bonds. However, *n*-dodecane and all extractants used in this master thesis project do not contain double c-c bonds.

These first stripping/extraction experiments were all performed on separate $[P_{44410}][Br_3]:GaAs$ and $[P_{44410}][Br_3]:InAs$ leachates using an O:A ratio of 0.1. The initial GaAs leachate contained 15 g/L gallium and 16 g/L arsenic, the InAs leachate contained 25 g/L indium and 16 g/L arsenic. Before and after stripping/extraction the metal concentrations were measured using TXRF. Note that later on in this master thesis project the switch was made to ICP-OES for the determination of metal concentrations because of a poor reproducibility and accuracy of the TXRF measurements. These first results should not be considered as very accurate. However, they do show interesting patterns and observations. The stripping/extraction efficiencies are shown in Table 8.

Table 8: Stripping/extraction efficiencies (%) of gallium, arsenic and indium for the initial experiments.

Strip/extraction solution	Ga	As	In
MilliQ	86.1	98.6	4.6
3 M HBr	0.0	98.5	6.8
6 M HBr	0.0	30.9	9.2
8.8 M HBr	0.0	18.8	29.2
0.1 M trisodium citrate	91.3	99.0	94.1
0.5 M sodium sulphate	99.6	99.5	54.5
9 wt% Cyanex 923	49.0	34.9	57.7
9 wt% D2EHPA	0.0	0.0	30.5

These results show that stripping with a concentrated HBr solution suppressed the stripping of gallium, while also lowering the arsenic stripping compared to stripping with MilliQ water. The stripping of indium seemed to be positively influenced by the addition of HBr, yet no high efficiencies were attained. Both 0.1 M trisodium citrate and 0.5 M sodium sulphate proved to be very effective for the stripping of all three elements. Cyanex 923 seemed to be the more effective extractant for gallium and arsenic and D2EHPA seemed to selectively extract indium, be it with a lower efficiency.

5.5.2 Sulphate salts

Based on the results in Table 8 the use of Na_2SO_4 seemed promising. It gives access to high stripping efficiencies and sulphate salts are also among the cheapest salts available on an industrial scale. To find out whether a separation between gallium and arsenic can be achieved, stripping experiments with varying sulphate concentration were conducted on the $[P_{44410}][Br_3]:GaAs$ leachate. Apart from Na_2SO_4 , $(NH_4)_2SO_4$ was used because of its higher and less temperature dependent solubility in water. Also $[BMIM][HSO_4]$ was used because it is a sulphate containing IL. The previously used O:A ratio of 0.1 is usually too low for industrial applications and a more reasonable ratio of 1 was used. The O:A ratio is preferably as high as possible because this combines the advantages of high metal concentrations with

a low solvent or water consumption. TXRF analysis was used for the determination of the stripping efficiencies and separation factors which are displayed in Table 9. No significant trend is observable in the stripping efficiencies of both elements nor the separation factor between them. However, one conclusion can be made. The stripping of gallium is suppressed when the aqueous phase is smaller, i.e. when an O:A ratio of 1 rather than 0.1 is used, while the stripping of arsenic is not. When no water is present (when pure [BMIM][HSO₄]⁻ was used) the stripping of arsenic is drastically reduced. It seems that arsenic is preferentially stripped to the aqueous phase over gallium. The high affinity of arsenic for the aqueous phase can be explained by its speciation. Arsenic is most likely present in the aqueous phase in the form H_{3-x}AsO₄^{x-} (with H₂AsO₄⁻ being the most prevalent at a slightly acidic pH). These are strongly hydrated anions with two water molecules being bound to each oxygen.⁸⁴

Table 9: Stripping efficiencies and separation factors (α) of gallium and arsenic with varying sulphate concentration.

Strip solution	Stripping efficiency (%)		α (Ga/As)
	Ga	As	
0.0 M Na ₂ SO ₄	15.4	91.7	61
0.1 M Na ₂ SO ₄	8.2	90.0	101
0.2 M Na ₂ SO ₄	13.0	89.5	57
0.3 M Na ₂ SO ₄	16.2	90.9	52
0.4 M Na ₂ SO ₄	15.5	88.4	42
0.5 M Na ₂ SO ₄	15.2	91.1	57
1.0 M Na ₂ SO ₄	19.0	91.7	46
2.0 M (NH ₄) ₂ SO ₄	47.5	94.0	17
3.0 M (NH ₄) ₂ SO ₄	44.9	98.3	69
[BMIM][HSO ₄] ⁻	10.6	48.4	8
[BMIM][HSO ₄] ⁻ 50 wt% in water	2.5	93.5	554

The stripping of gallium remained very limited in both [BMIM][HSO₄]⁻ experiments. This suggests that the use of a HSO₄⁻ rather than a SO₄²⁻ salt might be able to lower the stripping efficiency of gallium resulting in a larger separation factor. This theory was tested by performing stripping experiments with varying NaHSO₄ concentrations. From this point onwards all experiments were performed on a mixed GaAs/InAs leachate containing 7.5 g/L gallium, 12.5 g/L indium and 16 g/L arsenic as this more realistically reflects a leachate of a heterogeneous batch of LED semiconductors. The O:A ratio was kept at 1. The aqueous phases were analysed with TXRF and the results are displayed in Table 10. The stripping of gallium does indeed lower with increasing HSO₄⁻ concentration but a slight decrease in the stripping of arsenic was also observed. The stripping of indium on the other hand increases quite strongly with the HSO₄⁻ concentration. The results indicate that the use of a 2 M

NaHSO₄ solution in a multi-step stripping process should be able to quantitatively remove the arsenic with limited loss of gallium.

Table 10: Stripping efficiencies and separation factors (α) of gallium, arsenic and indium with varying NaHSO₄ concentration.

NaHSO ₄ concentration (M)	Stripping efficiency (%)			α
	Ga	As	In	Ga/As
1	12.3	73.9	8.2	20
2	4.0	72.4	20.8	63
3	0.7	67.9	29.8	287

5.5.3 MilliQ water

The results in Table 8 showed that MilliQ water was quite effective at stripping both gallium and arsenic. It was also concluded that the stripping of arsenic to an aqueous phase is rather unaffected by the O:A ratio and that when small aqueous phases were used arsenic is stripped preferentially over gallium. This was further investigated by performing a series of stripping experiments using MilliQ water in different O:A ratios. TXRF analysis of the aqueous phase resulted in the stripping efficiencies and separation factors displayed in Table 11. The separation factor between gallium and arsenic increases significantly with the O:A ratio. These results suggest that the use of a multi-step stripping process with MilliQ water using an O:A ratio of 2 is able to quantitatively remove the arsenic with limited loss of gallium and indium.

Table 11: Stripping efficiencies and separation factors (α) with varying O:A ratio of MilliQ water stripping experiments.

O:A ratio	Stripping efficiency (%)			α
	Ga	As	In	Ga/As
0.5	98.2	98.0	9.7	1
1	38.3	85.1	3.7	9
2	2.7	55.7	2.0	45
4	0.0	20.2	10.3	1383

5.5.4 Multi-step strippings

The results in Table 10 and Table 11 indicate that through the use of a multi-step stripping procedure arsenic can be quantitatively stripped from the IL without a significant loss of gallium or indium. Two three-step experiments were performed in which the IL was contacted three times with a stripping solution. After each step, the stripping solution was separated from the IL and a portion of the IL was used for the subsequent step. For the first experiment MilliQ water was used and in the second experiment a 2 M NaHSO₄ solution. The O:A ratio was 2 for both experiments. ICP-OES analysis after microwave digestion of the IL phase was

used for the determination the stripping efficiencies. The cumulative stripping efficiencies of arsenic, gallium and indium throughout the three stripping steps are shown in Figure 22.

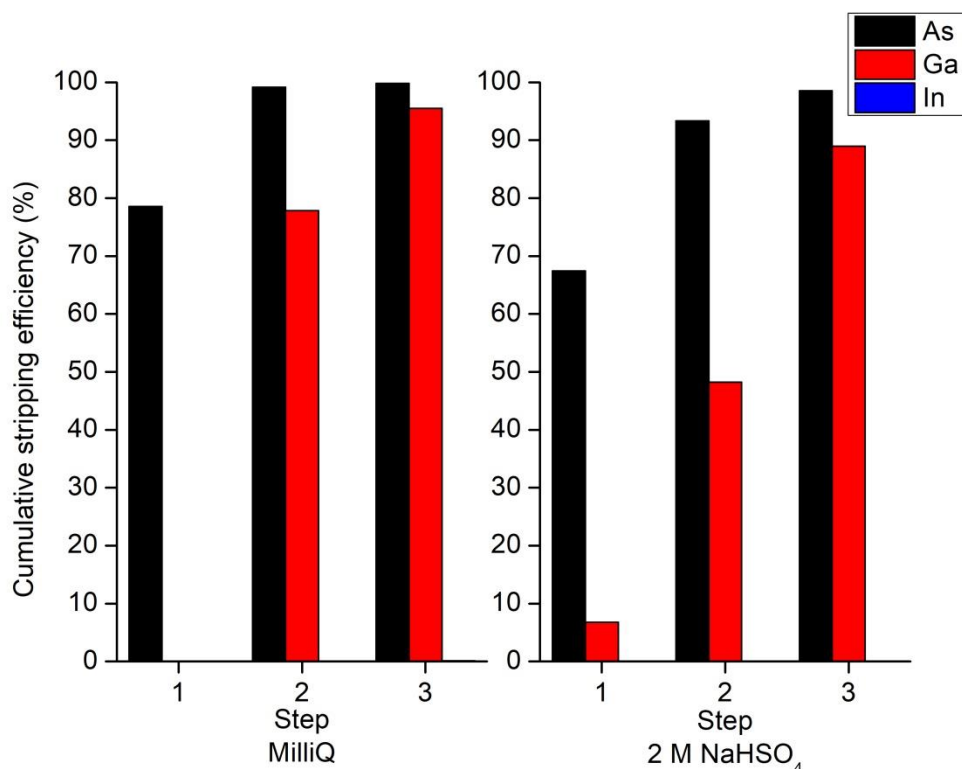


Figure 22: Cumulative stripping efficiencies of arsenic, gallium and indium in a three-step stripping experiment. Left: MilliQ water, O:A 2. Right: 2 M NaHSO₄, O:A 2.

Contrary to the results obtained by TXRF in Table 10 and Table 11, these first results obtained by ICP-OES analysis show that no indium is stripped. Repeating some of the initial stripping experiments of Table 8 it was shown that indium does not strip to any aqueous solution and that it has a high affinity for the ionic liquid phase. Indium will therefore no longer be included in the results of the succeeding experiments. The results on the left side of Figure 22 indicate that in the first step a large portion of the arsenic is stripped from the ionic liquid. In the second step, most of the gallium and the remaining arsenic is stripped. The last step raises the stripping efficiency of gallium to > 95%. The results on the right side of Figure 22 show that the stripping of both arsenic and gallium is lowered due to the presence of NaHSO₄ as is confirmed by Table 10.

With the aim of maximizing the stripping of arsenic in the first step while keeping the stripping of gallium minimal, some additional three-step experiments were performed with MilliQ water and NaHSO₄. For MilliQ, the O:A ratio was varied between 2 and 1.25. And for NaHSO₄, the concentration was varied between 0.5 and 2 M while the O:A ratio remained at 2. This time the aqueous phases were analysed with ICP-OES as this was less labour intensive. The gallium/arsenic separation factors of the first stripping step for both series of experiments are

given in Figure 23. The lower the O:A ratio, the more gallium is stripped and the lower the separation factor which confirms the TXRF results in Table 11. The stripping of arsenic was lowered with increasing NaHSO₄ concentration but the stripping of gallium was affected to a greater extent resulting in an increase of separation factor with NaHSO₄ concentration cfr. Table 10.

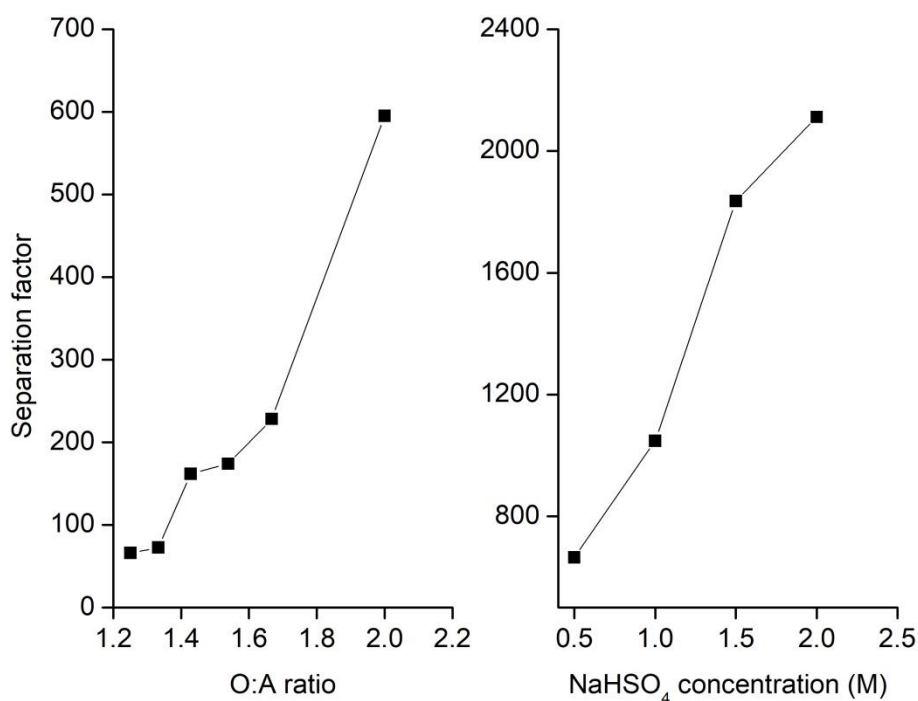


Figure 23: Separation factor (α) between gallium and arsenic in function of O:A ratio (left) and NaHSO₄ concentration (right).

The previous results show that through the manipulation of the O:A ratio and the NaHSO₄ concentration a high separation factor between gallium and arsenic can be attained. But how and why NaHSO₄ influenced the stripping equilibrium remained unknown. Was it the result of the Na⁺ or HSO₄⁻ ion or was it simply because the aqueous phase was already loaded with a salt? To find out, three step stripping experiments were performed with NaCl, KHSO₄ and CaCl₂. NaCl was chosen to test the effect of the Na⁺ ion. KHSO₄ was chosen to test the effect of the HSO₄⁻ ion. And CaCl₂ was chosen to determine whether the loading of the aqueous phase was the reason for the high separation factors. All experiments were performed with an O:A ratio of 2. The concentration of KHSO₄ and NaCl was 2 M while the concentration of CaCl₂ was 1.5 M. The cumulative stripping efficiencies are displayed in Figure 24.

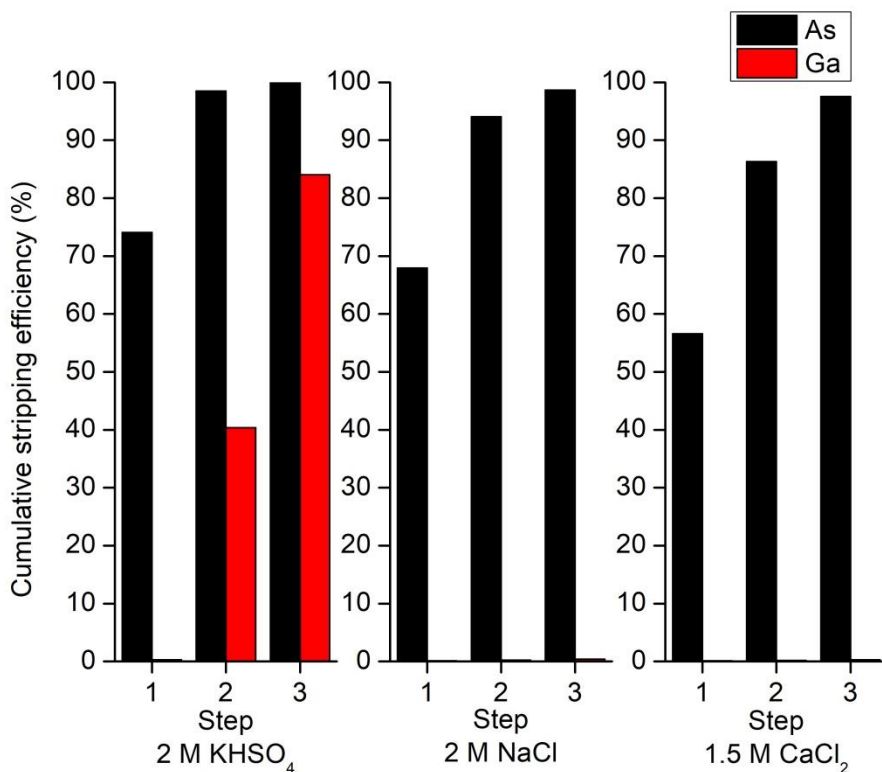


Figure 24: Cumulative stripping efficiencies of arsenic and gallium in a three-step stripping experiment. Left: 2 M KHSO₄, O:A 2. Middle: 2 M NaCl O:A 2. Right: 1.5 M CaCl₂ O:A 2.

The stripping efficiencies in Figure 24 show that the stripping of arsenic seems to be rather unaffected by the salt that is used. After three consecutive steps, nearly 100% of arsenic can be stripped from the IL. The stripping of gallium on the other hand is completely suppressed by the use of a chloride salt. This is remarkable as it is expected that, according to Equation (24), only bromide ions should influence the stripping equilibrium. The suppressing effect of bromide ions on the stripping of gallium was already shown in Table 8. However, these results were obtained by TXRF analysis, which since then had shown to be inconsistent. Some multi-step experiments were therefore performed using different concentrations of NaBr. Only two steps were performed as this would be sufficient to observe the differences between NaBr and NaCl. A higher NaBr concentration indeed resulted in a decreased gallium stripping, as would be expected from Equation (24). The stripping of arsenic was affected to a much lesser extent. In Table 12 the separation factors of the 2 M NaBr experiment are compared with the separation factors of the KHSO₄, NaCl and CaCl₂ experiments. The gallium/arsenic separation factor is considerably higher when using a chloride salt.

Table 12: Separation factors (α) between gallium and arsenic per stripping step of stripping experiments using KHSO_4 , NaCl , CaCl_2 and NaBr .

Strip solution	1	2	3
2 M KHSO_4	1062	23	/
2 M NaCl	1805	3258	2131
1.5 M CaCl_2	1296	2587	4396
2 M NaBr	588	35	/

5.5.5 Development of stripping procedure

Based on the preceding results, a stripping procedure can be proposed for the selective and consecutive stripping of arsenic and gallium from the IL. First, arsenic is selectively stripped from the IL using an aqueous solution of a chloride salt which is followed by the selective removal of gallium using MilliQ water. Throughout this entire process, indium remains in the IL phase. The proposed procedure was tested by performing a six step stripping experiment. First three stripping steps were performed with a 1.5 M CaCl_2 solution, which was followed by three stripping stages using MilliQ water. The O:A ratio was kept at 1. The cumulative stripping efficiencies are displayed in Figure 25.

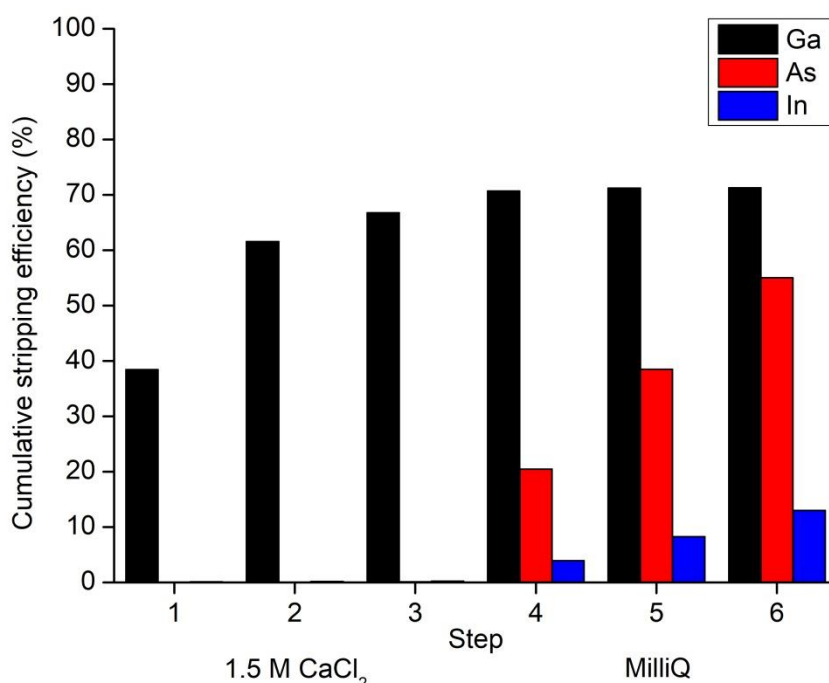


Figure 25: Cumulative stripping efficiencies in a six step stripping procedure O:A 1. Step 1-3: 1.5 M CaCl_2 . Step 4-6: MilliQ water.

As expected, only arsenic is stripped during the first three steps. However the cumulative stripping efficiency only reaches 67%, while values of at least 90% were expected. This can be explained by the slightly altered method of performing this multi-step stripping experiment.

In previous experiments a known fraction of the IL phase was taken and used in the subsequent step. In this experiment it was assumed that all steps were performed on the entire IL phase. However, this was not the case because of a small loss of IL that occurred by pipetting out the underlying aqueous phases. This loss was not taken into account in the calculation of the stripping efficiencies. This theory was tested by analysing some IL samples with microwave digestion and ICP-OES. Little to no arsenic was detected in these samples and the amount of remaining gallium was less than 1% after all six stripping steps. The reduced stripping efficiencies are thus indeed the result of a loss of IL during the stripping steps and should be rescaled to values close to 100%.

As was expected, gallium stripping occurs only after step three (however also with somewhat low efficiencies because of the loss IL). Some indium stripping was also observed after step 3. This might be explained by the fact that some IL seemed to have dissolved in the aqueous phase. This can be seen from the yellow colour, Figure 26, and was also confirmed by a comparative Raman analysis of the CaCl_2 and MilliQ phases in Figure 27. The spectra are compared with the spectrum of the pure IL in Figure 19 and the presence of a vibration around 2900 cm^{-1} confirms the dissolution of the IL into the aqueous phase. The shoulder which is present at 200 cm^{-1} might be attributed to the presence of the tribromide ion. Indium has a high affinity for the IL and would normally stay in the IL phase. However, due to dissolution of IL into the aqueous phase some indium can be measured. This dissolution of IL might be due to the conversion of tribromide IL to its chloride analogue whose solubility is expected to be higher due to a higher charge density of the anion. Considering the Hofmeister series this is not expected but a minimal conversion might still have occurred.

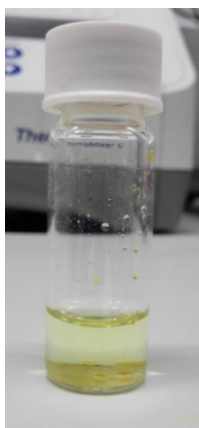


Figure 26: Picture of an aqueous phase of stripping step 4/5/6.

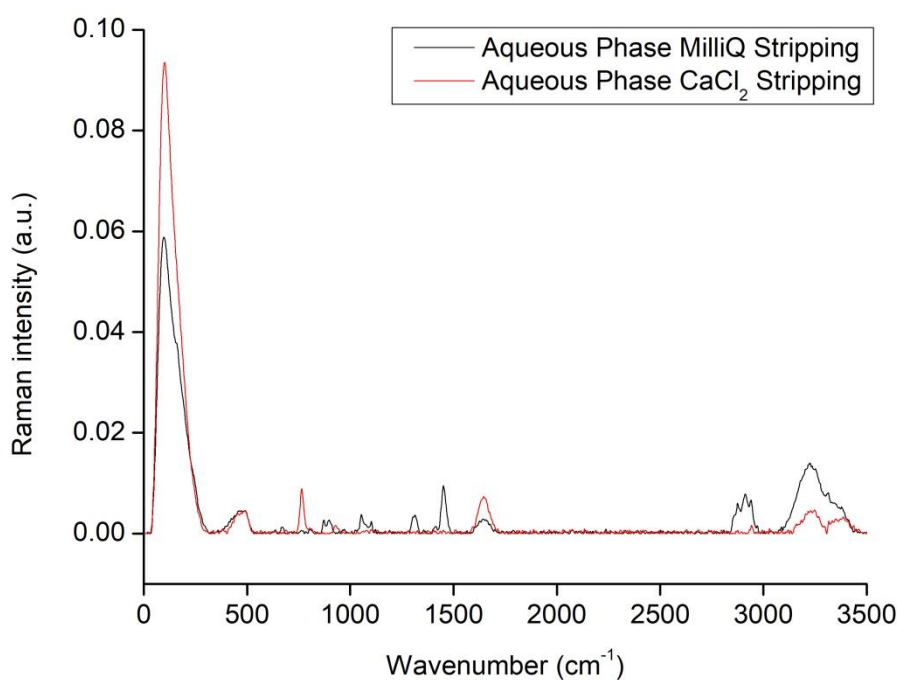


Figure 27: Raman spectra of the aqueous phases of the six step stripping experiment.

This dissolution of IL in the aqueous phase implies a small loss of the IL during each step. In a large scale application where the IL is recycled, this will result in a more significant loss over time. Two possible solutions were proposed to avoid this loss of IL. The first option is to use a salting out agent such as Na_2SO_4 during the last three stripping steps instead of stripping with MilliQ water. A second option is the use of a bromide salt in the first three stripping steps. Although this would result in lower separation factors, it would avoid the formation of the more soluble chloride IL. In a first experiment the first three stripping steps were performed using a 1.5 M CaCl_2 solution and the last three steps were performed with a 2 M Na_2SO_4 solution. In a second and third experiment, a 2 M NaBr solution was used for the first three steps. The last three steps of experiment 2 were performed with MilliQ water while those of experiment 3 were performed with a 2 M Na_2SO_4 solution. The non-cumulative stripping efficiencies of these three experiments are displayed in Figure 28. The use of Na_2SO_4 was able to prevent the yellow colour of the aqueous phases, indium was however still being stripped. The conclusion that chloride salts result in a higher separation factor between gallium and arsenic is also apparent here. When CaCl_2 is used no gallium is stripped in the first three steps while for NaBr there is some degree of gallium stripping. For all three experiments the first step resulted in a relatively pure arsenic fraction and the fourth step resulted in a relatively pure gallium fraction.

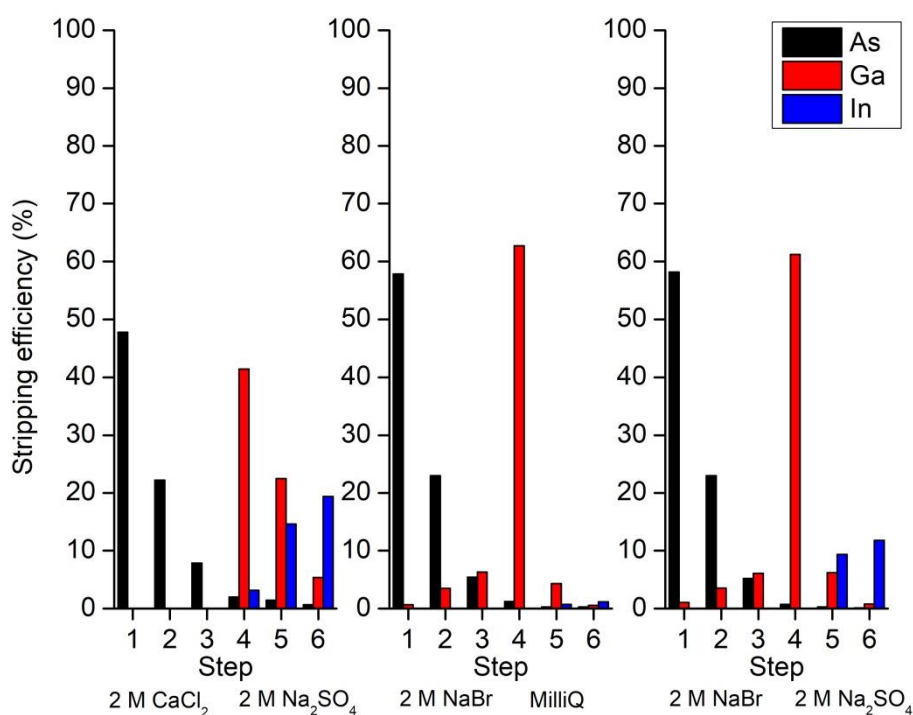


Figure 28: Stripping efficiencies in a six step stripping procedure. Left: step 1-3 1.5M CaCl₂, step 4-6 2M Na₂SO₄. Middle: step 1-3 2M NaBr, step 4-6 MilliQ. Right: step 1-3 2M NaBr, step 4-6 2M Na₂SO₄.

Figure 29 shows the IL phases after the entire procedures. After the NaBr – MilliQ procedure the IL is still clear while for the other experiments it is rather cloudy. Combined with the fact that almost no indium is being stripped and that relatively pure arsenic and gallium fractions can be obtained, the NaBr – MilliQ procedure is preferred.

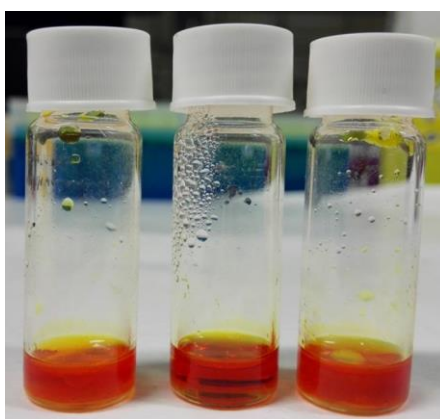


Figure 29: Appearance of IL phases after six a step stripping procedure. Left: step 1-3 1.5M CaCl₂, step 4-6 2M Na₂SO₄. Middle: step 1-3 2M NaBr, step 4-6 MilliQ. Right: step 1-3 2M NaBr, step 4-6 2M Na₂SO₄.

5.5.6 Optimization of the NaBr – MilliQ procedure

In the subsequent experiments, the NaBr concentration and the O:A ratio were optimized. For these experiments only 4 stripping steps were performed because of the minimal contribution of step 5 and 6 to the cumulative stripping efficiencies, Figure 28. NaBr was used in the first three steps and MilliQ water was used in the fourth step. The NaBr concentration was varied between 2 and 4 M and the O:A ratio was varied between 1 and 2. Note that also in these experiments the stripping efficiencies will not reach 100% because of a slight loss of IL. The magnitude of the error was however minimized by pipetting more carefully.

The stripping efficiencies of arsenic are displayed in Figure 30. A higher NaBr concentration and O:A ratio both lowered the stripping of arsenic during first step. These effects were however rectified during the second and third step. The stripping of arsenic is thus not effected by the NaBr concentration nor the O:A ratio when a multistep process is used.

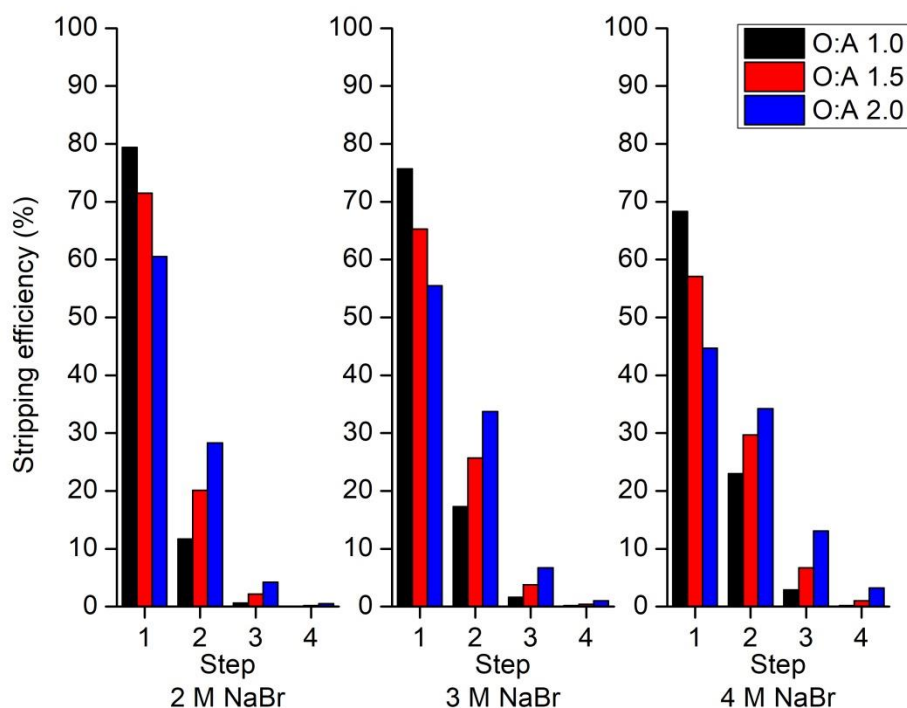


Figure 30: Stripping efficiencies of arsenic in a four step stripping procedure with varying O:A ratio. Left: Step 1-3 2 M NaBr, step 4 MilliQ. Middle: Step 1-3 3 M NaBr, step 4 MilliQ. Right: Step 1-3 4 M NaBr, step 4 MilliQ.

The stripping efficiencies of gallium are displayed in Figure 31. As expected, a higher NaBr concentration and a smaller aqueous phase result in a decreased gallium stripping during the first three stripping steps. For example, in the case of 4 M NaBr and an O:A ratio of 2, the separation factor between gallium and arsenic was 2419. Gallium is stripped quite

quantitatively using MilliQ water during the fourth step of the procedure, although the efficiency is negatively influenced by a higher O:A ratio. The stripping of indium was not included in the graphs but its cumulative stripping efficiency did not exceed 2%.

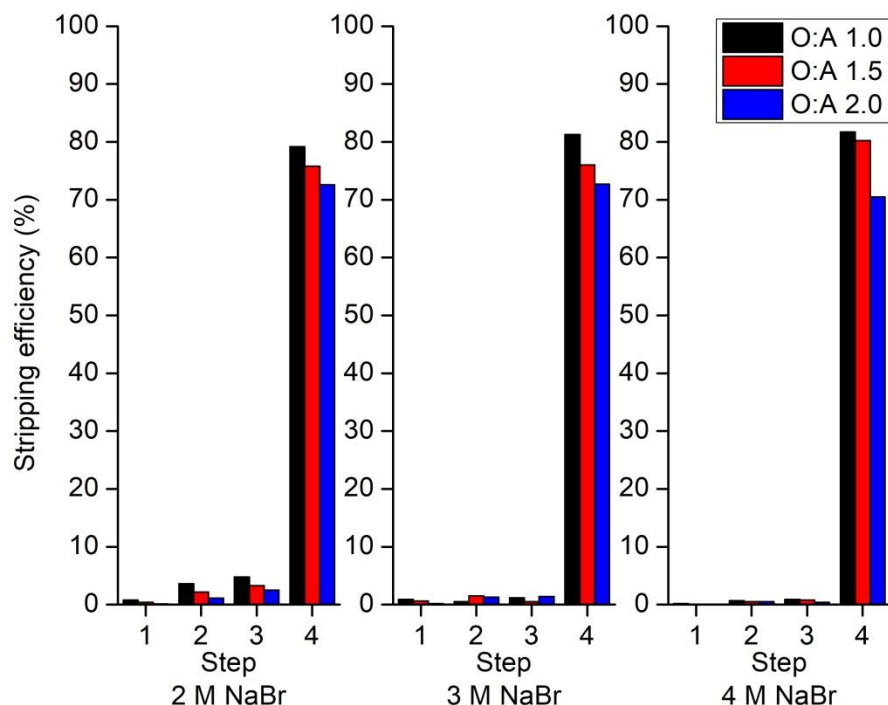


Figure 31: Stripping efficiencies of gallium in a four step stripping procedure with varying O:A ratio. Left: Step 1-3 2 M NaBr, step 4 MilliQ. Middle: Step 1-3 3 M NaBr, step 4 MilliQ. Right: Step 1-3 4 M NaBr, step 4 MilliQ.

To conclude, a solution of at least 4 M NaBr can be used to quantitatively and selectively strip arsenic from the ionic liquid in three steps. Here the O:A ratio should be at least be 2, to further limit the stripping of gallium. During these three stripping steps, gallium stripping remained below 1%. During a fourth step, gallium can be stripped quantitatively using MilliQ water. In this final step, the O:A ratio can be lowered to ensure a complete stripping of gallium.

5.5.7 Extraction/stripping of indium

The preceding paragraphs have all been dedicated to the selective stripping of gallium and arsenic from the $[P_{44410}][Br_3]$ IL phase. After the proposed stripping procedure using NaBr and MilliQ water, indium is still left in the IL. Previous experiments, e.g. Figure 22, showed that the stripping of indium to an aqueous phase was not a possibility because of its high affinity for the IL phase. However, extraction to an extractant containing organic phase remained a possibility. In the literature, the extractants Cyanex 923, D2EHPA and PC-88a have all been used for the selective extraction of indium from different media.^{54,60,61} These

three extractants were therefore used in extraction experiments on a mixed GaAs/InAs leachate. Of each extractant two different concentrations, 9 and 30 wt% in *n*-dodecane, were used. Metal concentrations were determined using ICP-OES analysis of the digested ionic liquid phase. The resulting extraction efficiencies are displayed in Figure 32.

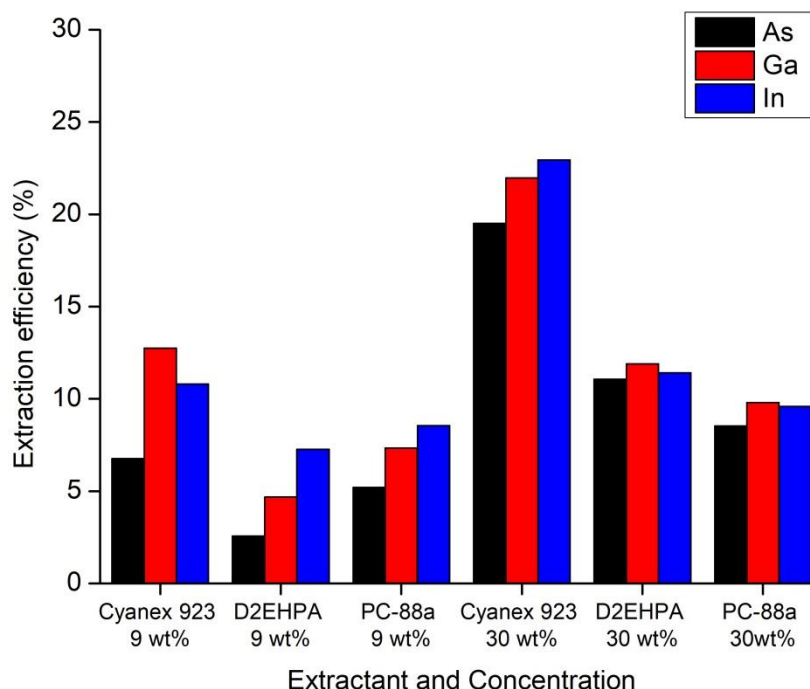
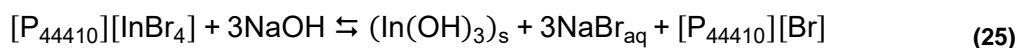


Figure 32: Extraction efficiencies of 9 and 30 wt% Cyanex 923, D2EHPA and PC88a in *n*-dodecane.

Although in Table 8 D2EHPA seemed to selectively extract indium, the results in Figure 32 indicate that none of the three extractants showed a particular selectivity for indium extraction from the $[P_{44410}][Br_3]$ phase. The extraction efficiencies are overall also quite low (< 25%). This can be explained by the fact that the majority of the extractant resides in the IL phase (cfr. Table 7) and will be unable to efficiently extract metals to the *n*-dodecane phase. It can also be concluded that a higher concentration of extractant results in slightly higher extraction efficiencies.

A second possibility for the removal of indium from the IL phase is the use of precipitation stripping.⁸⁵ Indium can be precipitated as an hydroxide using a dilute NaOH solution, Equation (25). The equilibrium can be manipulated through the pH, a higher pH will result in more indium being stripped. To perform this method, it must first be made sure that the IL is sufficiently stable in the alkaline environment. NMR analysis showed that $[P_{44410}][Br_3]$ was stable when in contact with a 1.3 M NaOH solution for the duration of the experiments.



Precipitation experiments with different equivalents of NaOH were performed on a 0.214 M indium metal leachate. O:A ratios smaller than 1 were also applied in order to avoid the use of too high NaOH concentrations which would result in the degradation of the IL through the formation of phosphine oxides. Unlike the other stripping experiments, the precipitation stripping was performed at room temperature to further avoid the decomposition of the IL. The concentrations of indium in the aqueous and IL phases were measured with ICP-OES to determine the amount of $In(OH)_3$ precipitation. All results are collected in Table 13.

Table 13: Indium precipitation efficiency (%) as a function of NaOH equivalents and O:A ratio.

Equivalents NaOH	O:A ratio	Used concentration NaOH (M)	Stripping efficiency (%)
3	1	0.64	59.9
4	1	0.86	65.4
5	1	1.07	87.6
	0.5	0.54	99.2
	0.25	0.27	99.8
6	1	1.28	99.5
	0.5	0.64	100.0
	0.25	0.32	99.8

With a solubility product of 10^{-33} in aqueous solutions it is expected that the addition of three equivalents NaOH should precipitate $In(OH)_3$ almost completely.⁸⁶ Nonetheless, at least five equivalents are necessary to quantitatively precipitate the indium. However, five equivalents of NaOH used in an O:A ratio of 1 are unable to strip all the indium while the same amount of NaOH used in an O:A ratio of 0.5 or 0.25 does strip practically all indium. Remarkably enough, the O:A ratio seems to effect the precipitation efficiency. A possible explanation for this might be found in the displacement of the produced NaBr. With an O:A ratio of 1 the aqueous phase is rather small and unable to dissolve all the NaBr hampering the total amount of indium precipitation.

5.5.8 Flowsheet for the selective stripping of arsenic, gallium and indium

Figure 33 summarizes the conclusions of the previous paragraphs in the form of a flowsheet for the recovery of arsenic, gallium and indium from a mixed GaAs/InAs $[P_{44410}][Br_3]$ leachate. First, arsenic can be selectively stripped using a 4 M NaBr solution with an O:A ratio of 2. Gallium can then be stripped using MilliQ water. For this the O:A ratio can be lowered to 1. Hereafter indium can be precipitated using at least 5 equivalents of NaOH in a sufficiently

large aqueous phase. Finally, the IL can be regenerated by bromination and reused in the leaching step.

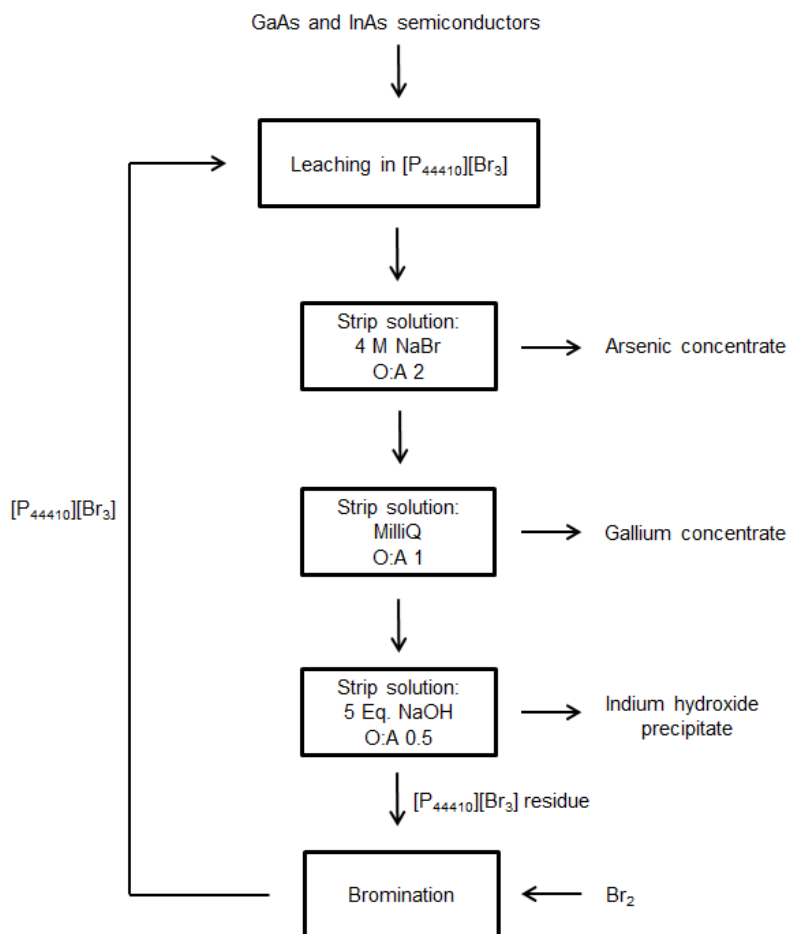
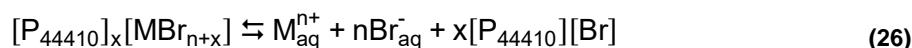


Figure 33: Flowsheet for the separation of arsenic, gallium and indium from a mixed GaAs/InAs [P₄₄₄₁₀][Br₃] leachate.

5.6 Mechanistic study

In this chapter a brief mechanistic study will be presented aimed at clarifying the differences in stripping between gallium, arsenic and indium. Equation (26) expresses the equilibrium which is present when stripping metals from the IL.



Based on the stripping experiments with varying NaBr concentrations presented in Figure 30 and Figure 31 a plot can be constructed in which the logarithm of the distribution ratios of gallium and arsenic are plotted versus the logarithm of the NaBr concentration, Figure 34. The slopes of these plots are equal to parameter *n* of Equation (26). Based on the larger slope of the gallium plot, it is concluded that the stripping of gallium is influenced to a greater extend by the bromide concentration than the stripping of arsenic, as was concluded earlier.

However, this plot should not be used for any quantitative description of stripping mechanisms because of the varying ionic strength of the solutions throughout the series of experiments. The ionic strength of the stripping solutions can be kept constant by addition of salts of non-coordinating anions such as ClO_4^- or Tf_2N^- . These anions will however cause an anion exchange of the IL.

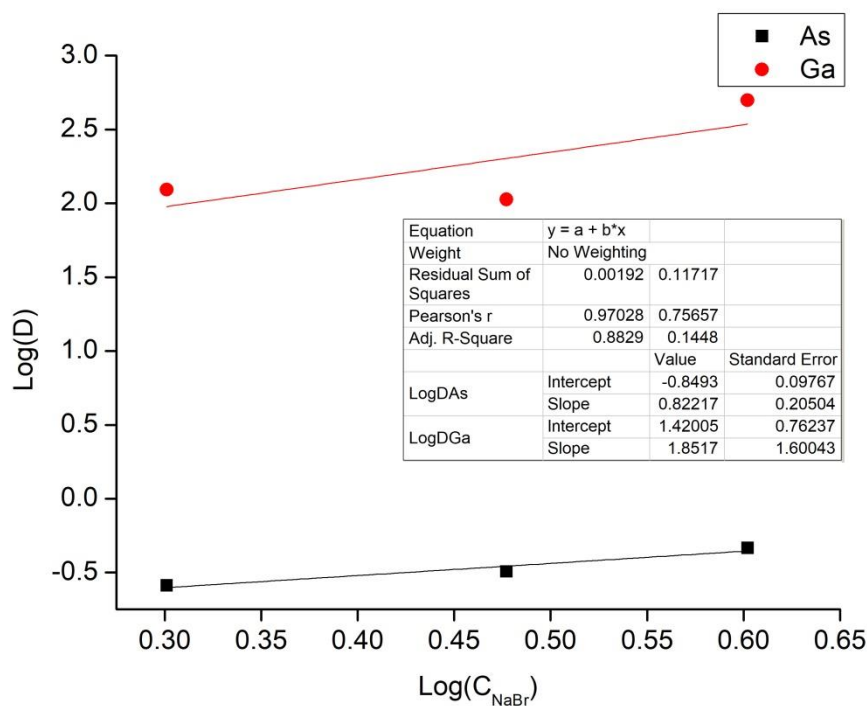


Figure 34: Plot of the logarithm of the distribution ratio in function of the logarithm of the NaBr concentration.

As an alternative to gain insight in the stripping mechanism one could manipulate the stripping equilibrium from the opposite direction and perform extraction experiments with varying $[\text{P}_{44410}][\text{Br}]$ concentration. Using this approach, the ionic strength of the aqueous solutions is kept constant. Starting from an aqueous phase of 2 M NaBr and 0.5 g/L Ga(III), As(V) or In(III) extractions were performed to a $[\text{P}_{44410}][\text{Br}]$ containing organic phase. Toluene was chosen as the diluent and the IL concentration was varied between 1.25 and 0.50 M. Both phases were shaken for 1 h at 60 °C and 2000 rpm and ICP-OES analysis was used to determine the equilibrium metal concentration in the aqueous phases. The resulting log-log plots are shown in Figure 35. The slopes of these plots are equal to the parameter x in Equation (26) and represent the number of IL molecules involved in the extraction. This can easily be confirmed mathematically, Equation (27), (28) and (29).

$$D = \frac{[P_{44410}]_x [MBr_{n+x}]}{[M_{aq}^{n+}]} \quad (27)$$

$$K_{eq} = \frac{[P_{44410}][Br]^{x+} [M_{aq}^{n+}]}{[P_{44410}]_x [MBr_{n+x}]} = \frac{[P_{44410}][Br]^{x+}}{D} \quad (28)$$

$$\log(D) = x \log([P_{44410}][Br]) - \log(K_{eq}) \quad (29)$$

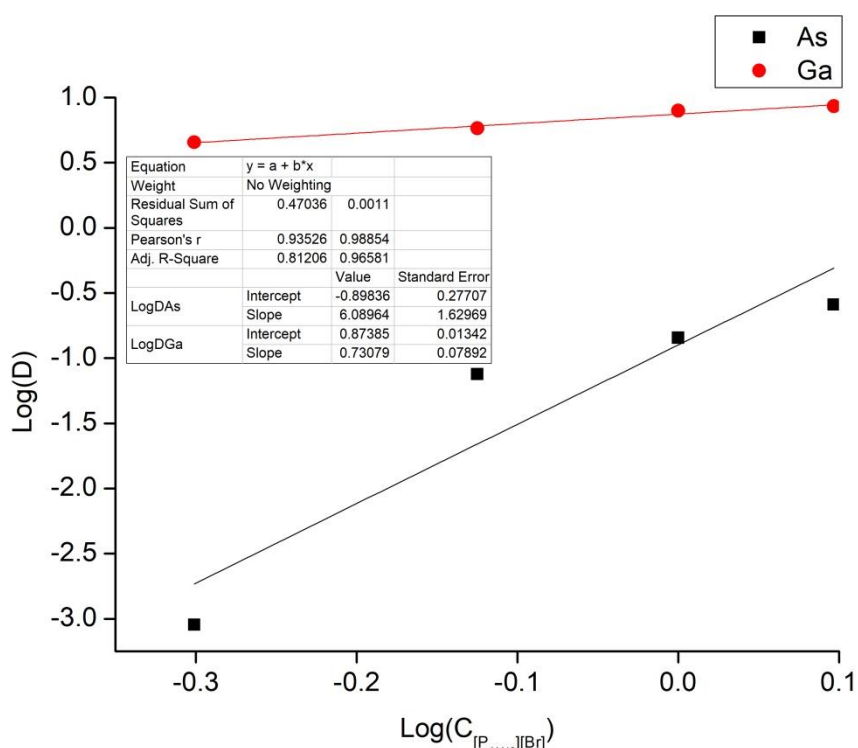


Figure 35: Plot of the logarithm of the distribution ratio in function of the logarithm of the $[P_{44410}][Br]$ concentration.

No results were obtained for indium as its affinity for the organic phase was so high that no measurable amount of indium was left in the aqueous phase. The slope of the gallium plot indicates that one IL molecule is involved in the extraction. Because gallium is in its 3+ state, this means that 3 Br⁻ ions have to be coextracted in order to conserve the electroneutrality of the solution. For arsenic however, the plot is not as evident. When the first data point is considered as an outlier and is left out of the calculation, the slope of the plot lowers to 2.39. Indicating that two IL molecules are involved in the extraction process. As the arsenic is in its 5+ state, 5 Br⁻ ions have to be coextracted. This would implicate that the stripping/extraction of arsenic is influenced to a greater extent by the bromide concentration than the stripping/extraction of gallium. This is the exact opposite of what is observed during the stripping experiments. Another implication is that arsenic is coordinated by 7 bromide ions when present in the organic phase. This is a doubtfully high value since the ionic radius of a

bromide ion is larger than that of arsenic. Lastly, it is also strange that the slope of the gallium plot has to be rounded upwards, while for arsenic the slope has to be rounded downwards. Due to all these reasons it was decided to repeat the experiment.

In the repeated experiment lower IL concentrations were used in order to obtain results for indium as well. However, the IL concentration cannot be taken too low and must still remain significantly higher than the metal concentration. If not, the assumption that the initial IL concentration is equal to the equilibrium concentration would be invalid and Equations (28) and (29) cannot be used. The concentration was varied between 0.125 and 0.2 M. The resulting log-log plots are shown in Figure 36. Despite using lower IL concentrations, no results were obtained for indium because its equilibrium concentrations in the aqueous phase were too low to be measured. This shows again the extreme affinity indium has for the organic phase and explains why indium cannot be stripped to any aqueous phase but has to be precipitated. For gallium the same result as before is obtained. The slope indicates that 1 IL molecule is involved in the extraction process. The slope of the arsenic plot is slightly negative, indicating the realistic slope (integer number) is zero. This implicates that there are no IL molecules nor bromide ions involved in the extraction/stripping of arsenic. This is exactly the result that is expected, based on the formation of arsenic acid (paragraph 5.5.2).

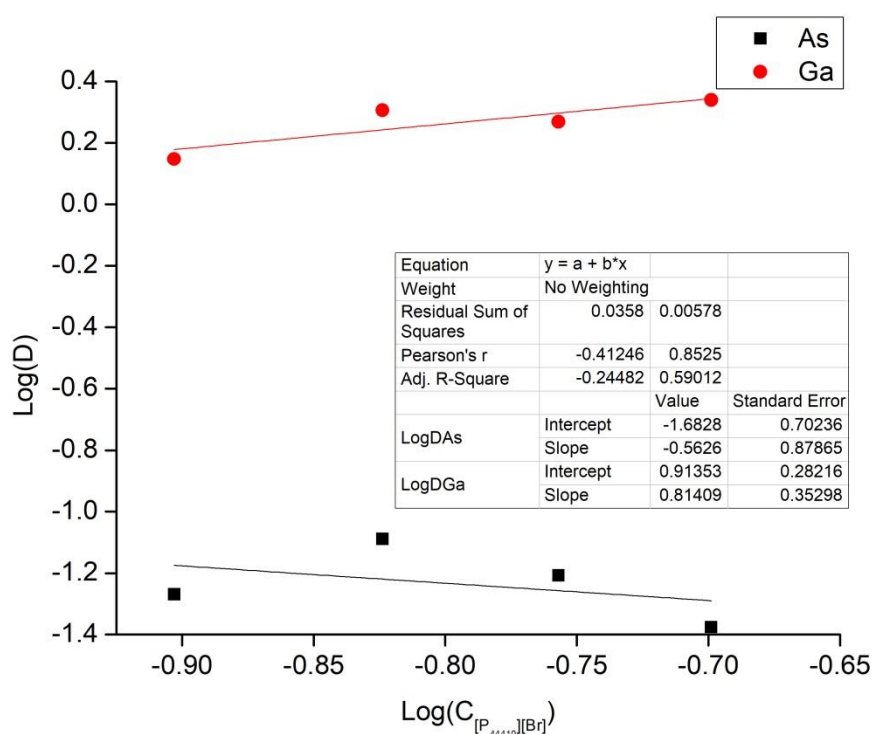


Figure 36: Plot of the logarithm of the distribution ratio in function of the logarithm of the $[P_{44410}][Br]$ concentration for the repeated experiment.

5.7 Light emitting diodes

To prove the applicability of tribromide ionic liquids for the recovery of gallium and/or indium from end-of-life LEDs, some experiments were performed on semiconductor material derived from real LEDs. Since no LED waste from industry is available, Vishay TSUS5400 LEDs were bought. These emit infrared (IR) light with a wavelength of 950 nm and are constructed with a GaAs semiconductor.

The first step in the entire recovery process is the isolation of the semiconductor material from the other constituent materials of the LEDs.

5.7.1 Grinding and milling

A first possibility to achieve the desired separation is the grinding or milling of the LEDs. Prior to any grinding or milling actions, the electrodes were cut from the LEDs to avoid an unnecessary excess of unwanted metals in the resulting powder. In a first attempt the LEDs were introduced in the planetary ball mill but no milling was achieved. The impact of the stainless steel balls was unable to break the LEDs because of the elasticity of the plastic material. In a second experiment a mechanical mortar grinder was used. Here, the LEDs are subjected to a shear stress as opposed to the compressive stress in the planetary ball mill. The mechanical mortar grinder was able to grind the LEDs into a fine powder. In Figure 37 the three stages of the LEDs are displayed.



Figure 37: Left: original LEDs; Middle: LEDs with cut off electrodes, Right: grinded (mechanical mortar grinder) LEDs.

As a third milling option, the disc mill was used. Also here, the LEDs are exposed to a shear stress rather than a compressive stress. Apart from the formation of very fine flakes the disc mill resulted in a slightly more coarse powder than the mortar grinder.

5.7.2 Thermal treatment

As a second option for the separation of the plastic and metallic materials a thermal treatment of the LEDs was investigated. Two mechanisms are possible through which the desired separation can be achieved. Firstly, the difference in thermal expansion coefficients of the plastic and the metals might promote their detachment. Secondly, the high

temperature can result in the decomposition of the plastic after which the metallic parts can easily be picked out.

To identify the surrounding plastic material, a fraction of the milled LEDs was subjected to an FTIR absorbance analysis. The spectrum is provided in Figure 38. The absence of an absorption in the 3500-3200 cm^{-1} region indicated that no alcohol functionalities were present and ruled out the possibility of an epoxy material. The presence of absorptions at 1731 and 1180 cm^{-1} can be associated with an ester-like functionality. This observation points in the direction of a polycarbonate, a material often used for LED applications because of its toughness and transparency.

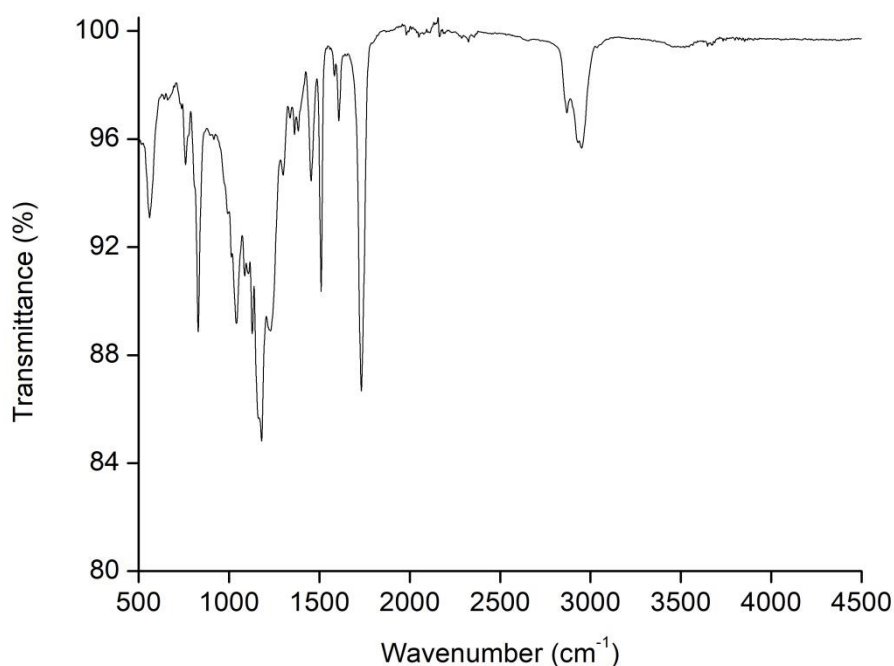


Figure 38: FTIR Vishay TSUS5400 LEDs.

These polycarbonate materials show decomposition temperatures around 500 °C.⁸⁷ Some LEDs were therefore heated for two hours at 500 °C. An inert argon atmosphere was chosen to avoid the possible oxidation of the metal parts which would render them insoluble in the tribromide IL. In Figure 39 a picture is shown of the LEDs after the thermal treatment. The LEDs had melted slightly and were caked together. Some of them had burst open but they were still quite tough. A thermal treatment was hereafter omitted as a possible route to the separation of the semiconductor material from the other constituent materials.



Figure 39: LEDs after thermal treatment at 500 °C in argon atmosphere.

5.7.3 Fractionalisation of the powders

Since the powder resulting from the mechanical mortar grinder was rather homogeneous, a density separation was proposed for the separation of the metals from the plastic material. As can be seen from the left side of Figure 40, the plastic material is heavier than water and no separation can be achieved by simply using water. The density of the aqueous phase was increased by the addition of NaCl. A 4 M (234 g/L) NaCl solution, which has a density of 1.15 g/mL, resulted in a slightly better separation as can be seen from the middle of Figure 40. However, a 5.14 M (300 g/L) NaCl solution with an approximate density of 1.20 g/mL resulted in the best separation, right side Figure 40. By scooping the plastic material from the top of the NaCl solution it could easily be separated from the metals. The resulting fractions were subsequently filtered, washed with deionized water and dried overnight in the vacuum oven. The metallic fraction had a brown colour, Figure 41, indicating some degree of corrosion.

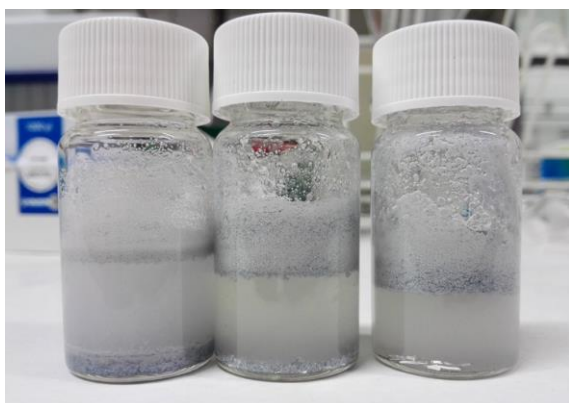


Figure 40: Small-scale density separations of the mortar ground LEDs. Left: water. Middle: 4 M NaCl. Right: 5.14 M NaCl.



Figure 41: Metallic (left) and plastic (right) fractions after mortar grinding, density separation, filtration and washing.

The powder which resulted from the disc mill was more heterogeneous and the fine flakes could easily be separated from the more coarse material by sieving to 710 μm . The electrodes were all contained in the coarse fraction and could be recovered using a magnet. The different fractions are shown in Figure 42.



Figure 42: Different fractions obtained after disc milling, sieving and magnetic separation. Left: fine plastic flakes. Middle: coarse plastic. Right: electrodes.

5.7.4 Analysis of the different fractions

Mechanical mortar grinder

A small portion of the metallic fraction was used in a dissolution experiment with $[P_{44410}][Br_3]$. The metal content was determined using ICP-OES analysis after microwave digestion and is shown in Table 14. Note that the accuracy of these results may be quite poor as for many elements the measured concentrations were in the 10-100 ppb range. The metallic fraction is mainly made up of iron with smaller amounts of copper, nickel and gold. Arsenic and gallium, which are the constituent elements of the semiconductor material, are only present in minute amounts.

Table 14: Elemental composition of $[P_{44410}][Br_3]$ leachate of metallic fraction obtained after mortar grinder and density separation.

	As	Ga	Al	Au	Cu	Fe	Pb	Sn	Ni
Concentration (ppm)	27	32	80	378	1711	67508	114	117	492

To determine whether there were still metals present in the remaining plastic material, some material was treated with a dilute (32.5 wt%) solution of nitric acid. This leachate was subsequently analysed using ICP-OES. On the basis of the masses used in both leaching experiments and the total masses of the metallic and plastic fractions, the distribution of each element over the different fractions could be calculated. This is presented in Table 15. Based on these results it seems that the GaAs semiconductor is largely still attached to the plastic material rather than to the metallic electrodes. All other elements seem to be mostly present in the metallic fraction.

Table 15: Distribution of each element over the metallic and plastic fraction after mortar grinder and density separation.

	As	Ga	Al	Au	Cu	Fe	Pb	Sn	Ni
% in metallic fraction	14.5	8.9	94.2 ¹	99.3 ¹	99.4	99.4	98.9	79.2	99.0
% in plastic fraction	85.5	91.1	5.8 ¹	0.7 ¹	0.6	0.6	1.1	20.8	1.0

¹ These percentages are not representative as nitric acid is unable to oxidize Au. The formation of a passivation layer is a hindrance for the dissolution of Al.

Disc mill

A small portion of the electrodes were used in a dissolution experiment with [P₄₄₄₁₀][Br₃]. Also here, the metal content was determined using ICP-OES analysis after microwave digestion, Table 16. The elemental composition is largely the same as the metallic fraction obtained with the mortar grinder. The leachate is mostly made up of iron, copper and nickel while the concentrations of gallium and arsenic are very low.

Table 16: Elemental composition of [P₄₄₄₁₀][Br₃] leachate of the electrodes obtained after disc mill and magnetic separation.

	As	Ga	Al	Au	Cu	Fe	Pb	Sn	Ni
Concentration (ppm)	24	44	141	124	2531	76864	66	190	442

The previously performed treatment of the plastic fractions with nitric acid is not very representative as some of the metals present (e.g. Au and Al) are unable to be dissolved. Both the fine flakes and more coarse plastic fractions were therefore leached with [P₄₄₄₁₀][Br₃]. The distribution of each element over the different fractions was calculated after microwave digestion and ICP-OES analysis. This is shown in Table 17. The results confirm the formerly made observation that the majority of the semiconductor material is present in the plastic fractions. Even though some other elements such as aluminium and lead are also quite significantly present, there is almost no iron or copper present. The latter are the most prominent metals of the LEDs, and can be considered as the main contaminants. In total, the fine flakes contain less of the semiconductor than the coarse plastic material. However the total mass of the fine flakes is significantly smaller than the coarse fraction and the concentration of gallium and arsenic will therefore be much higher in the fine flakes fraction.

Table 17: Distribution of each element over the different fractions obtained after disc mill and magnetic separation.

	As	Ga	Al	Au	Cu	Fe	Pb	Sn	Ni
% in electrodes	8.6	10.7	38.3	17.2	91.7	99.1	14.3	64.4	68.7
% in fine flakes plastic fraction	22.5	31.8	17.2	23.4	2.7	0.4	19.0	11.3	7.5
% in coarse plastic fraction	68.9	57.5	44.5	59.4	5.6	0.5	66.7	24.3	23.8

5.7.5 Stripping of LED leachates

Both plastic fractions origination from disc milling contain significant portions of the semiconductor material and are relatively free from the main contaminants iron and copper. For these reasons, some material of both fractions was leached with $[P_{44410}][Br_3]$. It was tried to use as little of the IL as possible to ensure sufficiently large concentrations of gallium and arsenic in the leachate. Both leachates were thereafter subjected to the optimized stripping procedure. Firstly, they were stripped three times with a 4 M NaBr solution handling an O:A ratio of 2. Secondly, two stripping steps with MilliQ water were performed in an O:A ratio of 1. All aqueous phases were analysed with ICP-OES and their composition is shown in Table 18 and Table 19. Note that the larger aqueous phases used in stripping steps 4 and 5 will result in lower measured concentrations.

Table 18: Metal concentrations (ppm) in the different aqueous phase after stripping $[P_{44410}][Br_3]$ leachate of coarse plastic fraction.

	As	Ga	Al	Au	Cu	Fe	Pb	Sn	Ni
Step 1	278.5	4.9	5.3	0.3	10.8	0.0	7.8	1.1	1
Step 2	24.2	4.8	3.6	0.5	9.1	0.0	4.2	0.8	0.6
Step 3	3.0	4.3	2.4	0.4	7.3	0.0	3.3	0.8	0.5
Step 4	1.5	25.3	3.1	1.1	11.6	0.4	0.7	0.0	0.1
Step 5	1.2	7.3	2.4	1.5	0.4	0.0	0.6	0.0	0.0

Table 19: Metal concentrations (ppm) in the different aqueous phase after stripping [P₄₄₄₁₀][Br₃] leachate of fine plastic fraction.

	As	Ga	Al	Au	Cu	Fe	Pb	Sn	Ni
Step 1	890.9	3.6	18.4	0.3	6.9	2.2	37.1	0.7	27.6
Step 2	62.8	4.4	7.1	0.1	6.9	0.6	22.3	0.4	1.9
Step 3	11.3	5.7	6.8	0.2	6.6	0.6	18.8	0.4	1.0
Step 4	3.3	342.2	5.7	30.9	65.3	195.2	1.9	0.0	0.5
Step 5	0.6	30.7	2.4	0.8	6.0	27.6	0.4	0.0	0.0

The concentrations of arsenic and gallium are, as expected, much higher in the strip solutions of the fine fraction than in those of the coarse plastic fraction. However this fraction is also more contaminated with other elements such as iron, copper and lead. The results show that the strip solutions of the first three steps consist mainly of arsenic with limited amounts of gallium. Also lead is stripped during these first steps. The strip solutions of the last two steps are mainly made up of gallium. In the case of the fine flakes, also significant amounts of iron and copper are present. Nevertheless, the use of the optimized stripping procedure was able to separate arsenic and gallium and worked therefore as intended.

5.7.6 Conceptual flowsheet

On the basis of all performed experiments a conceptual flowsheet for the recovery of gallium and indium from waste LEDs can be envisioned, Figure 43. The first step in the process consists of the grinding or milling of the LEDs. The grinded/milled LEDs are then subjected to several mechanical and physical separation steps (including sieving, density separations, magnetic separations, ...) resulting in the production of a concentrated fraction of the semiconductor materials which is subsequently leached in the [P₄₄₄₁₀][Br₃] IL. The remaining plastics and metallic elements can also be recovered and recycled.

The IL will leach arsenide semiconductors leaving others (e.g. GaN) in the residue. Since the residue does not contain any arsenic, it can easily be processed further using conventional acids without the possible production of the toxic arsine gas. The arsenic can then be stripped from the leachate using a 4 M NaBr solution with an O:A ratio of 2. Next, the gallium can be stripped using MilliQ water with an O:A ratio of 1. The resulting arsenic and gallium solutions can be purified further using additional and more conventional solvent extraction steps. Lastly, the indium is precipitated from the IL using at least 5 equivalents of NaOH in a sufficiently large aqueous phase. The produced In(OH)₃ can be treated similarly as In(OH)₃ recovered from zinc production. It can for example be redissolved using dilute hydrochloric acid and purified using several cementation steps.⁶ The remaining IL can thereafter be regenerated by bromination and recycled to the leaching step.

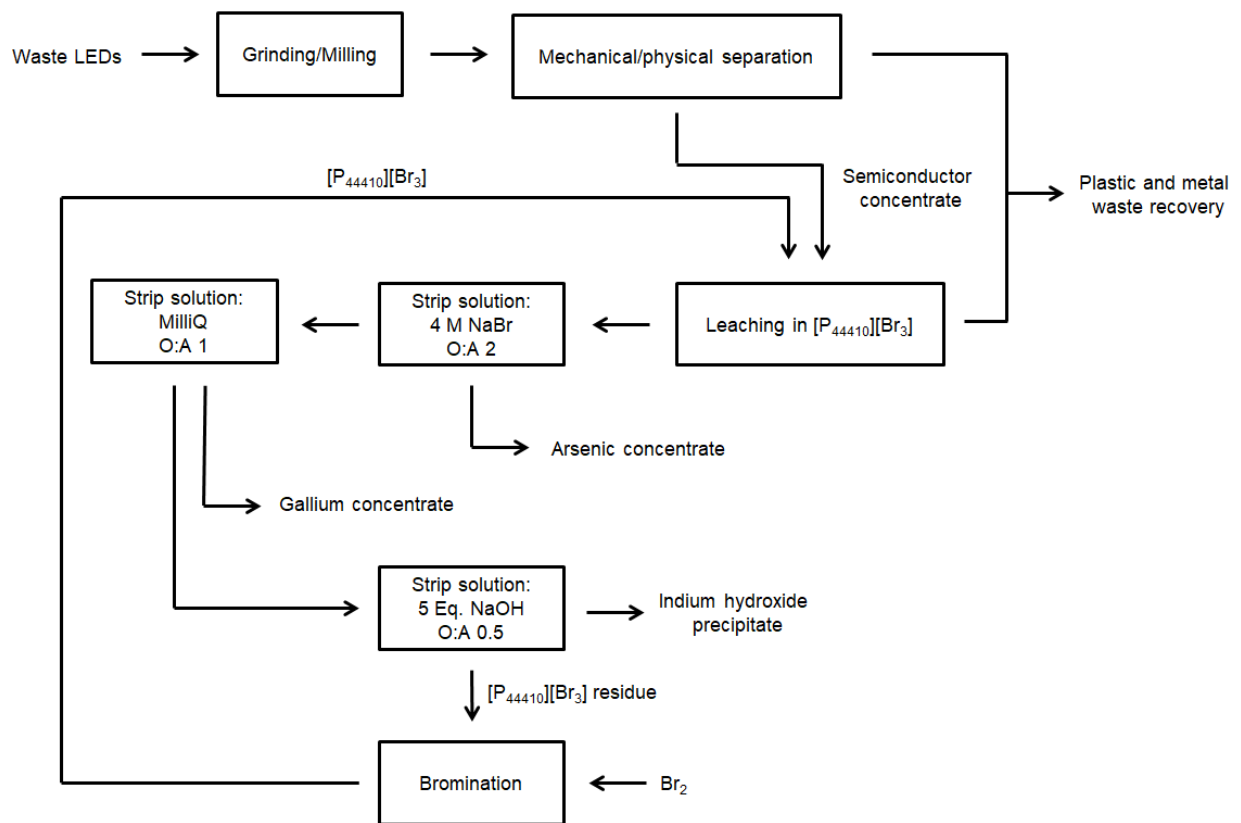


Figure 43: Conceptual flowsheet for the recovery of gallium and indium from waste LEDs.

6 Conclusion and outlook

The main objective of this master thesis project was the application of tribromide ILs for the recovery of gallium and indium from end-of-life LEDs. The first part of the project consisted of the determination of a suitable IL. This choice was firstly based on the mutual solubility of ILs with *n*-dodecane and water. Both [EMIM][Br] and [P₄₄₄₁₀][Br] showed a sufficiently low mutual solubility with dodecane. The influence of the addition of the extractants PC-88a, D2EHPA and Cyanex 923 on the mutual solubility was also investigated. In the case of [P₄₄₄₁₀][Br], the extractant resided almost entirely in the IL phase. In addition the *n*-dodecane content of the IL phase increased. For [EMIM][Br] the extractants did not cause a change in the mutual solubility and the extractant remained in the *n*-dodecane phase. [EMIM][Br] was however completely soluble in water, whereas [P₄₄₄₁₀][Br] was not. Secondly, the dissolution of semiconductor materials was considered in the choice of IL. GaN did not dissolve into [P₄₄₄₁₀][Br₃] nor [EMIM][Br₃]. GaAs and InAs dissolved into both ILs however the dissolution in [EMIM][Br₃] was slower and stagnated before completion. Using a 1:10 molar ratio metal to IL, both semiconductors were completely dissolved in [P₄₄₄₁₀][Br₃] within 24 h. Lastly, the ease of laboratory work was also considered. [P₄₄₄₁₀][Br₃] was liquid at room temperature which made laboratory work easier. [P₄₄₄₁₀][Br₃] was therefore used for the subsequent parts of this project.

[P₄₄₄₁₀][Br] and [P₄₄₄₁₀][Br₃] were synthesised and characterised by means of a Raman analysis and viscosity measurements. The tribromide displays a significantly lower viscosity than the monobromide, which is a major asset for the large scale application. The stability of the tribromide ion in the presence of water was confirmed using periodic Raman spectroscopic analyses. The dissolution kinetics of GaAs and InAs in [P₄₄₄₁₀][Br₃] were also compared. InAs showed a slightly faster dissolution because of its decreased bond strength. Overall the dissolution rates of both semiconductors were quite similar. This is probably because of a similar standard reduction potential and driving force.

The second major part of this project consisted of the development and optimization of a stripping/extraction procedure for the selective removal of gallium, arsenic and indium from the [P₄₄₄₁₀][Br₃] phase. Gallium and arsenic, contrary to indium, could easily be stripped to an aqueous phase. The stripping of gallium could largely be suppressed by an increase in the O:A ratio or the halide salt concentration. Although chloride salts resulted in the highest separation factors between gallium and arsenic, bromide salts were preferred to avoid a possible anion exchange of the IL. In the optimized procedure, arsenic is first stripped selectively from the [P₄₄₄₁₀][Br₃] phase using three stripping steps with a 4 M NaBr solution and an O:A ratio of 2. Hereafter gallium can be stripped selectively with MilliQ water and an

O:A ratio of 1. Throughout these manipulations indium remains in the IL phase. Extraction of indium to an organic phase was ruled out because none of the extractants showed a particular selectivity for indium and the extraction efficiencies remained too low. Indium could however quantitatively be precipitated from the IL phase using at least 5 equivalents of NaOH. A mechanistic study was performed with the aim of clarifying the differences in stripping between gallium, arsenic and indium. No results were obtained for indium because of its high affinity for the organic phase. This confirmed that it cannot be stripped to an aqueous phase. Slope analysis revealed that one IL molecule and three bromide ions are involved in the stripping/extraction of gallium. On the other hand, no IL molecules or bromide ions are involved in the case of arsenic, which formed the water soluble arsenic acid when contacted with the water phase. The stripping of gallium can therefore be suppressed using a bromide salt while the stripping of arsenic remains unaffected.

The last part of the project consisted of the application of the optimized stripping procedure to semiconductor material derived from real LEDs. For this purpose Vishay TSUS5400 IR LEDs with a GaAs semiconductor were acquired. The LEDs were first grinded or milled using the mechanical mortar grinder or the disc mill. The resulting powders were subsequently fractionalised using density separations, sieving and magnetic separations. Analysis of the different fractions revealed that the majority of the semiconductor material was present in plastic fractions rather than on the electrodes. Some plastic material was leached with the $[P_{44410}][Br_3]$ IL and subjected to the optimized stripping procedure. The metal concentrations in the different strip solutions indicated that the stripping procedure worked as was intended. Lastly, a conceptual flowsheet for the recovery of gallium and indium from waste LEDs was proposed.

There remains still some work for future research. Solvents other than dodecane and water in combination with other extractants could be used which could result in enhanced selectivities. In addition, the stripping/extraction behaviour of the other constituent elements of the LEDs such as iron, copper, lead and tin can be investigated. Based on these results the stripping procedure could be modified and the proposed flow sheet can be expanded. The main difficulty for the recovery of gallium and/or indium from end-of-life LEDs is the minute amount of the semiconductor material present per LED. The grinding/milling and the different mechanical and physical steps used for the separation and concentration of the semiconductor material can therefore also be optimized further. The dissolution of other semiconductor materials such as phosphides and mixed arsenides can also be researched. In this context also other polyhalide ILs could be used.

7 Bibliography

- 1 *Study on the review of the list of critical raw materials*, European Commission, Brussels, 2017.
- 2 F. Lu, T. Xiao, J. Lin, Z. Ning, Q. Long, L. Xiao, F. Huang, W. Wang, Q. Xiao, X. Lan and H. Chen, *Hydrometallurgy*, 2017, **174**, 105–115.
- 3 B. W. Jaskula, *Gallium*, U.S. Geological Survey, 2017.
- 4 R. R. Moskalyk, *Miner. Eng.*, 2003, **16**, 921–929.
- 5 B. Swain, C. Mishra, K.-J. Lee, H. S. Hong, K.-S. Park and C. G. Lee, *Int. J. Appl. Ceram. Technol.*, 2016, **13**, 280–288.
- 6 A. M. Alfantazi and R. R. Moskalyk, *Miner. Eng.*, 2003, **16**, 687–694.
- 7 A. C. Tolcin, *Indium*, U.S. Geological Survey, 2017.
- 8 D. Pradhan, S. Panda and L. B. Sukla, *Miner. Process. Extr. Metall. Rev.*, 2017, **0**, 1–14.
- 9 D. Chitnis, N. Thejo kalyani, H. C. Swart and S. J. Dhoble, *Renew. Sustain. Energy Rev.*, 2016, **64**, 727–748.
- 10 S. W. Sanderson and K. L. Simons, *Res. Policy*, 2014, **43**, 1730–1746.
- 11 A. De Almeida, B. Santos, B. Paolo and M. Quicheron, *Renew. Sustain. Energy Rev.*, 2014, **34**, 30–48.
- 12 *Global LED Lighting Market Size & Share Worth \$54.28 Billion by 2022 Zion Market Research*, 2017.
- 13 A. Nardelli, E. Deuschle, L. D. de Azevedo, J. L. N. Pessoa and E. Ghisi, *Renew. Sustain. Energy Rev.*, 2017, **75**, 368–379.
- 14 S.-R. Lim, D. Kang, O. A. Ogunseitan and J. M. Schoenung, *Environ. Sci. Technol.*, 2011, **45**, 320–327.
- 15 P. Atkins and J. de Paula, *Atkins' Physical Chemistry*, OUP Oxford, 2010.
- 16 G. Held, *Introduction to Light Emitting Diode Technology and Applications*, CRC Press, 2016.
- 17 T. Q. Khan, P. Bodrogi, Q. T. Vinh and H. Winkler, *LED Lighting: Technology and Perception*, John Wiley & Sons, 2015.
- 18 C. C. Lin and R.-S. Liu, *J. Phys. Chem. Lett.*, 2011, **2**, 1268–1277.
- 19 S. M. Mizanur Rahman, J. Kim, G. Lerondel, Y. Bouzidi, K. Nomenyo and L. Clerget, *Resour. Conserv. Recycl.*, 2017, **127**, 256–258.
- 20 S. Nagy, L. Bokányi, I. Gombkötő and T. Magyar, *Arch. Metall. Mater.*, 2017, **62**, 1161–1166.
- 21 L. Zhan, F. Xia, Q. Ye, X. Xiang and B. Xie, *J. Hazard. Mater.*, 2015, **299**, 388–394.
- 22 L. Zhan, J. Li, B. Xie and Z. Xu, *ACS Sustain. Chem. Eng.*, 2017, **5**, 3179–3185.
- 23 W.-T. Chen, L.-C. Tsai, F.-C. Tsai and C.-M. Shu, *CLEAN – Soil Air Water*, 2012, **40**, 531–537.
- 24 S.-H. Hu, M.-Y. Xie, Y.-M. Hsieh, Y.-S. Liou and W.-S. Chen, *Environ. Prog. Sustain. Energy*, 2015, **34**, 471–475.
- 25 B. Swain, C. Mishra, L. Kang, K.-S. Park, C. G. Lee, H. S. Hong and J.-J. Park, *J. Power Sources*, 2015, **281**, 265–271.
- 26 B. Swain, C. Mishra, L. Kang, K.-S. Park, C. G. Lee and H. S. Hong, *Environ. Res.*, 2015, **138**, 401–408.
- 27 A. Mohammad and D. Inamuddin, *Green Solvents II: Properties and Applications of Ionic Liquids*, Springer Science & Business Media, Dordrecht, 2012.
- 28 T. Welton, *Chem. Rev.*, 1999, **99**, 2071–2084.
- 29 P. Wasserscheid and T. Welton, *Ionic Liquids in Synthesis*, Wiley-VCH, Weinheim, 2008.
- 30 N. V. Plechkova and K. R. Seddon, *Chem. Soc. Rev.*, 2007, **37**, 123–150.
- 31 P. Barthen, W. Frank and N. Ignatiev, *Ionics*, 2015, **21**, 149–159.
- 32 K. Binnemans and P. T. Jones, *J. Sustain. Metall.*, 2017, **3**, 570–600.

- 33 M. Atilhan, J. Jacquemin, D. Rooney, M. Khraisheh and S. Aparicio, *Ind. Eng. Chem. Res.*, 2013, **52**, 16774–16785.
- 34 J. Pernak, T. Rzemieniecki and K. Materna, *Chem. Int.*, 2016, **70**, 476–480.
- 35 M. G. Freire, C. M. S. S. Neves, I. M. Marrucho, J. A. P. Coutinho and A. M. Fernandes, *J. Phys. Chem. A*, 2010, **114**, 3744–3749.
- 36 J. Gorke, F. Srienc and R. Kazlauskas, *Biotechnol. Bioprocess Eng.*, 2010, **15**, 40–53.
- 37 P. Wasserscheid and W. Keim, *Angew. Chem. Int. Ed.*, 2000, **39**, 3772–3789.
- 38 D. Depuydt, A. V. den Bossche, W. Dehaen and K. Binnemans, *RSC Adv.*, 2016, **6**, 8848–8859.
- 39 D. Dupont, D. Depuydt and K. Binnemans, *J. Phys. Chem. B*, 2015, **119**, 6747–6757.
- 40 M. A. A. Rocha, C. M. S. S. Neves, M. G. Freire, O. Russina, A. Triolo, J. A. P. Coutinho and L. M. N. B. F. Santos, *J. Phys. Chem. B*, 2013, **117**, 10889–10897.
- 41 M. A. A. Rocha, J. A. P. Coutinho and L. M. N. B. F. Santos, *J. Phys. Chem. B*, 2012, **116**, 10922–10927.
- 42 M. J. Earle, J. M. S. S. Esperança, M. A. Gilea, J. N. C. Lopes, L. P. N. Rebelo, J. W. Magee, K. R. Seddon and J. A. Widegren, *Nature*, 2006, **439**, 831–834.
- 43 H. D. B. Jenkins, *Sci. Prog. St Albans*, 2011, **94**, 265–297.
- 44 H. Haller and S. Riedel, *Z. Für Anorg. Allg. Chem.*, 2014, **640**, 1281–1291.
- 45 B. D. Stepin and S. B. Stepina, *Russ. Chem. Rev.*, 1986, **55**, 812–824.
- 46 J. C. Evans and G. Y. Lo, *J. Chem. Phys.*, 1966, **44**, 3638–3639.
- 47 O. Bortolini, M. Bottai, C. Chiappe, V. Conte and D. Pieraccini, *Green Chem.*, 2002, **4**, 621–627.
- 48 M. E. Easton, A. J. Ward, B. Chan, L. Radom, A. F. Masters and T. Maschmeyer, *Phys. Chem. Chem. Phys.*, 2016, **18**, 7251–7260.
- 49 R. Cristiano, K. Ma, G. Pottanat and R. G. Weiss, *J. Org. Chem.*, 2009, **74**, 9027–9033.
- 50 Z. Barnea, T. Sachs, M. Chidambaram and Y. Sasson, *J. Hazard. Mater.*, 2013, **244–245**, 495–500.
- 51 A. Matthew Wilson, P. J. Bailey, P. A. Tasker, J. R. Turkington, R. A. Grant and J. B. Love, *Chem. Soc. Rev.*, 2014, **43**, 123–134.
- 52 J. Rydberg, *Solvent Extraction Principles and Practice, Revised and Expanded*, CRC Press, 2004.
- 53 F. Xie, T. A. Zhang, D. Dreisinger and F. Doyle, *Miner. Eng.*, 2014, **56**, 10–28.
- 54 M. S. Lee, J. G. Ahn and E. C. Lee, *Hydrometallurgy*, 2002, **63**, 269–276.
- 55 Y. Baba, F. Kubota, N. Kamiya and M. Goto, *Solvent Extr. Res. Dev. Jpn.*, 2016, **23**, 9–18.
- 56 B. Gupta, N. Mudhar, Z. Begum and I. Singh, *Hydrometallurgy*, 2007, **87**, 18–26.
- 57 B. Gupta, N. Mudhar and S. N. Tandon, *Ind. Eng. Chem. Res.*, 2005, **44**, 1922–1927.
- 58 I. Mihaylov and P. A. Distin, *Hydrometallurgy*, 1992, **28**, 13–27.
- 59 R. G. Bautista, *JOM*, 2003, **55**, 23–26.
- 60 B. Gupta, A. Deep and P. Malik, *Anal. Chim. Acta*, 2004, **513**, 463–471.
- 61 H. N. Kang, J.-Y. Lee and J.-Y. Kim, *Hydrometallurgy*, 2011, **110**, 120–127.
- 62 X. Zhang, G. Yin and Z. Hu, *Talanta*, 2003, **59**, 905–912.
- 63 I. C. P. Smith and D. E. Blandford, *Anal. Chem.*, 1995, **67**, 509–518.
- 64 R. J. Carbajo and J. L. Neira, *NMR for Chemists and Biologists*, Springer Science & Business Media, Dordrecht, 2013.
- 65 A. Felgner, R. Schlink, P. Kirschenbühler, B. Faas and H.-D. Isengard, *Food Chem.*, 2008, **106**, 1379–1384.
- 66 *Good Titration Practice in Karl Fischer titration*, Mettler Toledo.
- 67 C. M. Clippard, J. C. Nichisti, R. A. Kreuter, B. S. Chohan and D. G. Sykes, *Food Anal. Methods*, 2015, **8**, 929–936.
- 68 G. S. Bumbrah and R. M. Sharma, *Egypt. J. Forensic Sci.*, 2016, **6**, 209–215.
- 69 E. González-Labrada and D. G. Gray, *Cellulose*, 2012, **19**, 1557–1565.
- 70 R. Klockenkämper and A. von Bohlen, *Total-Reflection X-Ray Fluorescence Analysis and Related Methods*, John Wiley & Sons, Dortmund, 2014.

- 71 *User Manual S2 PICOFOX*, Bruker Nano GmbH, Berlin, 2011.
- 72 C. B. Boss and K. J. Fredeen, *Concepts, Instrumentation and Techniques in Inductively Coupled Plasma Optical Emission Spectrometry*, PerkinElmer Instruments, 2004.
- 73 *Customer Hardware and Service Guide Optima 8000*, Perkin Elmer, Shelton, USA, 2014.
- 74 *Theory of Sample Preparation Using Acid Digestion, Pressure Digestion and Microwave Digestion (Microwave Decomposition)*, Berghof Product + Instruments GmbH.
- 75 *User Manual Speedwave Xpert Microwave Digestion System*, Berghof Products + Instruments GmbH, 2016.
- 76 Veiligheid, Gezondheid en Milieu, <https://chem.kuleuven.be/veiligheid/index.html>, (accessed September 30, 2017).
- 77 C. J. Bradaric, A. Downard, C. Kennedy, A. J. Robertson and Y. Zhou, *Green Chem.*, 2003, **5**, 143–152.
- 78 S. Riaño, M. Regadío, K. Binnemans and T. Vander Hoogerstraete, *Spectrochim. Acta Part B At. Spectrosc.*, 2016, **124**, 109–115.
- 79 X. Li, A. V. den Bossche, T. V. Hoogerstraete and K. Binnemans, *Chem. Commun.*, 2018, **54**, 475–478.
- 80 P. M. Dean, B. R. Clare, V. Armel, J. M. Pringle, C. M. Forsyth, M. Forsyth and D. R. MacFarlane, *Aust. J. Chem.*, 2009, **62**, 334–340.
- 81 A. Schnittke, H. Stegemann, H. Füllbier and J. Gabrusenoks, *J. Raman Spectrosc.*, 1991, **22**, 627–631.
- 82 S. J. Pearton, J. C. Zolper, R. J. Shul and F. Ren, *J. Appl. Phys.*, 1999, **86**, 1–78.
- 83 W. A. Harrison, *Electronic Structure and the Properties of Solids: The Physics of the Chemical Bond*, Courier Corporation, New York, 2012.
- 84 J. Mähler, I. Persson and R. B. Herbert, *Dalton Trans.*, 2013, **42**, 1364–1377.
- 85 C. Deferm, M. V. de Voorde, J. Luyten, H. Oosterhof, J. Fransaer and K. Binnemans, *Green Chem.*, 2016, **18**, 4116–4127.
- 86 A. I. Busev, *The Analytical Chemistry of Indium: International Series of Monographs on Analytical Chemistry*, Elsevier, Frankfurt, 2013.
- 87 W. Jiang and S. C. Tjong, *Polym. Degrad. Stab.*, 1999, **66**, 241–246.

FACULTY OF SCIENCE – DEPARTMENT OF CHEMISTRY
Celestijnenlaan 200F
3001 LEUVEN, BELGIË
tel. + 32 16 00 00 00
<https://chem.kuleuven.be/en>

